

AP2IX-4, A CELL CYCLE REGULATED NUCLEAR FACTOR, MODULATES
GENE EXPRESSION DURING BRADYZOITE DEVELOPMENT IN
TOXOPLASMA GONDII

Sherri Y. Huang

Submitted to the faculty of the University Graduate School
in partial fulfillment of the requirements
for the degree
Doctor of Philosophy
in the Department of Pharmacology & Toxicology
Indiana University

April 2017

Accepted by the Graduate Faculty, Indiana University, in partial fulfillment of the requirements for the degree of Doctor of Philosophy.

Gustavo Arrizabalaga, Ph.D., Chair

William J. Sullivan, Jr., Ph.D.

Doctoral committee

Tao Lu, Ph.D.

Yuichiro Takagi, Ph.D.

January 10, 2017

Jian-Ting Zhang, Ph.D.

ACKNOWLEDGEMENTS

My journey through graduate school would not have been possible without the mentorship, friendship and support of my scientific mentors, labmates, friends and family.

I would first like to thank my mentor and thesis adviser, Dr. William Sullivan Jr. Through these years, the mentorship of Dr. Sullivan has been invaluable. He has encouraged me to constantly hone my scientific communication skills and to evaluate my thoughts scientifically. He always took the time to sit down with me and review my lab presentations, posters, conference talks and my thesis dissertation. His love for microbiology is infectious, pun intended.

I would also like to thank members of my thesis committee: Dr. Gustavo Arrizabalaga, Dr. Tao Lu, Dr. Yuichiro Takagi, and Dr. Jian-Ting Zhang. Their help encompassed scientific experimentation and encouragement, both invaluable to a graduate student. I especially thank them for one thesis committee during which they encouraged me to take more intellectual risks. Through his tough scientific questions at lab and committee meetings, Dr. Arrizabalaga helped push me to become a better scientist. Drs. Takagi, Tao Lu, and Jian-ting Zhang, your humor and words of encouragement also helped me greatly when I doubted my abilities.

Next I would like to thank my zany and brilliant lab colleagues, past and present, in the Sullivan and Arrizabalaga labs: Dr. Michael Harris, Dr. Michael Holmes, Dr. Vicki Jeffers, Leah Padgett, Jen Martynowicz, Joe Varberg, Kaice LaFavers, Dr. Chunlin Yang, Tamila Garbuz, Dr. Raj Gaji, Dr. Robert Charvat, Sol Bogado, Dr. Anne Bouchut, Gian Gballou, Dr. Ting-Kai “Tank” Liu and Dr. Imaan Benmerzouga. Dr. Michael Holmes, thank you for your expertise and scientific opinion as we worked together on the AP2IX-4 story (I secretly hope to become brilliant like you, soon). Joe, Kaice and Leah, thank you for being wonderful and helpful fellow graduate students. Michael Harris and Jen, you two always made lab fun with talk of science and other geeky subjects. Vicki, you were the one who mentored me during my rotation, thank you for always being

patient as you demonstrated a technique or explained a concept to me. Tank, thank you for your friendship and obviously for the reagents you generated that launched my thesis work. Robert, thank you for being a great friend, fellow bubble tea aficionado, and ever-reliable encyclopedia of microscopy protocols. Raj, I remember I felt disappointed in my performance after my first lab meeting; thank you for talking with me. Imaan, thank you for all your work in teaching me how to perform mouse work, but no thank you to the “strawberry milkshake” analogy you made regarding homogenized mouse brains. Gian, thank you for your dedication in assisting with the cyst burden quantifications. Sol, you always inspired me with your fun and positive, Turbo-kicking attitude. Anne, I remember how you used to carry three grocery bags up five flights of stairs without huffing and puffing. This was the rigor with which you worked at the bench, and it was very inspiring.

I would also like to thank members of the Michael White Laboratory for their collaboration and scientific feedback. Thank you Dr. Michael White, Dr. Joshua Radke and Dr. Dong-Pyo Hong.

Many thanks to my dear friends in the IBMG program and IUSM Medical Scientist Training Program for their support through these years: Dr. Xin Tong, Abass Conteh, Dr. Sara Culleton, Dr. Alex Ocana, Kevin Ni, Adam Roth, Thao Trinh, Brian Grice, Dr. Rikki Enzor, Dr. Justin Johnson, Kurt Drury, Lisa Deng, Darrelle Colinot, Rochelle Frankson, Donna Cerabona, Dr. Han Wei, Rasika Mundade, Antja-voy Hartley, and Matthew Martin.

My scientific journey before IUSM was launched by three key role models, and I am grateful to have a chance to thank them here. First is my science teacher in eighth grade, Dr. Paul Ricks. It was in taking your physics course that gave me confidence I could possibly consider science. After I graduated from your class, you allowed me cherished moments after school where I could discuss with you my growing interest in biology and eventually college decisions. Through my academic life, I was always grateful to have had you as my constant mentor.

Second is the professor I worked with one summer at the University of California, Berkeley: Dr. Hiroshi Nikaido. I remember you allowing an unseasoned high schooler to try out bench science in your shiny laboratory. And I remember that on my second day in your lab, I broke a p1000 pipette and felt so awful I tried looking up how much it'll cost me to buy the lab a new p1000. You laughed and told me not to worry. The next day you started mentoring me one-on-one at the bench, teaching me how to use the pipette and aseptic techniques.

I would also like to thank my college mentor, Dr. Petra Levin. You taught me that a great scientist can be kind, patient and warm at the same time, and one day I hope to emulate you. You encouraged my creative pursuits and taught me not to fear failure. And through certain rough days in graduate school, I only have to recall the wisdom you imparted me, that we must always remember the big picture.

I would like to thank members of the King Laboratory at UC Berkeley for their scientific mentorship: Dr. Rosie Alegado and Dr. Nicole King. Thank you both for allowing me to work on a project in your laboratory after I graduated from college. I would like to thank the incredible directors of the IUSM Medical Scientist Training Program: Drs. Maureen Harrington, Raghu Mirmira, and Rebecca Chan. I would like to thank Jan Receveur, Amy Lawson and Joanna Plew for their help with coordinating important dates and events.

Another scientific mentor I would like to thank is Dr. Jer-Yen Yang. Thank you for always letting me drop by your laboratory and converse about science, graduate school and careers.

I would like to thank my friends who don't attend IUSM but whom have nevertheless walked with me in my academic journey. Thank you Reiri Sono, Ruth Howe, Elizabeth Watts, Crème Brulee and Pumpkin. I would like to thank my best friends Edward Lu, Han Wei, Eric Trieu, Christine Yeh, David Liu, Sachin Shah, Allan Gao, Daniel Besiada, Sol Bogado and Anne Bouchut for your loving support and confidence in my dreams.

Importantly, I cannot thank my parents, David and Carol, enough. Mom, you continue to inspire my life choices every single day. I'll always remember

your words to me and the promises I made to you. Both you and dad have been my biggest role models and always inspired me with your hard work, careful thinking, and constant love, sacrifice and support. It was from you both that I first learned lessons of compassion, then the importance of education, and finally the value of confidence, persistence and keeping an open mind.

And finally, I would like to thank my best friend and soulmate, Joshua Elkins. You walked with me every step of the way through some of the tougher times in graduate school. Even though my MD/PhD program is a relatively long program, you never cease to remind me of how I can eventually make a difference in science and medicine. Your enthusiasm for science, engineering and art always reminds me to live a life filled with exploration and creativity.

Sherri Y. Huang

AP2IX-4, A CELL CYCLE REGULATED NUCLEAR FACTOR, MODULATES
GENE EXPRESSION DURING BRADYZOITE DEVELOPMENT IN
TOXOPLASMA GONDII

Toxoplasma gondii is a ubiquitous, protozoan parasite contributing significantly to global human and animal health. In the host, this obligate intracellular parasite converts into a latent tissue cyst form known as the bradyzoite, which is impervious to the immune response. The tissue cysts facilitate wide-spread transmission through the food chain and give rise to chronic toxoplasmosis in immune compromised patients. In addition, they may reactivate into replicating tachyzoites which cause tissue damage and disseminated disease. Current available drugs do not appear to have appreciable activity against latent bradyzoites. Therefore, a better understanding of the molecular mechanisms that drive interconversion between tachyzoite and bradyzoite forms is required to manage transmission and pathogenesis of *Toxoplasma*.

Conversion to the bradyzoite is accompanied by an altered transcriptome, but the molecular players directing this process are largely uncharacterized. Studies of stage-specific promoters revealed that conventional *cis*-acting mechanisms operate to regulate developmental gene expression during tissue cyst formation. The major class of transcription factor likely to work through these *cis*-regulatory elements appears to be related to the Apetala-2 (AP2) family in plants. The *Toxoplasma* genome contains nearly 70 proteins harboring at least

one predicted AP2 domain, but to date only three of these *T. gondii* AP2 proteins have been linked to bradyzoite development.

We show that the putative *T. gondii* transcription factor, AP2IX-4, is localized to the parasite nucleus and exclusively expressed in tachyzoites and bradyzoites undergoing division. Knockout of AP2IX-4 had negligible effect on tachyzoite replication, but resulted in a reduced frequency of bradyzoite cysts in response to alkaline stress induction – a defect that is reversible by complementation. Microarray analyses revealed an enhanced activation of bradyzoite-associated genes in the AP2IX-4 knockout during alkaline conditions. In mice, the loss of AP2IX-4 resulted in a modest virulence defect and reduced brain cyst burden. Complementation of the AP2IX-4 knockout restored cyst counts to wild-type levels. These findings illustrate the complex role of AP2IX-4 in bradyzoite development and that certain transcriptional mechanisms responsible for tissue cyst development operate across parasite division.

Gustavo Arrizabalaga, Ph.D., Chair

TABLE OF CONTENTS

LIST OF TABLES	xi
LIST OF FIGURES	xii
LIST OF ABBREVIATIONS	xiii
CHAPTER 1: INTRODUCTION	1
I. <i>T. gondii</i> converts between life cycle stages to propagate and transmit	2
A. Life cycle	2
B. Transmission	3
C. The host immune response	6
D. Toxoplasmosis	8
E. Genetic lineages of <i>T. gondii</i> and toxoplasmosis	14
II. The bradyzoite is important to transmission and pathogenesis	18
A. Structural morphology of bradyzoite cysts	18
B. Inducers and molecular changes of bradyzoite differentiation	20
C. Gene expression changes accompanying bradyzoite development	24
D. <i>T. gondii</i> cis-regulatory elements	26
III. ApiAP2s represent a primary lineage of transcription factors	29
A. Discovery of the ApiAP2s	29
B. Function of AP2s in plants and in Apicomplexa	32
C. Function and mechanism of <i>T. gondii</i> AP2s	34
IV. Goals for this thesis	36
CHAPTER 2: MATERIALS AND METHODS	39
I. Tissue culture techniques	39
A. Parasite strains and sources	39
B. Host cell and parasite culturing	40
C. Parasite growth assays	43
D. <i>In vitro</i> bradyzoite induction.....	43
E. Harvesting of parasites	44
F. Freezing and thawing of cells	44
G. Transfection	45
H. Drug selection of transfected parasites	46
I. Cloning by limiting dilution	48
II. Plasmid construction	48
A. General PCR protocol	49
B. General molecular cloning guidelines	51
C. Construct for endogenous tagging of AP2IX-4	54
D. Construct for knocking out <i>ap2IX-4</i>	54
E. Construct for complementation of AP2IX-4 in Δ <i>ap2IX-4</i> parasites	56
III. Biochemical techniques	61
A. Western blot	61
B. Indirect immunofluorescence assay	62
IV. Gene expression analysis	64
A. Purification of total RNA	64
B. ToxoGeneChip description	65
C. Target sequence synthesis, hybridization, and statistical analysis	66
V. Modeling of parasite infection in mice	67

A.	Acquisition, housing and general care of mice	67
B.	Preparation of parasites for injection of mice.....	67
C.	Injection and monitoring of mice	68
D.	Preparation of IFA samples for <i>in vivo</i> cyst burden quantification	68
E.	Quantification of mouse brain cysts.....	69
VI.	Yeast two-hybrid library construction	70
A.	General schematic.....	70
B.	Preparation of total RNA.....	74
CHAPTER 3: RESULTS	75
I.	Alignment and phylogenetic analysis of the predicted AP2 DNA-binding domain of AP2IX-4	75
II.	The predicted and confirmed protein size of AP2IX-4	80
III.	AP2IX-4 is expressed in the parasite nucleus during the S-M phase of the tachyzoite cell cycle	81
IV.	AP2IX-4 is dispensable for <i>in vitro</i> tachyzoite replication	82
V.	AP2IX-4 is expressed throughout bradyzoite development	86
VI.	Deletion of AP2IX-4 reduces <i>in vitro</i> bradyzoite cyst efficiency	91
VII.	Analysis of $\Delta ap2IX-4$ in mouse models of acute and chronic toxoplasmosis.....	92
VIII.	Loss of AP2IX-4 results in enhanced bradyzoite gene expression	95
IX.	Strategies to generate overexpression of AP2IX-4.....	101
X.	Yeast two-hybrid screen uncovers AP2IX-4 protein interactors.....	101
CHAPTER 4: DISCUSSION	107
I.	AP2IX-4 is a nuclear factor expressed in the S/M phase of the tachyzoite cell cycle, but is dispensable for tachyzoite replication	108
II.	AP2IX-4 is expressed in dividing bradyzoites	109
III.	Ablation of AP2IX-4 decreased cyst frequency in alkaline induction and in brains of chronically infected mice	112
IV.	AP2IX-4 as a transcriptional repressor of a subset of bradyzoite-associated genes.....	113
V.	Conclusions and future studies	114
APPENDIX	121
REFERENCES	123
CURRICULUM VITAE		

LIST OF TABLES

Table 1: Parasite lines	40
Table 2: PCR primers	50
Table 3: Plasmids	53
Table 4: Differentially expressed genes (FC \geq 2) under tachyzoite conditions in PruQ Δ <i>ap2IX-4</i> compared to parental PruQ parasites	98
Table 5: Differentially expressed genes (FC \geq 2) under tachyzoite conditions in PruQ Δ <i>ap2IX-4</i> compared to parental PruQ parasites	99
Table 6: Protein interactors of AP2IX-4 from yeast two-hybrid screen	105

LIST OF FIGURES

Figure 1: Common transmission routes of <i>T. gondii</i> in intermediate hosts	5
Figure 2: HXGPRT drug selection employs the biochemical basis of purine salvage in <i>T. gondii</i>	47
Figure 3: Final construct used to tag endogenous AP2IX-4 in RH Δ <i>ku80</i> with three tandem HA tags.....	58
Figure 4: Final construct used to delete AP2IX-4	59
Figure 5: Construct used to complement AP2IX-4 in Δ <i>ap2IX-4</i> parasites	60
Figure 6: Schematic of yeast two-hybrid concept	71
Figure 7: Amino acid sequence alignment of AP2 domain of AP2IX-4.....	77
Figure 8: Predicted secondary structures in the AP2IX-4 AP2 domain.....	78
Figure 9: Phylogenetic relationship of <i>T. gondii</i> AP2 domains.....	79
Figure 10: Generation of parasites expressing HA-tagged AP2IX-4.....	81
Figure 11: AP2IX-4 is localized to the parasite nucleus and expressed predominantly in the S and M phases.....	83
Figure 12: Generation of PruQ Δ <i>ap2IX-4</i> parasites.....	84
Figure 13: AP2IX-4 is dispensable for tachyzoite replication and viability	85
Figure 14: Complementation of the AP2IX-4 knockout.....	87
Figure 15: Expression of AP2IX-4 in Δ <i>ap2IX-4::AP2IX-4^{HA}</i> tachyzoites.....	88
Figure 16: Expression of AP2IX-4 in developing bradyzoites <i>in vitro</i>	90
Figure 17: Loss of AP2IX-4 results in lower frequency of bradyzoite cyst formation <i>in vitro</i>	91
Figure 18: Role of AP2IX-4 in acute and chronic infection in Balb/c mouse model	94
Figure 19: Expression of AP2IX-4 under constitutive tubulin promoter results in mis-expression.....	102

LIST OF ABBREVIATIONS

AP2	Apetela2
DMEM	Dulbecco's Modified Eagle Medium
bp	Base pairs
DAPI	4',6-diamidino-2-phenylindole
ddH ₂ O	Double-distilled H ₂ O
DHFR-TS	Dihydrofolate reductase-thymidylate synthase
DMSO	Dimethyl sulfoxide
GFP	Green fluorescent protein
FBS	Fetal bovine serum
HFF	Human foreskin fibroblast
HXGPRT	Hypoxanthine-xanthine-guanine phosphoribosyl transferase
IFA	Immunofluorescence assay
kDa	Kilodaltons
mg	Milligrams
mL	Milliliters
MPA	Mycophenolic acid
PBM	Protein binding microarray
PBS	Phosphate-buffered saline
uL	Microliters
WB	Western blot
XAN	Xanthine
Y2H	Yeast two-hybrid

CHAPTER 1: INTRODUCTION

Toxoplasma gondii is a prevalent and versatile pathogen. This obligate intracellular parasite infects up to a third of the world population, and in certain countries, the seroprevalence reaches as high as 80% (1). The transmission of this parasite is multi-route, and patient populations that suffer the potentially fatal disease caused by this parasite include HIV/AIDS patients, patients receiving immunosuppressive therapies, organ transplant recipients, and developing fetuses (2).

The role that bradyzoite tissue cysts play in the parasite's success cannot be understated. *T. gondii* is able to infect virtually any warm-blooded animal, and the tissue cysts play an important role in transmission between intermediate hosts as they are prevalent and found in a wide range of animals (2). In its host, these tissue cysts are able to remain latent, but when a loss of immune response occurs, such as in immunocompromised patients, this parasite is able to reactivate, rupture tissues, and disseminate systemically where it causes further damage (2). There are no FDA-approved therapies that can eradicate the tissue cysts.

Unfortunately, much of bradyzoite biology remains a mystery. At the basis of bradyzoite development is a cascade of gene expression changes; however, the key molecular players that direct this gene expression are unknown. The goal of this thesis is to characterize a putative transcription factor, AP2IX-4, whose transcript expression increases during bradyzoite development.

I. *T. gondii* converts between life cycle stages to propagate and transmit

A. Life cycle

T. gondii is an obligate intracellular protozoan parasite that converts between three stages in its life cycle: the sporozoite (contained within the oocyst), the tachyzoite (replicative stage inside host cells), and the bradyzoite (contained within the tissue cyst). The definitive host of the parasite in which it completes sexual replication is the cat (3). The sexual cycle in the cat produces oocysts that are shed from cat feces in oocysts. In intermediate hosts, which can be any warm-blooded animal (2), *T. gondii* differentiates between its two asexual stages, the tachyzoite and the bradyzoite (**Figure 1**).

Oocyst development begins in the intestinal epithelium of the cat (3). Cats acquire the parasite from ingesting oocysts in its environment or tissue cysts containing bradyzoites. Once in the cat, tissue cyst bradyzoites or oocyst sporozoites invade the feline gut and commence replication, undergoing an asexual replication phase followed by sexual replication (2, 3). The appearance of oocysts depends on the form of the parasite ingested; for example, oocysts are excreted in just a few days in cats fed tissue cysts, in about a week in cats fed intracellular or free tachyzoites, and 20-24 days in cats fed feces from an infected cat (3).

After feline ingestion of tissue cysts, stomach and small intestine proteolytic enzymes dissolve the cyst wall, releasing bradyzoites that invade

epithelium along the entire length of the feline intestine (4). Asexual stages appear as early as 12 hours post-ingestion and develop sequentially as five morphologically distinct types designated A through E (4, 5). Sexual stages appear subsequently 3-15 days post-ingestion, coinciding with the late asexual D and E stages (4). The mature male sexual stage, termed the microgamont, swims to and fertilizes macrogametes to form zygotes. The development of zygotes into the oocyst is accompanied by formation of a wall at the surface of the zygote. Oocysts are released into the intestinal lumen when the infected intestinal epithelium ruptures (5).

The number of oocysts a cat sheds following ingestion of bradyzoite cysts is in the millions, and intermediate hosts may acquire these oocysts through ingestion (6). Digestive enzymes of the intermediate host gastrointestinal tract rupture the oocyst wall, releasing the sporozoites within. These sporozoites transform into tachyzoites, which invade the small intestine, disseminating in the bloodstream to various tissues before converting into the bradyzoite cyst form (5, 7). Subsequently, the bradyzoite cysts remain latent. They may be further transmitted to other intermediate hosts through carnivorousism or can reactivate spontaneously to cause focal and systemic disease in human patients (2).

B. Transmission

A major reason behind the widespread prevalence of *T. gondii* is its ability to transmit through multiple routes. The parasite can be transmitted between its definitive host (the cat) to its intermediate hosts, which include any warm-blooded

animal, and vice versa (**Figure 1**). In addition, transmission occurs both horizontally and vertically in humans, who can contract any of the infectious forms of *T. gondii* (2):

- A. Oocysts distributed from cat excrement into the environment (2)
- B. Bradyzoite tissue cysts in uncooked, raw meat or animal viscera (2)
- C. Tachyzoites in organ transplants, blood products and unpasteurized dairy products (2)
- D. Tachyzoites transplacentally in the case of congenital toxoplasmosis (2)

Toxoplasmosis in the fetus can be contracted when a pregnant woman becomes infected with *T. gondii* as a primary infection (2, 8). Exactly how the parasite infects the developing fetus is unknown, although it's possible the parasite invades and replicates in the placenta (9). Congenital toxoplasmosis represents only a small percentage of all acquired *T. gondii* infections (2). Other patient populations include those receiving organ transplants and immunocompromised patients (10). Patients receiving heart, kidney, liver or bone marrow transplants may acquire both the bradyzoite and free tachyzoite form residing in the donor organ (11). In immunocompromised patients whose altered immune response fails to control the parasite, toxoplasmosis can arise from reactivation of latent tissue cysts acquired from a previous infection (10). Encephalitis and disseminated disease are common presentations for these patients (10). Immunocompromised patients may also contract severe disease from primary infection (10). The clinical presentation of the patient populations affected by severe *T. gondii* disease will be reviewed in a later section.

The major route by which healthy individuals acquire the parasite is through ingestion of oocysts or bradyzoite tissue cysts (2). Tissue cysts can be found in common livestock animals such as pigs, sheep and goat, and less frequently in poultry (13, 14). In consuming pork, lamb, poultry and other meats, humans can limit the risk of ingesting tissue cysts by thoroughly cooking their food (2).

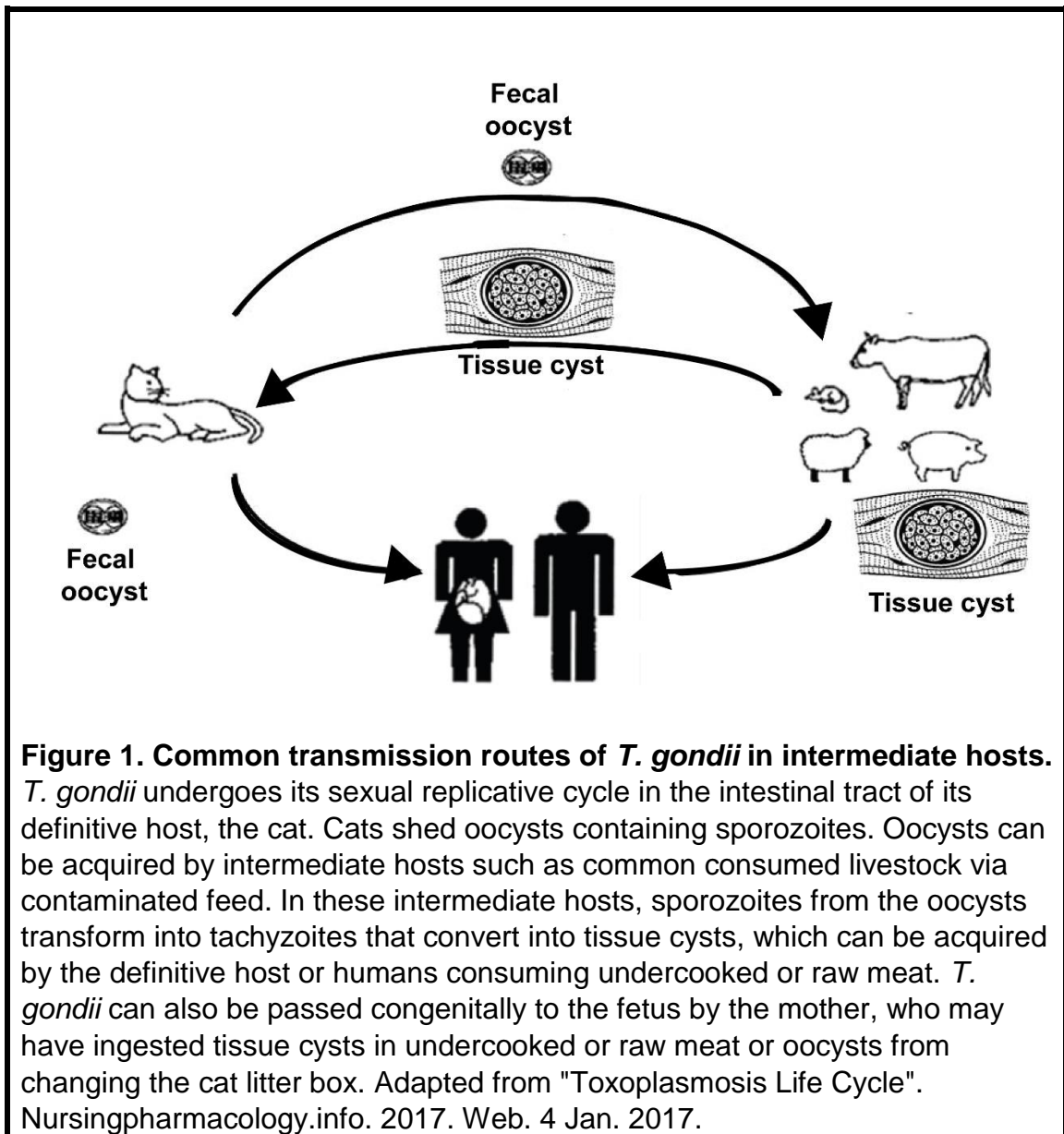


Figure 1. Common transmission routes of *T. gondii* in intermediate hosts. *T. gondii* undergoes its sexual replicative cycle in the intestinal tract of its definitive host, the cat. Cats shed oocysts containing sporozoites. Oocysts can be acquired by intermediate hosts such as common consumed livestock via contaminated feed. In these intermediate hosts, sporozoites from the oocysts transform into tachyzoites that convert into tissue cysts, which can be acquired by the definitive host or humans consuming undercooked or raw meat. *T. gondii* can also be passed congenitally to the fetus by the mother, who may have ingested tissue cysts in undercooked or raw meat or oocysts from changing the cat litter box. Adapted from "Toxoplasmosis Life Cycle". Nursingpharmacology.info. 2017. Web. 4 Jan. 2017.

C. The host immune response

Innate and adaptive immunity overview

Most studies of the *T. gondii*-host immune interaction have been performed in mice. However, studies employing human cell lines or patient data suggest that parallels exist between mice and human models of the immune response to *T. gondii*. First, in both mice and humans, IFN- γ has been shown to be a major lymphokine in the killing of the parasite (15-17). IFN- γ was shown to be the component from lymphoid supernatant collected from human macrophages stimulated with *T. gondii* antigen (18). This fraction enhanced human macrophage ability to secrete H₂O₂ and to kill *T. gondii* tachyzoites, and both H₂O₂ secretion and toxicidal activity was abolished by anti-IFN- γ (18). Consistent with these findings showing the essential role of IFN- γ in macrophage antimicrobial ability, macrophages isolated from AIDS patients stimulated with lymphokine fractions containing IFN- γ secreted H₂O₂ and inhibited *T. gondii* replication, and these effects were again abolished by treatment with IFN- γ antibody (19).

In mice, immune control of acute *T. gondii* infection employs the IL-12/IFN- γ axis. It was shown that in IFN- γ knockout mice, survival was significantly reduced, however IL-12 production was not (20). However, inhibition of IL-12 with anti-IL-12 ablated the ability of natural killer cells to produce IFN- γ (21). Injection of IL-12 into mice in early acute infection enhanced mice survival (22). Together, these results suggest that IL-12 precedes and initiates IFN- γ production. In response to *T. gondii* antigen, human innate immune cells

such as neutrophils and dendritic cells also release IL-12, although the specific subsets of dendritic cells that release IL-12 upon parasite exposure differ from mice (23).

Much remains unknown about how human immune cells recognize *T. gondii*. In mice, a fraction from a *T. gondii* lysate that induced IL-12 release from dendritic cells was further separated, resulting in the identification of profilin, a protein involved in actin reorganization during parasite invasion of host cells (24). Mice lacking toll-like receptor (TLR) 11 or 12 failed to induce IL-12 release in response to profilin stimulation, suggesting that *T. gondii* recognition relies on TLR11 and TLR12 (25-27). However, the gene for TLR11 in humans does not encode a functional protein and TLR12 is entirely absent in the human genome (28). In addition, heat-killed tachyzoites failed to elicit cytokine release from human monocytes and dendritic cells (29). Therefore, while the detailed mechanisms of how human immune cells recognize *T. gondii* are unknown, they most likely occur independently of TLR11/TLR12/profilin system and involve live tachyzoites (30).

Both humoral and cellular immunity play important roles in the immune reaction against *T. gondii*, and cellular immunity involves both CD4+ and CD8+ T-cells (31, 32). Human CD4+ and CD8+ cytotoxic T-cells were isolated from a patient chronically infected with *T. gondii*, and both T-cell populations exhibit cytotoxicity to *T. gondii*-infected cells (33). *T. gondii*-infected antigen presenting cells elicited proliferation of human CD4+ cells as well as generation of specific CD8+ memory cells (34). Compared with the role of CD8+ cells, the role of CD4+

may be mostly supplemental and synergistic, as treatment of mice with anti-CD4+ caused no significant changes in mortality or reactivation (32, 35-37).

Immune inducers of bradyzoite conversion

The release of nitric oxide, stimulated by IFN- γ signaling, is critical for reducing parasite replication and inducing the expression of bradyzoite antigens (38, 39). The role of nitric oxide in bradyzoite conversion supersedes that of IFN- γ as nitric oxide is sufficient to induce the conversion, while culturing of certain cell types with IFN- γ fails to induce bradyzoite antigen expression (39-41). However, IFN- γ is required for maintaining parasite latency, as inhibition of IFN- γ with antibody to this lymphokine results in reactivation of cysts and development of toxoplasmic encephalitis (42).

D. Toxoplasmosis

Healthy adults

Immunocompetent adults who are able to produce normal immune responses to *T. gondii* are usually asymptomatic (43). About 10-20% of acutely infected adults will develop flu-like symptoms, including muscle aches and pains and swollen lymph nodes; these symptoms can resolve without treatment within weeks to months (43, 44). The incubation period after consumption of meat contaminated with tissue cysts is 10 to 23 days and 5 to 20 days after exposure to oocysts (45).

T. gondii is one of the most common causes of posterior inflammation of the uvea in immunocompetent hosts. Acute *T. gondii* infection in the eyes of

immunocompetent adults may manifest as inflammation of the retina at one focus with subsequent involvement of the choroid (46). Eye involvement is usually unilateral (46). On clinical inspection, the eye presents an area of focal retinal necrosis adjacent a choroidal scar (47).

Congenital toxoplasmosis

For the United States, it is estimated that about 400-4,000 cases of congenital toxoplasmosis occur annually (48). Congenital toxoplasmosis occurs when the parasite crosses the placenta to the developing fetus. Prior infection resulting in congenital toxoplasmosis usually occurs in the case of immune-compromised women such as HIV patients (8). Otherwise, infection of the fetus generally only occurs when a woman contracts a primary infection during gestation (8). The pregnant woman can contract toxoplasmosis through ingesting raw or undercooked meat or in handling cat excrement (such as through changing the cat litter box) (49). The infection is usually asymptomatic for the woman during pregnancy but can cause miscarriage, stillbirth, or severe symptoms in the newborn (8, 50). Around 30% of women transmit primary-acquired toxoplasmosis to their fetus. The risk of transmission is lowest during the first trimester of pregnancy, with a rate of 10-15%. The rate of vertical transmission in the second trimester is 25% and is highest during the third trimester, at a rate of 60-90% (51). Disease severity in the fetus correlates with earlier infection (52).

The majority of infants with congenital toxoplasmosis will present with eye disease, brain calcifications, and hydrocephalus; 61% of patients presenting

concurrently with all three signs (53). Other signs the newborn may present with include epilepsy and developmental delays (53). Some infants are asymptomatic at birth, but develop neurological deficits or developmental disabilities later in life (54).

Acute toxoplasmosis infection might be suspected in a pregnant woman if she is immune-compromised or if ultrasound demonstrates findings such as hydrocephalus, intracranial calcifications or fetal development abnormalities. Diagnosis of acute infection in the woman is based on *T. gondii* IgG and IgM antibody titers (54, 55). Elevated IgG antibody levels indicate that infection by *T. gondii* had occurred in the past, although the exact time of occurrence is unknown (56, 57). Elevated IgM antibody levels indicate acute infection (57). Because diagnosis of acute toxoplasmosis in a pregnant woman will influence pregnancy treatment and even termination decisions, extra care is given to validate diagnosis results. Unfortunately, IgM antibody tests are complicated by false positives; therefore, specific blood re-testing and antibody avidity test guidelines are given to pinpoint diagnosis (58). If a pregnant woman is found to be infected with *T. gondii* during her pregnancy, her fetus will then be tested for infection as well. This is accomplished through PCR analysis of amniotic fluid (59).

If a pregnant woman is diagnosed with acute toxoplasmosis, efforts will be taken to prevent transmission to the fetus and the patient may be treated with spiramycin (56). Fetal toxoplasmosis is treated by switching the woman to pyrimethamine and sulfadiazine after the first trimester (56). To protect against

bone marrow suppression, one of the side effects of pyrimethamine, folinic acid is added to the therapeutic regimen (56).

Toxoplasmosis in the immunocompromised

Severe toxoplasmosis can also occur in humans with compromised immune systems. These include patients with HIV/AIDS, hematologic cancers, and organ transplant patients receiving immunosuppressive agents. Disease initiates from reactivation of latent tissue cysts from prior infection, however primary infection may also cause devastating disease in the immunocompromised (2, 10). For seropositive AIDS patients who have CD4+ T cell count of less than 100 cells/uL, the rate of reactivation can be up to 30% (60). Most commonly, infected patients exhibit symptoms such as headaches, seizures, ocular inflammation, and focal neurological defects (10). On autopsy, “space-occupying lesions” and abscesses in the brain are often found (10). The parasite also commonly targets the lung and the heart, causing pneumonitis and myocarditis (61). Left unrecognized or untreated, the infection is usually fatal (61).

Treatment consists of an initial therapy to limit the acute infection, then secondary therapy to prevent against recurrence (62). The therapies consist of sulfadiazine and pyrimethamine to target the parasite, with lower dosages administered for the secondary therapy (62). Folinic acid is added to guard against pyrimethamine-induced bone marrow suppression (63). Prophylactic therapy is necessary for as long as the patient is immune-compromised, because the drugs do not target the latent tissue cysts, which may reactivate (62).

Toxoplasmosis in organ transplant patients

Toxoplasmosis may affect patients receiving either solid organ transplants or hematopoietic stem cell transplants (11). In solid organ transplant recipients, disease usually results from transmission of the tissue cysts through the donor organ and reactivation of these cysts in the recipient who is receiving immunosuppressive therapy, while in hematopoietic stem cell patients, the cause of toxoplasmosis is usually from reactivation of a pre-existing, latent infection in the recipient (11). The major clinical signs associated with transplant toxoplasmosis include pneumonitis and encephalitis, often with dissemination to multiple organ systems (11).

Diagnosis of toxoplasmosis by serology is often difficult in organ transplant patients who usually present with an altered immune status. Diagnosis therefore relies on confirming the presence of the parasite such as through PCR analysis or microscopic examination of bone marrow aspirates, bronchoalveolar lavage, and tissue biopsies (64).

For hematopoietic stem cell recipients who are seropositive for antibodies to *T. gondii* or for seronegative solid organ recipients receiving from a seropositive donor, prophylaxis before the transplant procedure is recommended to guard against reactivation disease (64). In this case, co-trimoxazole is the preferred therapy in the United States (64).

Current drug therapeutics for *T. gondii*

The first-line drug therapy for patients with *T. gondii* infection (including women with acute *T. gondii* infection, infants with congenital toxoplasmosis,

AIDS and other immune-compromised patients who develop toxoplasmic encephalitis, or patients with ocular toxoplasmosis) is pyrimethamine and sulfadiazine (65). Leucovorin is usually added to the therapy regimen because it protects against bone marrow suppression (65). Clindamycin may be substituted for sulfadiazine if the patient is allergic to sulfa drugs, and the pyrimethamine plus clindamycin regimen has been shown to be equally efficacious as pyrimethamine plus sulfadiazine for AIDS patients with toxoplasmic encephalitis (65, 66). The trimethoprim-sulfamethoxide combination can be used if pyrimethamine is not available and if patients do not have allergies to sulfamethoxide, another sulfa drug; no differences in clinical response to either drug combination was detected in HIV patients with toxoplasmic encephalitis (67).

Pyrimethamine, sulfadiazine, trimethoprim, and sulfamethoxazole are compounds that act on separate steps in the folic acid metabolism pathway (68). Sulfadiazine and sulfamethoxazole are competitive inhibitors of dihydropterate synthetase, and pyrimethamine and trimethoprim inhibit dihydrofolate reductase (68-70). Clindamycin has been demonstrated to reduce protein synthesis and inhibit parasite replication at low concentrations in mouse macrophage cultures, with 50% inhibitory concentration of 32.50ug/mL (71). Leucovorin, used to rescue bone marrow suppression, is a reduced form of folic acid that can be converted into tetrahydrofolate without DHFR, thus bypassing the blockage of tetrahydrofolate synthesis during pyrimethamine inhibition of dihydrofolate reductase (69).

E. Genetic lineages of *T. gondii* and toxoplasmosis

Strain isolates of the parasite from Europe or the USA group into three main lineages based on genotype analysis (72). However, genotypes not belonging to the three main lineages exist and appear to be attributed to higher genetic variations and recombination among these parasite groups, which are found outside Europe and North America such as in Africa and South America (73, 74). The three main lineages that are predominant isolates from Europe or the USA are designated Type I, II and III and were classified based on restriction fragment length polymorphism (RFLP) analysis of six different *T. gondii* genetic loci (75). The analysis also revealed that these lineages are $\geq 95\%$ similar, suggesting clonal population structure and an absence of random mating (75). Despite this degree of genetic similarity, the three lineages differ in their epidemiological prevalence in human toxoplasmosis and also exhibit clear phenotypic differences when studied in mice models of acute and chronic infection (75-78). Of clinical importance, type II isolates were found to predominate human toxoplasmosis. Type III strains are common in animals and significantly less observed in human disease cases (75). An assay consisting of PCR amplification followed by RFLP of the SAG2 locus was subsequently developed and used to classify parasite samples isolated from toxoplasmosis patients (77). The SAG2 assay revealed that 81% of strains isolated from patient samples were grouped as type II, further buffering the observation that the majority of human disease is caused by type II strains of *T. gondii* (77).

In mice models of acute infection, the three lineages segregate strongly into virulent and non-virulent strains (75-78). The distinction for virulence is based on 100% lethal dosage in outbred Swiss mice, with “virulent” strains exhibiting $LD_{100} < 10$ and “non-virulent” strains exhibiting $LD_{100} > 1000$ (78). Type I strains (i.e. RH, GT1, OH3, PT, and ENT isolates) which are highly virulent lead to systemic dissemination and death of mice within ten days in mice following inoculation of less than ten parasites (78, 79). Type II (ME49, Prugniaud) strains exhibit intermediate virulence compared to the low virulence of type III strains like VEG (78). The genetic loci responsible for the virulence differences between the three lineages is a topic of intense interest, with new “virulence factors” revealed through forward and reverse genetic approaches through the years (80, 81). These mediators of acute virulence appear to modulate the host immune response (81).

Differences in strain virulence can be mapped to genetic variation in *SAG1* alleles (78, 82). Comparison of the lengths of restriction digest fragments of *SAG1* revealed specific patterns to mouse-virulent versus mouse-avirulent strains (78). Subsequent analyses of *SAG1* revealed seven nucleotide mismatches between mouse-virulent and mouse-avirulent strains occurring in the 322-bp region upstream of the AUG start codon (82). In addition, mouse-avirulent strains lacked one stretch of 27-bp repeats found in the this upstream region, such that mouse-virulent strain contained five of these repeats compared to four in the mouse-avirulent strain (82). Finally, transcript expression of *SAG1* was at least four-fold higher in the mouse-virulent strain (82). These results suggested

that SAG1 is a factor contributing to virulence differences between the three prominent *T. gondii* lineages (78, 82).

Besides virulence, other traits such as tissue cyst-forming rate, host mitochondria association, and gene expression differ between strains. Strains exhibiting lower virulence in mice produce higher numbers of cysts compared to the higher virulence strains (83, 84). There is a correlation between the strain replication rate and its cystogenic rate; for example, Type II and Type III strains exhibit lower replication rates and form higher numbers of cysts (85).

Host mitochondria association (HMA) has been observed in organisms besides *T. gondii*, such as in *L. pneumophila* and *C. psittacci* (86, 87). The functional consequences of HMA in these organisms is not understood, but pathogens such as hepatitis C virus and *H. pylori* manipulate host mitochondria to induce specific immune responses or cellular apoptosis (88, 89). Examination for HMA using Mitotracker in human foreskin fibroblasts (HFFs) infected with either Type I RH, Type II ME49 or Type III CEP strains revealed that while association of host mitochondria at the parasitophorous vacuole membranes (PVMs) of RH and CEP strains was observed, this was not the case for ME49 (90). The experiment was repeated with Type II Pru strains, which also demonstrated absence of HMA as well as significantly lower expression of the gene *MAF1* discovered to mediate HMA (90). The exact reason for this strain-specific difference is currently unknown. Since it has been shown that host mitochondria-pathogen interaction can modulate immune signaling in some host-pathogen systems, and since there are strain-specific differences in cytokine

release, the role of *T. gondii* HMA in immune signaling is possible (91, 92).

Together, these observations provide examples of strain-specific phenotypes which can possibly impact the pathogen-host interaction.

Type II and Type III strains exhibit higher efficiency tissue cyst formation *in vitro* and *in vivo* (83-85). This observation has been correlated with the hypovirulence of these strains compared to Type I, their lower replication rates, and specific gene expression patterns in these strains (83-85, 93). Differences in the specificity and expression levels of genes between Type I, Type II, and Type III parasites were implicated in a comparison of SAGE tag libraries from Type I RH, Type II ME49 and Type III VEGmsj parasites (93). The identity and expression levels of genes between each strain as compared to libraries from different timepoints of the sporozoite-to-bradyzoite development pathway (93). The Type I RH library was most similar to Day-6 post-sporozoite infection parasites, which have emerged from sporozoite-infected cells, re-invaded and are rapidly replicating. In contrast, the Type II and Type III libraries exhibited basal levels of bradyzoite markers such as ENO1 and Sag4.2, which are not detected in the Type I RH library (93). While the basal bradyzoite expression may be a result of a subpopulation of differentiated Type II and Type III parasites, these results are consistent with the observation that Type II and Type III strains are more efficient at bradyzoite differentiation (83-85). Consistent with these findings, Saeij et. al found an apparent inverse relationship between strain virulence and bradyzoite gene expression when examining the gene expression

and growth rate of an avirulent and virulent progenitor from a Type II and Type III cross (94).

II. The bradyzoite is important to transmission and pathogenesis

A. Structural morphology of bradyzoite cysts

Bradyzoites are contained in the host cell inside a modified parasitophorous vacuole, which is bound by the parasitophorous vacuole membrane (PVM) derived from the plasma membrane of the host (83). Early electron microscopy of a type II *T. gondii* strain revealed that cyst wall material is deposited gradually at the membrane, with early cysts showing patchy aggregation and mature cysts showing a continuous thick wall (83). Specifically, the cyst wall material is a “dense granular precipitate” found scattered between bradyzoites, leading the authors to believe the granular matrix is parasite-secreted (83). The composition of the cyst wall is now believed to contain both parasite-derived and host-derived components. Staining of the cyst wall with protargol silver, in a protocol used to detect neuronal-specific elements, suggested that the walls of neuronal cysts are composed in part of host cell constituents (95).

Studies on the composition of the cyst wall suggest that this structure is composed of specific polysaccharides and glycosylated proteins. The walls stain with specific lectins, carbohydrate-binding proteins derived from plants. In one study, only two lectins out of twelve tested were able to bind the bradyzoite cyst

wall (96). These were succinylated wheat germ agglutinin (S-WGA), which binds N-acetyl-glucosamine (GlcNac)-like residues, and *Dolichos biflorus* lectin (DBA), which binds N-acetyl-galactosamine (96). *Dolichos* lectin remains one of the most common tools to stain cyst walls for the field.

The bradyzoite cyst wall also binds Concanavalin A (Con A), a lectin that specifically binds D-mannose or D-glucose-like residues and soy bean agglutinin (SBA), which binds N-acetyl-galactosamine-like residues (97). In addition, the composition of the cyst wall may be similar to chitin, a major cell wall component in yeast. GlcNac polymers are a constituent of chitin, a yeast cell wall protein, and treatment with chitinase disrupted both the integrity of the cyst wall and S-WGA binding (97).

The protein CST1 is a major constituent of the bradyzoite cyst wall. Electron micrographs show that this protein is localized to the PVM (98). CST1 is responsible for the majority of *Dolichos biflorus* lectin binding, as immunoblotting of a 2D gel with CST1 with DBA resulted in a detectable single band at 116 kDa, the size of CST1. Knocking out CST1 resulted in near-complete loss of DBA binding (99). CST1 was not essential for cyst formation, but is important for structural integrity of the cyst wall as its deletion resulted in fragile cysts that ruptured easily (99).

In addition to CST1, the cyst wall is composed of proteins released by secretory organelles called dense granules (100, 101). These dense granule or “GRA” proteins include nearly the entire repertoire as that found for tachyzoites (100, 101) and localize to the parasitophorous vacuole. However, the sizes of

these proteins may differ between stages, possibly due to modifications such as glycosylation. In support of the possibility that the same protein product is differentially modified between the stages, a monoclonal rat antibody recognizes a 40kDa antigen in the tachyzoite stage and a 115 kDa antigen in the bradyzoite stage (102).

The importance of secreted proteins in forming the bradyzoite cyst wall prompted screens for proteins secreted during the bradyzoite stage. A list of genes that are differentially expressed between the tachyzoite and bradyzoite stage was obtained from transcriptomic analysis of the M4 Type II strain. This list was then narrowed to those with putative signal peptides (103). Two genes – bradyzoite pseudokinase 1 and microneme-adhesive repeat containing protein 4 (MCP) – were tested and confirmed for their localization at the PVM (103). While the specific function and localization of the majority of these putative secreted proteins is unknown, the screen expands the catalogue of potential cyst wall constituents.

B. Inducers and molecular changes of bradyzoite differentiation

Tachyzoites convert to bradyzoites in a process called bradyzoite differentiation. While immune modulators such as IFN- γ and IL-12 induce this process, *in vitro* methods are able to induce the expression of tissue cyst markers. In 1994, Soete et al. identified several *in vitro* conditions that induce the expression of bradyzoite antigens (104). The authors subjected RH tachyzoites to several stress conditions, including alkaline pH, incubation at high

temperatures (43°C), sodium arsenite (a chemical stress inducer) and IFN- γ (104). In their experiments, with exception of IFN- γ , all of these stress conditions were effective at inducing bradyzoite antigen expression (104). Alkaline pH (pH 8.0-8.2) remains one of the most convenient and effective *in vitro* inducers of bradyzoite differentiation for the field. Induction of bradyzoite-specific antigens is also triggered by application of sodium nitroprusside to parasite cultures; sodium nitroprusside acts as an exogenous source of nitric oxide (38). The mechanism of nitric oxide is supposedly binding to iron-sulfur clusters in mitochondrial electron transport chain proteins, inhibiting their function (38). Other drugs that interfere with mitochondria function, such as olivomycin A and atovaquone, also trigger bradyzoite differentiation (38, 105).

As discussed earlier, the relative frequency of differentiation depends on the *T. gondii* strain, where slower-replicating and lower virulent strains such as ME49 exhibit a higher differentiation frequency compared to fast-replicating virulent strains such as RH (83-85, 104, 106). These observations are consistent with those demonstrating a longer G1/S cell cycle length for slower-replicating strains and that a decrease in growth rate precedes bradyzoite differentiation (38, 107, 108). In summary, bradyzoite differentiation is accompanied by a decrease in parasite replication rate.

Bradyzoite development and relationship to the tachyzoite cell cycle

Initiation of bradyzoite development is accompanied by reduced parasite replication (38). This is observed in treatment of tachyzoites with all the classic *in vitro* bradyzoite inducers, including alkaline pH, nitric oxide, and mitochondrial

inhibitors. Molecular dynamics of the cell cycle are clearly important for bradyzoite development, as cell cycle arrest precludes bradyzoite differentiation (107). Furthermore, analysis of differentiating parasite populations reveals an enrichment for parasites in the S/M phase of the tachyzoite cell cycle. For example, an increase in the number of parasites with 1.8-2N amount of nuclear DNA accompanies the appearance of BAG1 antigen in alkaline-treated parasites, concomitant with a decrease in parasites in the M/C phase (108). Furthermore, the population of parasites containing the 1.8-2N amount of DNA is both positive for SAG1 and BAG1, suggesting parasites at the onset of the tachyzoite-to-bradyzoite transition (108). Supporting the view that the S/M boundary is important for the commitment to bradyzoite differentiation, peak expression of bradyzoite transcripts during the tachyzoite cell cycle occurs at this phase boundary (109). Therefore, although the molecular events are not clearly understood, it is evident that bradyzoite differentiation is associated with the S/M phase of the tachyzoite cell cycle. To fully understand how the tachyzoite cell cycle and bradyzoite development are linked, the function and mechanism of cell cycle-regulated molecular players involved in bradyzoite differentiation should be identified. Of interest are those transcriptional factors with peak expression around the S/M boundary, which possibly play a role in the commitment to bradyzoite differentiation.

Upregulation of stress responses

In response to stress such as high pH, *T. gondii* launches a common environmental stress response (ESR) characterized by upregulation of genes

involved in detoxification, metabolism (ie. glycogen and trehalose synthesis), protein folding and degradation, and oxidative protection and mitochondrial function (110). Specifically to alkaline pH, *T. gondii* also upregulates PHO84, a member of the phosphate transport and metabolism family that is upregulated in yeast as a response to alkaline stress.

Through the years, a number of “bradyzoite-specific” genes have been characterized for their function in stress response. Screening of a bradyzoite expression library with bradyzoite-specific monoclonal antibody mAB 7E5 identified a ~30 kDa protein that shared homology with plant small heat shock proteins (111). This protein is now annotated as HSP30 or BAG1 (111). BAG1 polyclonal antiserum reacted only to bradyzoite but not to tachyzoite lysate, suggesting that this protein is bradyzoite-specific (111). As a bradyzoite-specific antigen, BAG1 remains an important marker of differentiation for the field. BAG1 is induced by day three of bradyzoite induction and is localized to the bradyzoite cytoplasm (111). Another heat shock protein, DnaK-TPR, is also bradyzoite-specific, and yeast-two hybrid screening revealed this protein interacted with a co-chaperone protein, suggesting a role for this protein as a molecular chaperone (112).

In both higher eukaryotes and in yeast, stress conditions result in the phosphorylation of serine 51 of eIF2 α , which then inhibits its guanine nucleotide exchange factor eIF2B (113). This precludes the methionine-tRNA charging ability of eIF2A, leading to a global decrease in translation. A protein homologue of eIF2 α was cloned in *T. gondii* and demonstrated to be phosphorylated at

serine 51 under different bradyzoite-induction conditions, including heat shock, alkaline pH, tunicamycin and sodium arsenite (114, 115). TgIF2 α phosphorylation was accompanied with a global decrease in translation initiation in parasites treated with tunicamycin (115). Bradyzoites exhibit significantly higher levels of TgIF2 α phosphorylation compared to unstressed tachyzoites (115). Furthermore, inhibition of dephosphorylation by treating parasites with salubrinal resulted in induction of bradyzoite genes (115). These observations suggest that translational control plays an important role in bradyzoite differentiation, which is accompanied by a global reduction of protein translation. As in higher eukaryotes where different eIF2 α kinases phosphorylate eIF2 α under different stress conditions, separate eIF2 α kinases have been cloned in *T. gondii* (114). TgIF2K-A localizes to the *T. gondii* endoplasmic reticulum while TgIF2K-B localizes in the cytosol (114). Therefore, the translational reduction conserved in higher and lower eukaryotes under stress conditions also accompany bradyzoite development.

C. Gene expression changes accompanying bradyzoite development

A number of transcriptome approaches have been undertaken to understand the gene expression changes accompanying bradyzoite development. One of the earliest explorations into the bradyzoite transcriptome utilized sequencing a library of expression sequence tags (ESTs) generated from ME49 bradyzoite cysts in chronically infected mice (116). Comparison of the bradyzoite cDNA sequences to a parallel tachyzoite library identified a set of

genes restricted to the bradyzoite stage. However, this EST sequencing approach had limitations since it did not measure transcript abundance or timing of expression. To solve this problem, Cleary et al. constructed microarrays, using DNA derived from the bradyzoite EST library for spotting the arrays (117). This approach identified developmentally regulated genes that were either induced or repressed in bradyzoites compared to tachyzoites. Comparison of transcript levels from two-, three- and four-day *in vitro* bradyzoite to tachyzoite cultures allowed identification of those bradyzoite transcripts that were “induced, constitutive, or repressed” relative to tachyzoite transcripts (117). Novel developmentally regulated genes such as SRS9 (induced in the bradyzoite) and rhoptry protein 1 and 4 (repressed) were also revealed (117).

Finally, it was evident that induction of bradyzoite transcripts occurs in a temporal fashion (117, 118). For example, BAG1 and enolase 1 (ENO1) were classified as “mid-late” genes as their transcripts expression relative to that in tachyzoites did not peak until day four post bradyzoite-induction (117). In contrast, other genes such as lactose dehydrogenase 2 (LDH2) were expressed from day two through day four of the experiment, suggesting that LDH2 expression may be induced as early as day two post-induction (117).

Gene expression changes accompanying the tachyzoite-to-bradyzoite conversion were further assessed in 2005 by Benhke et al. (119). In addition to demonstrating the existence of developmentally regulated genes, this study demonstrated that these genes are regulated in cohorts (119). In other words, transcripts are expressed through the cell cycle with a “just-in-time” control.

Clearly, a mechanism exists that allows for both specific and temporal timing of gene expression in parasite replication and development.

In part, gene expression changes accompanying stage conversion can be explained by the dynamic nature of chromatin remodeling and association of epigenetic complexes. In the *T. gondii* genome, the players for epigenetic modulation are readily present and include histone acetyltransferases (HATs) from the GCN5 and MYST families (120, 121), histone deacetylases (HDACs) and histone arginine methyltransferase (122) and chromatin remodeling complexes such as those from the SWI/SNF family (123). Furthermore, epigenetic marks follow stage-specificity. The tachyzoite stage is marked by hyper-acetylation at tachyzoite-specific genes such as SAG1 and SAG2A and a hypo-acetylation at bradyzoite-specific genes such as BAG1 and LDH2 (122). In the bradyzoite stage, these acetylation patterns are reversed, with a hyper-acetylation of promoters at BAG1 and LDH2 and hypo-acetylation of promoters at the tachyzoite-specific genes.

D. *T. gondii* cis-regulatory elements

In other species, gene expression is modulated by transcription factors that bind to specific motifs called *cis*-regulatory elements upstream of the coding sequence. Stage-specific *cis*-regulatory elements have been shown to exist in *T. gondii*. Promoter mapping experiments have been undertaken for the purpose of expression control in transgenic parasites, understanding developmental switches, and understanding basic *cis*-regulatory sequences controlling

transcription. Promoter truncation demonstrated that the motifs essential for SAG1 expression consist of six 27 bp repeats with no requirement on their orientation and dictate the location of the transcriptional start site. In addition, these repeats were sufficient to induce expression from a heterologous promoter (124). Truncation mutations with the 5' regions of the NTP 1, 2 and 3 genes identified the approximate upstream bp region necessary for expression (125). In addition, deletion of a segment of the NTP3 5' region altered downregulation in the bradyzoite stage, suggesting transcriptional elements regulate stage expression for NTP3 (125). Both SAG1 and NTP upstream lacked a canonical TATA box; with NTP3 it was shown an initiator-element (Inr) consensus was necessary for basal expression (125). The pH 8-inducible expression of hsp70 has been mapped to a 70bp region which was shown to be sufficient for increased pH 8 induction using GFP reporter construct (126). This 70bp cis-regulatory element was the first to be shown to be able to bind with a protein in a *T. gondii* lysate, assumed to be a putative transcription factor (126). Interestingly, homologies to the 70bp region was not found for hsp60 and hsp90, suggesting unique promoter motifs exist for bradyzoite-specific gene expression (126). The promoter mapping for dihydrofolate thymidylate synthase emphasized the importance of GC-rich regions upstream of the transcriptional start site (127). Such GC-rich regions were also found in the BAG1 promoter.

First, the 324 base pairs immediately upstream of the BAG1 initiation codon were demonstrated to be essential for induction of expression (128). Another study further fine-mapped the promoter region for BAG1 to the

nucleotide motif TACTGG required for expression (129). Fine-mapping was also accomplished for the bradyzoite NTPase gene (129). The promoter elements were sufficient to induce the expression of bradyzoite genes under both Compound 1 and alkaline pH, suggesting that bradyzoite expression is activated through common promoter sequences (129). Finally, nuclear extracts applied to electromobility shift assays, using the minimal genomic elements required to induce bradyzoite gene expression, demonstrated that unspecified nuclear factors indeed bind specific promoter motifs (129).

Therefore in these studies, the upstream sequences of bradyzoite-specific genes that contain *cis*-regulatory sequences were shown to be 1.) necessary and sufficient for bradyzoite gene transcription, 2.) able to activate gene expression under a variety of bradyzoite induction conditions and 3.) bound by nuclear factors. However, the identity of these nuclear factors remained unknown.

Moreover, the study of the *SAG2CDXY* promoter demonstrates the importance of *cis*-regulatory sequences in regulating the time course of *in vivo* infection. The *SAG2CDXY* locus is a cluster of genes encoding bradyzoite-specific surface markers (130). Tachyzoites containing a truncation of the *SAG2CD* promoter fused to firefly luciferase exhibited bioluminescence levels comparable to that in bradyzoites, suggesting that the truncated promoter portion may repress the expression of the gene in the tachyzoite stage (130). In addition, mice infected with parasites expressing firefly luciferase under the full *SAG2D* promoter exhibited signal starting at day 9 post-infection (130). These studies with the *SAG2CD* promoter demonstrated both a temporal regulation of

bradyzoite gene expression and stage-specific control of these genes by possible repression in the tachyzoite stage. The *in vivo* switch of tachyzoites to bradyzoites is the first step to establishing chronic infection; identification of temporally-regulated specific transcription factors will help illuminate the mechanism by which stage-specific gene expression occurs.

III. The ApiAP2s represent a primary lineage of putative transcription factors

A. Discovery of the ApiAP2s

Transcription in both prokaryotes and eukaryotes utilize three basic classes of machinery: RNA polymerase II, general transcription factors and specific transcription factors. Basal transcription begins with formation of the preinitiation complex consisting of RNA polymerase II and general transcription factors (TFIIA, TFIIB, TFIID, TFIIIE, TFIIIF, and TFIIH) that bind core promoters proximal to the transcription initiation site (131-133). Enhancement or repression of basal transcription occurs via binding of specific transcription factors to cis-regulatory elements upstream or downstream of the core promoter (133, 134). Once a specific transcription factor binds to its regulatory motif, it may recruit the preinitiation complex via its transactivation domain or epigenetic machinery such as chromatin remodeling enzymes, histone acetyltransferases or deacetylases. The specific transcription factor can also modulate basal gene expression by

blocking the assembly of the preinitiation complex or activator specific transcription factors or blocking the recruitment of HATs (135).

Based on homology, all three RNA polymerases have been identified in the *T. gondii* genome (136). All twelve subunits of RNA polymerase II, whose main role is mRNA transcription, are present (134). Various components of the general transcription factors have been located in the *T. gondii* genome, including some but not all subunits of TFIID, TFIIE, TFIIIF and TFIIH. TFIIA is missing entirely along with most of the TATA-box protein-associating factors (136). This suggests that basal *T. gondii* transcription shares certain mechanistic features with higher eukaryotes yet exhibits unique features as demonstrated by its simplified or yet unidentified repertoire of general transcription machinery.

An evolutionarily expanded group of specific transcription factors populates the genome of eukaryotes. Major classes are grouped by their structure and include the helix-turn-helix class of specific transcription factors, consisting of two α -helices connected by a short loop and includes the homeodomain and forkhead proteins; the zinc finger factors which is further subdivided based on fold groups but are united by coordination of a zinc ion within their folds; the basic zipper proteins; and the helical domain proteins which include the bZip and basic helix-loop-helix proteins (137). The *T. gondii* genome contains putative DNA-binding proteins belonging to various classes of major eukaryotic transcription factors, such as members of the MYB, C2H2 zinc finger, HMG1, and AT-hook proteins (138). However, compared to higher eukaryotes, expansion of these classes of transcription factors is not observed; animals for

example contain more than 100 members of the C2H2 zinc finger factors compared to less than ten as annotated in the *T. gondii* ME49 genome (ToxoDB.org). In addition, Apicomplexan genomes reveal a complete lack of other members of the major transcription factor classes such as the forkhead, basic helix-loop-helix, homeodomain, STAT, retinoblastoma, MADS-domain and CENPB proteins (138). This called into question the identity of the primary lineage of specific transcription factors for *T. gondii*.

Therefore, Balaji et al. in 2005 explored the possibility that the predominant specific transcription factors of Apicomplexa were distantly related or even unrelated to conserved eukaryotic specific transcription factors. Searching for predicted proteins with DNA domains and motifs in the Apicomplexan *Plasmodium*, they focused on a DNA-binding motif called the AT-hook, which is found in a number of chromosomal proteins (139). Importantly, the AT-hook is often associated with larger globular DNA-binding domains. Indeed, the AT-hook containing protein also contained a domain which BLAST searches revealed to belong to the *apetela2* (AP2) class of DNA-binding domains. The AP2 domain was discovered to be well-conserved in other Apicomplexa such as *Theileria* and *Cryptosporidium* (139).

The AP2 class of DNA-binding domains has been previously characterized as developmental transcription factors in plants (137). Structurally, the ApiAP2s consist of three strands and a helix that is a conserved backbone structure involved in DNA sequence binding. Unlike the plant AP2s, however, the ApiAP2s include a hairpin linker structure between two of the strands that is

hypothesized to be important for specifying DNA contact (139, 140). The ability of several ApiAP2 proteins to bind specific DNA sequences has been validated using “protein binding microarrays” or PBMs (142). These arrays are spotted with DNA 10-mers, to which a recombinant, tagged AP2 domain is applied (141). The structural and functional homology of the AP2s and their ability to bind potential *cis*-regulatory sequences cast the ApiAP2s as the primary lineage of putative specific transcription factors for the Apicomplexa.

B. Function of AP2s in plants and in Apicomplexa

In plants, the AP2s are responsible for proper development and response to environmental stress. Mutations in AP2 proteins result in abnormal patterning of flower organs, shape of leaf epidermal cells, and plant height (142-144). The response of plants to various environmental stresses is mediated by different subgroups of AP2s, with the DRE-motif binding transcription factors (DREBs) responding to drought and cold and ERF class responding to biotic factors such as pathogens (145). Other plant AP2s integrate multiple stress responses through triggering crosstalk with other AP2s or forming differential protein complexes (146-148).

A number of Apicomplexan AP2s have been functionally characterized and play roles ranging from parasite development to virulence. PfSIP2 was found to bind to subtelomeric regions of heterochromatin at the SPE2 motif, a conserved sequence hypothesized to be important for silencing of the virulence *var* genes (149). Consistent with the temporal cascade of just-in-time expression,

Plasmodium AP2s have been demonstrated to regulate gene expression within specific developmental stages, for example, AP2-O binds a specific six-mer DNA sequence to activate genes for midgut invasion (150). Expressed in the mosquito gut late-stage oocyst and the salivary gland sporozoite, AP2-Sp is essential for sporozoite formation and recognizes a specific eight-mer motif to regulate gene expression during this stage (151).

Following injection of sporozoites into the host, the parasites invade liver hepatocytes. AP2-L has been identified that is crucial for successful infection of the liver; although AP2-L knockout parasites invaded hepatocytes normally, they growth-arrested in the schizont stage which precedes merozoite formation (152). During their development in the human liver, malarial merozoites must either continue replicating asexually or commit to gametocyte production. Recently it was shown that nuclear factor PfAP2-G is essential for commitment to the gametocyte stage, as null mutants failed to form any gametocytes (153, 154). In addition, electromobility shift assays confirmed the ability of PfAP2-G to bind specific DNA motifs found upstream of gametocyte development genes (154). Transcripts for early gametocyte development were also downregulated in PfAP2-G null mutants (154). Together these results demonstrate that PfAP2-G is a transcriptional activator of genes involved in the gametocyte stage for *Plasmodium*. Deletion of PfAP2-G2, on the other hand, allows commitment to the sexual development stage but precluded complete development of the gametocyte (153, 155).

C. Function and mechanism of *T. gondii* AP2s

Only three of the 68 *T. gondii* AP2s have been functionally characterized, with two (AP2IX-9 and AP2XI-4) identified with roles in bradyzoite development (156-158). Since the bradyzoite cyst is essential for pathogenesis and transmission, identifying the transcriptional players directing bradyzoite differentiation is crucial. Of the 68 *T. gondii* AP2 proteins, mRNAs of 15 are induced during early *in vitro* bradyzoite development (159), with a subset of these also induced at least ten-fold in mouse brain cysts (160).

AP2IX-9 has been characterized as a bradyzoite repressor (156). It is expressed in early but not late *in vitro* bradyzoites, and ablation of the factor in RH and the PLK strain of ME49 resulted in an increased frequency of bradyzoite development, suggesting that AP2IX-9 is a repressor of bradyzoite development (156). Conditional overexpression of the factor further supported this model, as enhancement of AP2IX-9 expression limited bradyzoite cyst formation (156). As a putative transcription factor, AP2IX-9 was demonstrated to bind a specific *cis*-regulatory element that includes a motif in the B-NTPase promoter (156). It directly downregulates the expression of bradyzoite-specific genes such as BAG1, LDH2, and ENO1 besides B-NTPase (156). Finally, chromatin immunoprecipitation experiments confirmed that AP2IX-9 associates with the promoter of BAG1 (156). As a transcriptional repressor of bradyzoite gene expression, AP2IX-9 may act to prevent premature commitment to bradyzoite development. This might occur to allow the parasite to balance latency with

replication when faced with the host immune response or when the parasite infects a host tissue unfavorable for differentiation (156).

While AP2IX-9 has been characterized as a bradyzoite repressor, AP2XI-4 appears to be a bradyzoite activator (157). AP2XI-4 is expressed in bradyzoites in a cell cycle-regulated manner (157). Although its mRNA profile suggests its peak expression is between the mitotic and cytokinesis stage of the cell cycle, endogenously tagged AP2XI-4 demonstrated robust expression in the cytokinesis and G1 phase with minimal expression in S and M (157). No significant difference in growth rate was observed between wild-type and AP2XI-4 parasites (157). However, knockout of this factor resulted in downregulation of bradyzoite transcripts, suggesting a role for this factor as an activator of bradyzoite expression (153). Mice infected with a knockout strain of AP2XI-4 subsequently carried five-fold fewer brain cysts compared to mice infected with the wild-type (157).

AP2XI-5 appears to regulate virulence genes during the tachyzoite stage of the parasite (158). AP2XI-5 binds preferentially to promoters of genes involved in parasite invasion such as rhoptry and microneme proteins (158). A specific *cis*-regulatory motif (GCTAGC) was enriched in the chromatin immunoprecipitation peaks for AP2XI-5, which was confirmed to bind to the nucleotides encompassing this motif upstream of the ROP18 promoter (158).

IV. Goals for this thesis

T. gondii is a prevalent pathogen transmitted in intermediate hosts as the bradyzoite tissue cyst. In immune-compromised individuals, these tissue cysts may spontaneously reactivate, causing local organ damage and disseminated disease. As bradyzoites are crucial for transmission and pathogenesis, they are also crucial candidates for drug targeting. Diverse aspects of bradyzoite cellular biology have been uncovered, including the general composition of the cyst wall and bradyzoite surface antigens, the role of heat shock proteins and translational control and the role of epigenetic histone modification in stage switching.

Transcriptional changes clearly underlie the transition from tachyzoite to bradyzoite and identifying the molecular players that regulate these expression changes would reveal the mechanism of stage reprogramming. Cis-regulatory sequences for tachyzoite- and bradyzoite-specific genes have been identified that are essential for complete expression, and proteins in parasite lysate were shown to bind several of these cis-regulatory sequences. These observations strongly suggest a role for specific transcription factors. However, bioinformatics mining of the *T. gondii* genome had revealed few members of the canonical eukaryotic classes of DNA-binding proteins.

The identification of nearly 70 proteins with ApiAP2 domains suggest that this class of DNA-binding proteins may serve as the primary lineage of specific transcription factors for *T. gondii*. Three of these 70 have been functionally characterized, with two involved in bradyzoite activation and repression. Novel AP2s are ideal candidates to further understanding some of the most important

questions remaining for bradyzoite biology. These include mapping the molecular networks driving bradyzoite differentiation along with the exact timing of transcriptional changes occurring as the bradyzoite develops. Fortunately, stage conversion transcriptome data has provided clues to which AP2 factors may be involved in bradyzoite conversion. In addition, the association of the S/M phase of the tachyzoite cell cycle with bradyzoite conversion encourages closer look at those AP2 factors with cyclical or “cell cycle regulated” mRNA expression.

Of the 68 *T. gondii* AP2 proteins, 24 exhibit cyclical mRNA profiles through the tachyzoite cell cycle. The temporally-specific expression of this subset of the *T. gondii* AP2s may also be central for their method of mediating parasite development. Indeed, in *Plasmodium*, the 28 ApiAP2s are expressed at distinct periods during development, aligning with the temporal appearance of developmentally regulated genes (141). This “just-in-time” mechanism may be important to ApiAP2s in other Apicomplexans as well. In particular, the cellular changes linking the tachyzoite cell cycle and initiation of bradyzoite development at the S/M phase require further clarification.

Evaluation of transcriptome data revealed that four of AP2 factors which are induced under *in vitro* bradyzoite conditions also demonstrate S phase peak expression (156). One of these, AP2IX-4, is also upregulated during chronic infection in mice (159). These data demonstrate that transcript levels of AP2IX-4 are upregulated in both *in vitro* and *in vivo* bradyzoite conditions. In addition, AP2IX-4 transcript expression is cell cycle-regulated in the tachyzoite stage, and AP2IX-4 contains a putative DNA-binding domain. **Therefore, we hypothesize**

that AP2IX-4 is a cell cycle-regulated transcription factor that contributes to the biology of bradyzoite cysts. This hypothesis will be dissected using the following aims:

- (1) Using molecular genetics and IFA, evaluate the expression of AP2IX-4 protein in the bradyzoite stage compared to the tachyzoite stage
- (2) Examine the role of AP2IX-4 in tachyzoite replication and in both *in vitro* and *in vivo* models of bradyzoite induction.
- (3) Evaluate the genes whose expression are under direct or indirect control of AP2IX-4.
- (4) Generate reagents for a yeast two-hybrid screen towards the goal of identifying AP2IX-4 interacting proteins.

The long-term goals of this thesis are to illustrate the molecular basis for the transcriptional reprogramming that occurs in the tachyzoite-to-bradyzoite conversion. Based on previous studies, this transcriptional reprogramming is accompanied by a temporal cascade of gene activation or repression and changes in acetylation status on promoters of stage-specific genes. The evaluation of AP2IX-4 protein expression throughout the tachyzoite cell cycle and bradyzoite time course aims to compare this data with existing transcriptome data of AP2IX-4 expression. Knockout and transcriptional analysis experiments will specify possible functions this factor plays in bradyzoite development, with eventual Y2H results indicating the mechanistic complexes in which the factor participates towards its role.

CHAPTER 2: MATERIALS AND METHODS

I. Tissue culture techniques

A. Parasite strains and sources

Modified versions of two parental parasite lines were used for this thesis: a type I strain, RH, a type II strain Prugniaud (abbreviated “Pru”). All the parasite lines used in this thesis are summarized in **Table 1**. Parasites were modified to contain deletions of the non-homologous end joining enzyme *ku80* and/or the *hxgprt* gene, resulting in the parasite lines used as parental backgrounds in this thesis, $RH\Delta ku80::HXGPRT$ and $Pru\Delta ku80\Delta hxgprt$. Wild-type RH parasites were used to generate the total RNA for construction of the yeast two-hybrid library, described in **Section VI.A**.

The $Pru\Delta ku80\Delta hxgprt$ line in this thesis was originally generated in (160), and the $RH\Delta ku80::HXGPRT$ line is derived from the parasite line originally generated in (161). These two studies demonstrated that deletion of *ku80* promotes DNA repair via homologous recombination over non-homologous end joining, a manipulation employed in the generation of parasite mutants for allelic replacement via homologous recombination (160, 161). $Pru\Delta ku80\Delta hxgprt$ parasites also contain ectopic integration of three copies of a construct that expresses green fluorescent protein (GFP) under the bradyzoite-specific LDH2 promoter (118). This line was generated at the John Boothroyd Lab at Stanford University and is described in (118). Deletion of *hxgprt* sets up a selection system discussed in **Section I.H**.

Table 1. Parasite lines

Line	Parental Strain	Features and Notes
RH $\Delta ku80::HXGPRT$	RH	Deletion of <i>ku80</i> promotes homologous recombination over non-homologous end-joining DNA repair
Pru $\Delta ku80\Delta hvgprt$	Pru	Deletion of <i>hvgprt</i> sets up drug selection system explained in Chapter 2 Section I.H. ; Contains ectopic integration of three copies of a construct that expresses <i>gfp</i> under the bradyzoite-specific LDH2 promoter
RH	RH	Wild-type RH used for preparation of total RNA for yeast two-hybrid screen
AP2IX-4 ^{HA}	RH $\Delta ku80::HXGPRT$	Parasite line containing AP2IX-4 endogenously tagged at its C-terminus with three tandem HA tags
$\Delta ap2IX-4$ in Pru	Pru $\Delta ku80\Delta hvgprt$	Deletion of <i>ap2IX-4</i>
$\Delta ap2IX-4::AP2IX-4^{HA}$	$\Delta ap2IX-4$ in Pru	Complementation of AP2IX-4 in Pru $\Delta ap2IX-4$ parasites; rescued AP2IX-4 is tagged at its C-terminus with three tandem HA tags

B. Host cell and parasite culturing

T. gondii is capable of invading virtually any nucleated cell in the body. In tissue culture work, human foreskin fibroblasts (HFFs) are widely used for

several reasons. These cells are easy to culture, reaching confluence in days and exhibiting contact inhibition. Invaded parasites form rosettes which, along with the large and flat host cells, are easily visualized under the microscope. Parasites were cultivated in confluent monolayers of HFFs (ATCC #CRL-4001) grown in T25cm² or T150cm² flasks (Corning Life Sciences, #353109 or 353110). HFFs were cultured in host medium that consisted of Dulbecco Modified Eagle Medium (DMEM; Corning #10-017-CV) supplemented with 10% heat-inactivated fetal bovine serum (FBS, Gibco #16000). The HFF cultures were grown at 37°C in a humidified incubator with 5% CO₂. All host cell and parasite culturing was performed under sterile conditions in a laminar flow hood.

To expand HFF cultures, HFFs in T150cm² flasks were trypsinized, diluted in HFF medium, and allocated into new T25cm² or T150cm² flasks. The host medium was aspirated from the HFF monolayer which was then washed with 1x phosphate-buffered saline (PBS). Monolayer cells were released for passaging using trypsin digestion at 37°C for two minutes. Following digestion, the monolayers were thoroughly separated from the flask surface by banging the sides of the flask using the palm of the hand. The cells were then resuspended in new host medium at a dilution of 1:5 or 1:10. This cell resuspension was then allocated into T25cm² flasks with 10 mL of culture per flask or into T150cm² flasks with 50 mL of culture per flask. The new monolayers were then cultured at 37°C with 5% CO₂.

HFFs lose their ability to reach confluency as they age; they cannot be expanded indefinitely. Therefore, the number of expansions or “passage number”

of an HFF culture is recorded on the flask with each trypsinization. To maintain healthy, confluent HFF cultures for both tachyzoite and bradyzoite growth, HFF cultures were discarded after passage 20. Younger passage HFF cultures from either existing in-culture lines or thawed lines were then used to generate new lines.

Indirect immunofluorescence (IFA) experiments utilized HFFs cultured in 12-well plates (Fisher, #07-200-81) with coverslips. The wells of the plate were first populated with coverslips by aspirating autoclaved coverslips from a storage dish and depositing the coverslips into the well via gentle dislodging motion of the aspirator. 2 mL of trypsinized and resuspended HFFs were cultured per well.

Cloning with the limiting dilution technique employed 96-well plates (Fisher, #07-200-90), which were prepared by resuspending trypsinized HFFs in 20 mL of host medium. From this, 2.7 mL was added to 115 mL of host medium and the diluted culture was then allocated into a sterile solution basin (VWR, #21007-972). Using a multi-channel pipettor, the mixture was aliquoted into the wells of the 96-well plate with 200 uL per well.

Depending on the volume of *T. gondii* used to infect HFFs in a flask, parasites invade, replicate and lyse a monolayer in the span of several days. Since *T. gondii* is an obligate intracellular parasite, an absence of HFF monolayer for invasion means parasites linger without host cells. Viability of the parasites declines with increasing time outside of host cells, therefore propagation of parasite cultures requires fresh host cells before or immediately following complete lysis of the original monolayer. To propagate parasite

cultures, aliquots of extracellular parasites were passed into T25cm² flasks with fresh HFF monolayers whose host medium had been replaced with parasite medium. Parasite medium consists of DMEM supplemented with either 1% (for type I, RH background parasites; see **Section I.A** and **Table 1**) or 5% (for type II, Pru background parasites; see **Section 1.A** and **Table 1**) FBS. Parasites were then cultured in at 37°C in a humidified incubator with 5% CO₂.

C. Parasite growth assays

Parasite doubling assays were performed as previously described (148). In brief, 10⁶ freshly lysed tachyzoites were inoculated onto host cell monolayers. After 24 hours, the number of tachyzoites present within 50 random vacuoles was recorded at 12 hour intervals. For plaque assays, infected monolayers in 12-well plates were fixed with 4% para-formaldehyde (PFA) and stained with crystal violet to visualize and count plaques, which are areas of parasite lysis in the host monolayer (149).

D. *In vitro* bradyzoite induction

To initiate conversion to bradyzoites *in vitro*, type II parasites were allowed to invade HFF monolayers for four hours under normal culture conditions, then the medium was replaced with Roswell Park Memorial Institute (RPMI) medium without sodium bicarbonate (Sigma-Aldrich #R6504) adjusted to pH 8.2 with NaOH. Cultures were then moved to a 37°C incubator with ambient CO₂.

E. Harvesting of parasites

To control for consistent viability between strains, parasites were harvested when they were intracellular. Parasites were harvested by scraping the infected HFF monolayer with a cell scraper (Fisher, #50-476-477) and passing the culture through a 25-gauge syringe needle (Excel International, #26046) to extrude the parasites from the host cells. HFF debris was separated from the parasites by passing the syringe-lysed mixture through a 3-micron pore filter (Fisher # NC9655197).

F. Freezing and thawing of cells

Parasites were frozen down in parasite freeze mix to create stocks for future use. To prepare freeze mix, 6.3 mL of dimethyl sulfoxide (DMSO) was added to 13.8 mL of DMEM and sterile-filtered with a 0.2-micron pore filter unit. 5 mL of 1% or 5% heat-inactivated FBS was added to the mix, which was then stored at 4°C. For freezing, intracellular parasites were harvested by scraping their host monolayer without syringe-lysing, and the cells were pelleted in by centrifugation at 1500xg at room temperature for 10 minutes. The pellet was then resuspended in a 1:1 ratio of ice cold parasite medium to freeze mix, and the cells then transferred into sterile CryoTubes (Cole-Parmer, #368632). The tubes were stored at -80°C immediately followed by transfer to the liquid nitrogen storage. Frozen parasite stocks were thawed by incubating the CryoTubes in a 37°C water bath. Immediately after thawing, the cells were transferred into T25 flasks containing parasite medium.

G. Transfection

Electroporation, a technique which introduces pores in the plasma membrane, remains a successful method-of-choice to introduce DNA into *T. gondii* parasites (162). It has been shown that cell survival is improved when electroporated cells are buffered in a medium that closely mimics the osmolarity and ionic composition of the cytosol (163). For this reason, *T. gondii* tachyzoites are electroporated in the presence of a potassium phosphate-based buffer called Cytomix consisting of 120 mM KCl, 0.15 mM CaCl₂, 10 mM K₂HPO₄/KH₂PO₄ at pH 7.6, 25 mM HEPES at pH 7.6, 2 mM EGTA, and 5 mM MgCl₂. (164).

For electroporations, 50ug of DNA was first linearized via digestion overnight using a single-cut restriction enzyme. The digested DNA was purified with ethanol precipitation, by combining the DNA with a 0.1 volume of 3M sodium acetate, pH 5.2 and 2.5 volume of 100% ice cold ethanol followed by centrifugation of the mixture at 21,000xg at 4°C for 20 minutes. The pellet was then washed with 70% ethanol before final centrifugation at 21,000xg at 4°C for 5 minutes. The ethanol was removed in the sterile laminar flow hood where the DNA pellet was allowed to dry for one hour.

Freshly lysed or intracellular parasite vacuoles were harvested for electroporation. The infected monolayer within the flask was scraped, passed through a 25-gauge syringe needle, and filtered using a sterile 3-micron pore filter unit. The purified parasites were quantified using a hemocytometer to allocate 2×10^7 parasites, which were spun down at 1,500xg at room temperature for 10 minutes. Parasites were resuspended in 350 uL of sterile-filtered Cytomix

and combined with the purified DNA. The sample was then transferred to a 2 mm gap cuvette (Fisher #BTX620). Parasites were pulsed with 1.5 kV, 25 Ω and 25 μ F using a BTX ECM 630 electroporator. Following electroporation, parasites were allowed to recover in the cuvette at room temperature for 20 minutes. The transfected parasites were then allocated at equal volume into three flasks containing confluent HFF monolayers whose host medium was replaced with parasite medium.

H. Drug selection of transfected parasites

Purine salvage and folate synthesis underlie the biochemical basis for two common methods of selection of transgenic *T. gondii*. HXGPRT, one of the enzymes in the purine salvage pathway, catalyzes the conversion of hypoxanthine, xanthine or guanine to intermediates or products of guanine-monophosphate (GMP) synthesis (165, see **Figure 2**). Treatment of $\Delta hxgp rt$ parasites with mycophenolic acid (MPA) is efficiently lethal as MPA inhibits IMP dehydrogenase and thus production of inosine monophosphate (IMP) and GMP (165). On the other hand, $\Delta hxgp rt$ parasites transfected with a copy of the *HXGPRT* gene and supplemented with xanthine can rescue GMP production (166, **Figure 2**). MPA and xanthine can thus be used to select for $\Delta hxgp rt$ parasites transfected with plasmids encoding a copy of HXGPRT. MPA is added to cultures post-transfection at a final concentration of 25 μ g/mL, and xanthine at 50 μ g/mL.

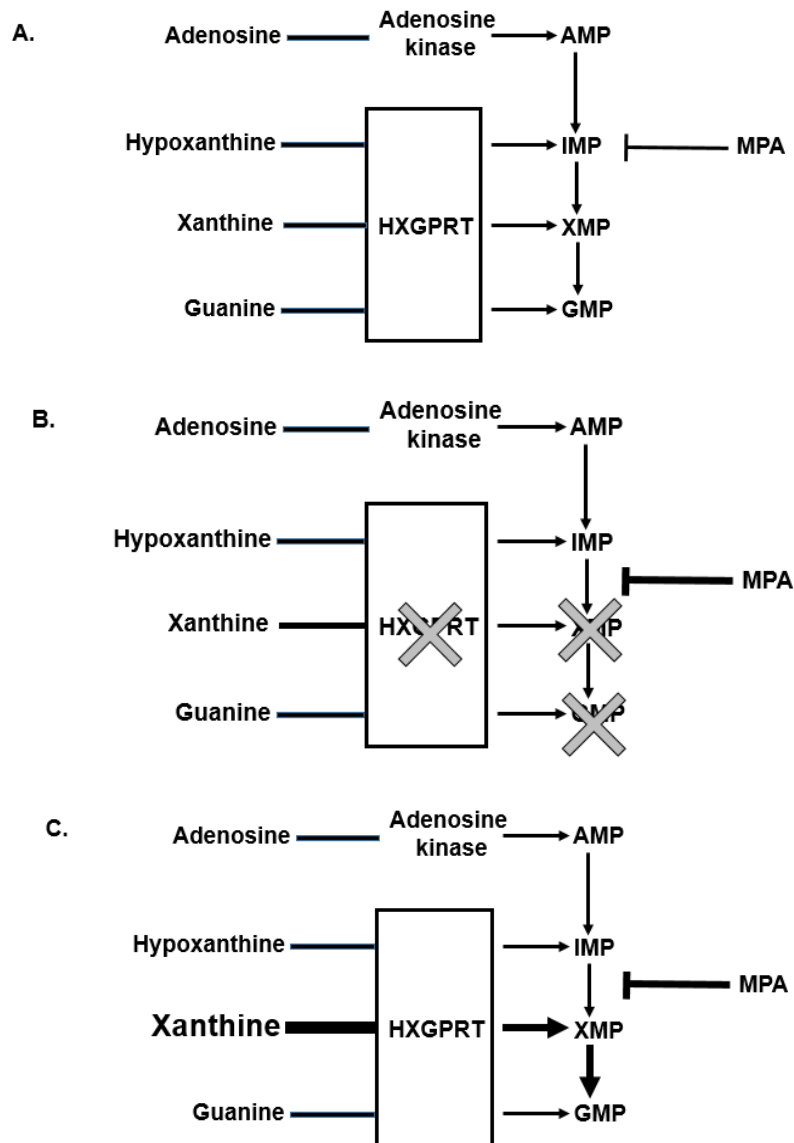


Figure 2. HXGPRT drug selection employs the biochemical basis of purine salvage in *T. gondii*. **A.** A simplified schematic of the purine salvage pathway in *T. gondii*. The adenosine kinase and HXGPRT pathways are two pathways of adenosine monophosphate (AMP) and guanosine monophosphate (GMP) production. Hypoxanthine, xanthine and guanine are all potential substrates of hypoxanthine-xanthine-guanine phosphoribosyl transferase (HXGPRT). **B.** Steps in the pathway that are inhibited in $\Delta hxpgrt$ parasites with mycophenolic acid (MPA) treatment. MPA inhibits IMP dehydrogenase that catalyzes the conversion of IMP to xanthosine monophosphate (XMP). With inhibition of both HXGPRT and IMPDH, GMP synthesis does not occur and parasites perish. **C.** $\Delta hxpgrt$ parasites rescued with an ectopic copy of *HXGPRT* and xanthine supplementation restore GMP synthesis.

Pyrimethamine inhibits dihydrofolate reductase-thymidylate synthase (DHFR-TS), the enzyme catalyzing the conversion of tetrahydrofolic acid from dihydrofolic acid (68). Inhibition of this biochemical step prevents the production of thymine for DNA synthesis. The DHFR*-TS drug selection cassette carried by plasmids used for parasite cloning contains a mutation that renders the enzyme resistant to pyrimethamine (167). For selection, pyrimethamine is added at a final concentration of 1 μ M to transfected cultures.

I. Cloning by limiting dilution

Transfected parasites were passed at least three times in the presence of drug before single parasite clones were isolated using the limiting dilution method accomplished in 96-well plates containing HFF monolayers. Dilutions were prepared that estimated the allocation of one parasite per well. The plates were placed in humidified incubators at 37°C with 5% CO₂ and left undisturbed for 6-7 days. The wells were then checked for the presence of single plaques representing the lysis of a single population of parasites. Wells containing single clones were marked and scraped with the tip of a p200 pipette and the cultures transferred into the wells of a 24-well plate containing an HFF monolayer.

II. Plasmid construction

All primers used for construct generation are summarized in **Table 2**.

All plasmids generated for this thesis are summarized in **Table 3**.

A. General PCR protocol

Components of the PCR reactions were assembled according to protocols optimal for either Taq DNA Polymerase (NEB, #M0273S) or Phusion High-Fidelity DNA Polymerase (NEB, #M0530S). The high-fidelity Phusion polymerase was used for molecular cloning applications in which the accuracy of amplicons for sub-cloning was crucial, while Taq polymerase was used for diagnostic screening of cloning products. All components of the PCR reactions were assembled on ice, with the polymerase aliquoted last. Annealing temperatures for Taq polymerase reactions were in general determined by subtracting five degrees from the lower annealing temperature of the primer pair, while annealing temperatures for Phusion polymerase reactions were determined through <http://tmcalculator.neb.com/#/>. The general PCR protocols and cycling conditions for the Taq and Phusion polymerase systems are given below:

Components	Taq polymerase	Phusion polymerase
	5 uL, 10x Standard Taq polymerase buffer 1 uL, 10mM dNPT 1 uL, 10uM sense primer 1 uL, 10 uM antisense primer Variable, DNA template To 50 uL: nuclease-free water 0.25 uL, Polymerase	10 , 5x Phusion HF buffer 1 uL, 10 mM dNTPs 2.5 uL, 10 uM sense primer 2.5 uL, 10 uM antisense primer Variable, DNA template To 50 uL: nuclease-free water 0.5 uL, Polymerase
Cycling		
Denaturation	95°C, 30s	98°C, 30s
25-30 cycles	95°C, 30s T _m , 30s 68°C, 1 minute/kb	98°C, 30s T _m , 30s 72°C, 30s/kb
Final extension	68°C, 5 minutes	72°C , 10 minutes
Hold	4°C	4°C

Table 2. PCR primers

Underlined and bold indicate sequences for molecular sub-cloning purposes.

Application	Primer	Amplicon	5' → 3' Sequence
Endogenous tagging	F1	C-terminus of AP2IX-4	<u>TACTTCCAATCCAATTTAATGCA</u> GCACGATCCAACCTCGCCCT
Endogenous tagging	R1	C-terminus of AP2IX-4	<u>TCCTCCACTTCCAATTTAGCTC</u> GCAGGACGGGGACGCTG
Deletion of AP2IX-4	F2	AP2IX-4 upstream genomic	<u>GGGGACAACCTTTGTATAGAAAA</u> <u>GTTG</u> CTCGCAACAGCCACTCCCC G
Deletion of AP2IX-4	R2	AP2IX-4 upstream genomic	<u>GGGGACTGCTTTTTTGTACAAAC</u> <u>TTG</u> CCAACAACGCAAGCACGCC C
Deletion of AP2IX-4	F3	AP2IX-4 downstream genomic	<u>GGGGACAGCTTTCTTGTACAAA</u> <u>GTGG</u> TCAACACGGCGTCCAGCG TC
Deletion of AP2IX-4	R3	AP2IX-4 downstream genomic	<u>GGGGACAACCTTTGTATAATAAA</u> <u>GTTG</u> GCCGATCACGCCACTCCCT G
Deletion of AP2IX-4	F4	DHFR*-TS minigene	<u>GGGGACAGCTTTCTTGTACAAA</u> <u>GTGGCT</u> CAGGAAAGACAGGCTC CGGA
Deletion of AP2IX-4	R4	DHFR*-TS minigene	GGGGACAACCTTTGTATAATAAAG TTGCTGACCGCTGATACATGATG CA
Deletion of AP2IX-4	F5	DHFR*-TS minigene	TATCTAGAGACCCCAAGAGGG GCATC
Deletion of AP2IX-4	F6	DHFR*-TS minigene	<u>TAGCGGCCGCGGGGACCACTTT</u> <u>GTACAAGAAAGCTGGGTAGGAT</u> CGATCCCCCGTTTTG
Complementation	F7	AP2IX-4 upstream	<u>TTCCAATCCAATTTAGCCACCCG</u> TACCATGACTGGGGA
Complementation	F8	AP2IX-4 upstream	CCCCCGTGTCTACCGACAT

Complementation	F9	AP2IX-4 CDS	ATGTCGGTAGACACGGGGGG
Complementation	F10	AP2IX-4 CDS	TGCGAGATACTTGGGGACGCA
Complementation	F11	AP2IX-4 CDS	TGCGTCCCCAAGTATCTCGCA
Complementation	F12	AP2IX-4 CDS	<u>CCACTTCCAATTTAGC</u> TGCGAG GACGGGGACGCT

B. General molecular cloning guidelines

In-Fusion® HD Cloning (Clontech, # 638910) was used for the construction of the plasmids detailed in this thesis. In-Fusion cloning operates on the ligation of a linearized vector to PCR-amplified fragments that contain extensions complementary to the vector at its restriction cut site. These homologous end sequences are appended onto the fragments through PCR amplification with primers that contain both vector- and insert-specific sequences. Therefore, the first step of In-Fusion cloning is to generate the linearized vector through restriction digest and to amplify the insert fragment.

To purify the insert fragment and linearized vector, the products were resolved on a 0.8% agarose gel, and bands of the correct sizes were excised using a metal scalpel. The vector and insert fragment were gel-purified using the PureLink Quick Gel Extraction Kit (ThermoFisherScientific, # K210012), then combined in an In-Fusion Reaction at a 2:1 insert-to-vector molar ratio, with at least 50 ng of insert. The final component of the In-Fusion Reaction is the In-Fusion HD enzyme, which generates single-stranded 15-nucleotide regions at

the ends of the insert and vector. These single-stranded regions then ligate due to their complementarity. All components of the In-Fusion Reaction were added to an Eppendorf tube on ice, and the completed reaction was incubated at 50°C for 15 minutes according to the protocol before cooling on ice.

Recombinant clones were isolated through transformation in DH5α high-efficiency competent *E. coli* (NEB, #C2987H). 50 uL of the competent DH5α cells were thawed on ice and then combined with 2.5 uL of the In-Fusion reaction. The mixture was incubated on ice for 30 minutes, heat-shocked for 45 seconds at 42°C, then placed on ice for two minutes. 500 uL of Super Optimal Broth with Catabolite Repression (S.O.C) medium (Invitrogen #15544034) was added to the cells before the cells were incubated with shaking at 37°C for one hour. The transformation reaction was then plated at two separate volumes onto LB plates containing antibiotic for selection. Plates were incubated overnight at 37°C for 12-16 hours.

To screen for molecular clones containing the insert, bacterial colonies were picked at random from the LB plate using the tip of a p20 pipette and deposited into 5 mL of LB broth containing the selection antibiotic. The bacteria was grown at 37C with shaking for up to 16 hours. Up to 2 mL of the culture was spun down in 15-mL conical tubes into a pellet for miniprepping, which were performed using the FastPlasmid Mini Kit (5 Primer, #2300010). The extracted plasmids were screened for the presence of insert using either restriction digest and/or diagnostic PCR. Putative positive clones were sent for sequencing at ACGT, Inc., and glycerol stocks of confirmed clones were prepared by adding

700 uL of culture to 300 uL of glycerol. Maxipreps of plasmids for transfection were prepared by inoculating 125 mL of LB broth containing the selection antibiotic, shaking the culture for up to 16 hours at 37°C, and extracting the plasmid using the GenElute™ HP Plasmid Maxiprep Kit (Sigma-Aldrich, #NA0310-1KT).

All primers utilized to generate constructs and the plasmid maps for all constructs utilized in this thesis are provided at the end of this chapter (**Figures 3-5**).

Table 3. Plasmids

Plasmid	Purpose in this thesis	Features and Notes
pLIC-3HA-DHFR	Parent for pLIC-AP2IX-4-3HA-DHFR	
pLIC-AP2IX-4-3HA-DHFRTS	Endogenous tagging of <i>AP2IX-4</i>	
pDONR_P2R-P3-3arm	Deletion of <i>AP2IX-4</i>	Entry vector for Gateway cloning; contains 3' homology arm
pDONR_P4P1R-5arm	Deletion of <i>AP2IX-4</i>	Entry vector for Gateway cloning; contains 5' homology arm
pDONR221-DHFRTS	Deletion of <i>AP2IX-4</i>	Entry vector for Gateway cloning; contains DHFR* - TS
pDEST_AP2IX-4KO	Deletion of <i>AP2IX-4</i>	Construct transfected into PruQ parasites
pLIC-3HA-HXGPRT	Parent of pLIC-AP2IX-4-3HA-HXGPRT	
pLIC-AP2IX-4-3HA-HXGPRT	Complementation in $\Delta ap2IX-4$ parasites	

C. Construct for endogenous tagging of AP2IX-4

RH Δ ku80::*HXGPRT* parasites were engineered to express endogenous AP2IX-4 tagged at its C-terminus with three hemagglutinin (3xHA) epitopes. Modification of the endogenous *AP2IX-4* locus was achieved through allelic replacement of parasites lacking the non-homologous end joining repair enzyme KU80 to promote homologous recombination. The construct to append the endogenous copy of *ap2IX-4* with three HA tags was derived from the pLIC-3HA-DHFRTS vector, which contains three HA tags preceded by a *PacI* restriction cloning site (**Figure 3**). Ligation of the insert at the *PacI* site appends the three epitope tags at the C-terminus of the insert.

The final tagging construct, pLIC-*ap2IX-4-3HA-DHFRTS*, employed a 1514 bp C-terminal sequence from genomic *AP2IX-4* for homologous recombination, amplified with primers F1 and R1 shown in **Table 2**. The fragment was ligated to the *PacI*-linearized vector in an In-Fusion reaction, which was then transformed into DH5 α competent *E. coli*. An ampicillin resistance cassette on the plasmid allowed positive selection of bacteria clones, which were then screened for transformation with vector containing the 1514 bp insert. Plasmids containing the 1514 bp were sent for sequencing to confirm correct sequence in the recombinant construct.

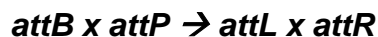
D. Construct for knocking out *ap2IX-4*

Deletion of *AP2IX-4* in Pru Δ ku80 Δ *hxgpRT* (PruQ) parasites was achieved using allelic replacement of the endogenous *AP2IX-4* locus with a DHFR*-TS

drug selection cassette. The “knockout construct” flanks the *dhfr^{*}-ts* minigene with 1.6-1.9kb sequences that are homologous to regions of the *ap2IX-4* locus up- and downstream of the coding region. To design this multi-fragment construct, the MultiSite Gateway Three-Fragment Vector Construction Kit (ThermoFisherSci, # 12537100) was utilized by adapting manufacturer protocol.

One attractive feature of the MultiSite Gateway Three-Fragment cloning method is its restriction enzyme-free system that allows recombination of several sequences in one reaction. Gateway Cloning is an *in vitro* modification of events occurring during the integration of lambda (λ) bacteriophage DNA into *E. coli*. The λ phage is able to integrate into *E. coli* DNA at *att* sites. The phage *attP* targets the bacterial *attB* site, generating *attL* and *attR* sites at the recombination loci. In Gateway Cloning, the *att* sites have been modified such that directional recombination can occur. DNA sequences-of-interest, usually generated in PCR reactions, contain the *attB* sites while “donor” vectors contain the *attP* sites. In brief, Gateway cloning is divided into two steps:

- (1) Generation of entry vectors. Entry vectors are generated in a “BP” reaction which mixes *attB* site-flanking PCR products and *attP*-containing donor vectors. At the recombination sites, *attL* and *attR* sites are generated:



Entry clones are transcriptionally silent. They must be subcloned into a destination vector, a reaction that generates the expression clone.

(2) Generation of the expression clone. Entry vectors, containing their *attL* sites, are combined with a destination vector to produce the expression clone.

To generate the AP2IX-4 deletion plasmid, two entry vectors were constructed that included 5' and 3' flanking sequences for homologous recombination at the *AP2IX-4* genomic locus. Entry vector pDONR_P4P1R-5arm contained a 1,660 bp sequence upstream of the *AP2IX-4* genomic sequence, while entry vector pDONR_P2R-P3-3arm contained the 1,875 bp sequence downstream. A third entry vector, pDONR221-DHFRTS, was constructed to contain the *dhfr⁺-ts* minigene. The three entry vectors were combined in a Gateway LR reaction with the destination vector pDEST_R4R3 to create the final knockout plasmid pDEST_AP2IX-4KO (**Figure 4**). All PCR primers used to generate these vectors are listed in the **Table 1**.

E. Construct for complementation of AP2IX-4 in $\Delta ap2IX-4$ parasites

Complementation of AP2IX-4 in $\Delta ap2IX-4$ parasites was achieved with ectopic expression of triple HA-tagged AP2IX-4. The complementation plasmid was generated from the pLIC-3HA-HXGPRT plasmid. This plasmid contains a *PacI* site to integrate the sequence-of-interest which would then be fused at its C-terminus to the 3HA tags engineered into the plasmid.

The sequence-of-interest cloned into the pLIC-3HA-HXGPRT vector is a 2,116 bp sequence used for homology recombination, followed by the entire coding sequence of *ap2IX-4* (minus the stop codon). The 2,116 bp sequence

immediately upstream the *ap2IX-4* start codon was amplified from PruQ cDNA using primers F7 and F8 (see **Table 2**) and ligated to *ap2IX-4* coding sequence. Primers F9, F10, F11 and F12 were used to amplify the *ap2IX-4* coding sequence, with F9 and F10 amplifying the upstream and F11 and F12 amplifying the downstream region. The coding sequence amplicons and the 2,116 bp homology amplicon were then ligated using In-Fusion Cloning and integrated into pLIC-3HA-HXGPRT at the *PacI* restriction site. The resulting plasmid (**Figure 5**) was electroporated into Δ *ap2IX-4* PruQ parasites. Transgenic parasites were selected for using mycophenolic acid and xanthine and cloned by limiting dilution.

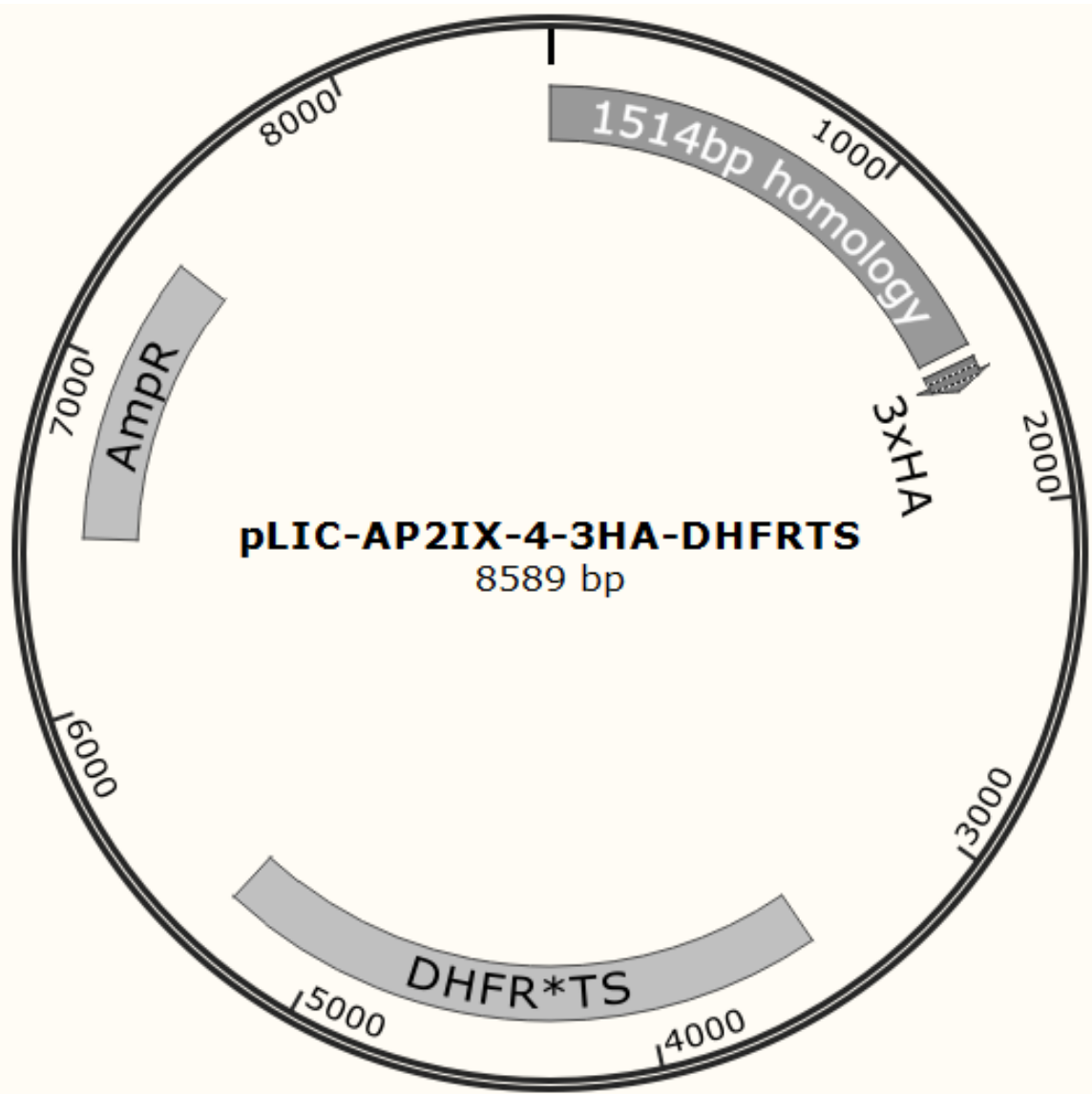


Figure 3. Final construct used to tag endogenous AP2IX-4 in RHΔku80 with three tandem HA tags. Features of the plasmid include the three HA epitopes preceded by a 1,514 bp homology region used for allelic replacement through homologous recombination. The ampicillin resistance cassette allows for selection of bacteria clones containing the construct, and the DHFR*TS drug selection cassette allows for pyrimethamine selection of transgenic parasites. Schematic generated with SnapGene® software (from GSL Biotech; available at snapgene.com).

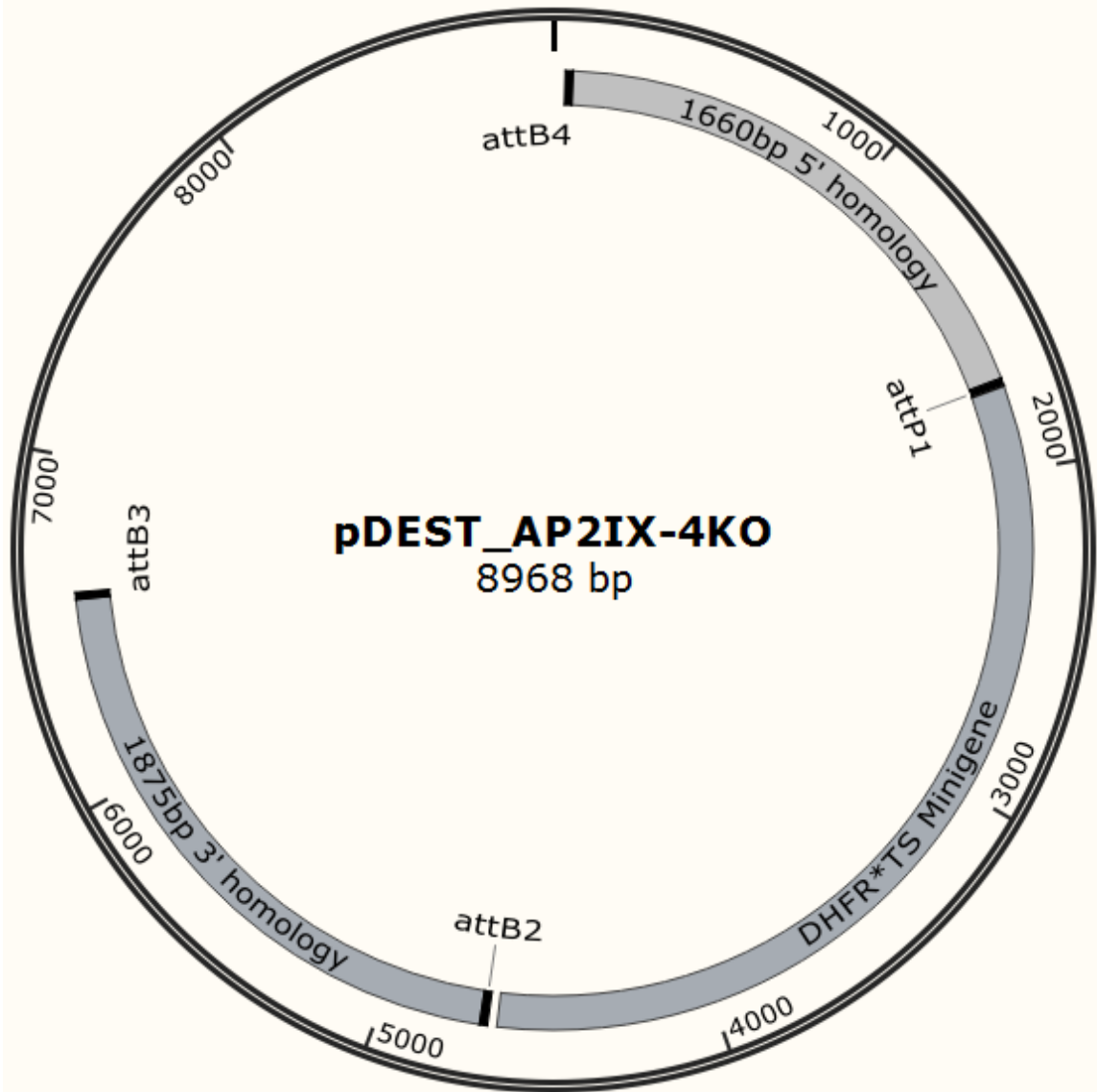


Figure 4. Final construct used to delete AP2IX-4. Flanking the DHFR*TS drug selection cassette are sequences upstream (1,660 bp) and downstream (1,875 bp) to genomic *AP2IX-4* which are used for homologous recombination. Schematic generated with SnapGene® software (from GSL Biotech; available at snapgene.com)

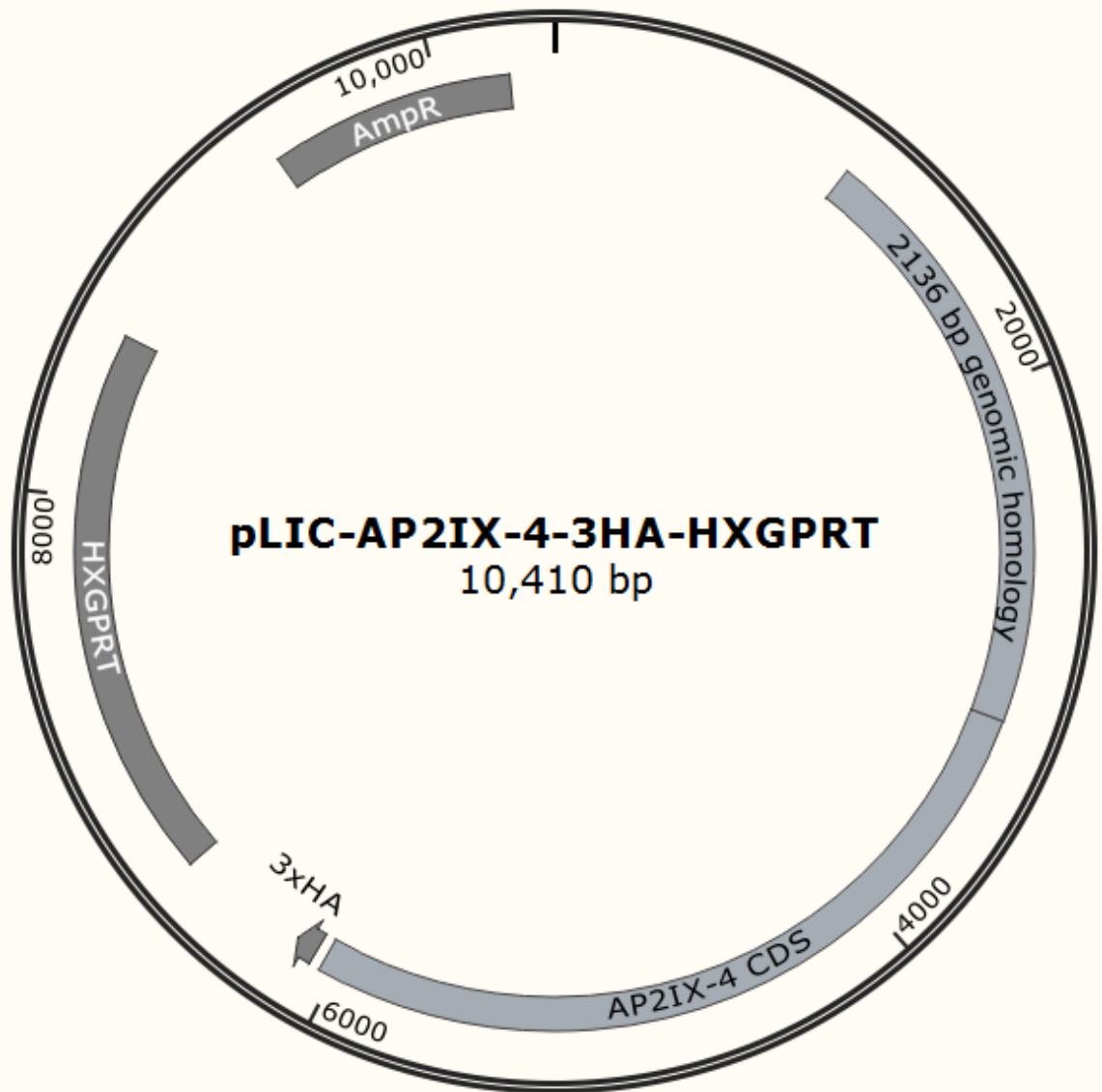


Figure 5. Construct used to complement AP2IX-4 in $\Delta ap2IX-4$ parasites. Upstream of the AP2IX-4 is a 2,116 bp genomic sequence used for homologous recombination at the *AP2IX-4* locus. Re-constitution of AP2IX-4 in $\Delta ap2IX-4$ parasites appends three HA epitopes at its C-terminus through the tandem HA repeats in the construct. Schematic generated with SnapGene® software (from GSL Biotech; available at snapgene.com).

III. Biochemical techniques

A. Western blot

Parasites were harvested when intracellular by scraping infected host monolayer and extruding the intracellular parasites with passage through a 25-gauge syringe. Host debris was filtered out by passing this mixture through a 3 micron pore membrane. To prepare pellet samples with equal parasite material, purified parasites were quantified using the hemocytometer and an equal number of parasites for each parasite strain was allocated into 15-mL conical tubes before centrifugation at 1,500xg for 10 minutes at room temperature. The parasite medium was aspirated and the parasite pellet was resuspended in parasite lysate buffer (150 mM NaCl, 50 mM Tris-Cl pH 7.5, 0.1% NP40) mixed with mammalian protease inhibitor cocktail (Sigma, # P8340-5ML) to prevent enzymatic degradation of proteins. The mammalian protease inhibitor cocktail was added at 10 μ L per 1 mL of parasite lysis buffer. The parasite sample was then incubated at 4°C for 30 minutes with gentle shaking. Afterwards, the lysate was sonicated 15 seconds three times, with 30 seconds on ice between each sonication. Insoluble debris was separated from soluble cellular components by centrifugation at 21,000xg at 4°C for 20 minutes and discarding the pellet.

Denaturation and reduction of disulfide bonds in the soluble proteins was achieved by preparing β -mercaptoethanol in 4x NuPAGE LDS Sample Buffer (Fisher # NP0007), adding this buffer at a ratio of 1:4 to the lysate, and incubating the sample on a 95°C for ten minutes. Samples were then loaded into

the wells of a pre-cast 4-12% Bis-Tris gel (Fisher, #NP0322BOX) and electrophoresed in MOPS buffer for 55 minutes at 200 V, 120 mA and 25 W. Nitrocellulose membrane (GE Healthcare Life Sciences, # 10600004) was used for transfer of protein performed at 35V for 1.5 hours, after which the quality of transfer was assessed using Ponceau staining. Membranes were blocked in 4% milk/TBST for 30 minutes.

Rat anti-HA primary antibody (Roche, #11867423001) was applied at 1:5000 dilution to the membrane overnight at 4°C with gentle shaking followed by anti-rat antibody conjugated to horseradish peroxidase (HRP) (GE Healthcare Life Sciences, #NA935) at 1:2000 dilution. Rabbit anti- β -tubulin antibody (kindly supplied by Dr. David Sibley, Washington University) was applied at 1:2,000 dilution followed by HRP-conjugated donkey anti-rabbit antibody (GE Healthcare) at 1:2,000. Proteins were visualized using chemiluminescence catalyzed by HRP on SuperSignal™ West Femto Maximum Sensitivity Substrate (ThermoFisherScientific, #34094) and detecting the signals using the FluorChem E Imager and AlphaView® software (Protein Simple).

B. Indirect immunofluorescence assay

HFF monolayers grown on coverslips in 12-well plates were inoculated with freshly lysed parasites. Infected monolayers were fixed in 4% para-formaldehyde (PFA) for 10 min, quenched in 0.1 M glycine for 5 min, and then permeabilized with 0.3% Triton X-100 for 20 min with blocking in 3% BSA/1xPBS for 30 min.

IFAs of tachyzoite cultures: Rabbit polyclonal anti-HA primary antibody (Invitrogen) was applied at 1:2,000 dilution overnight at 4°C, followed by goat anti-rabbit Alexa Fluor 488 secondary antibody (Thermo Fisher) at 1:4,000 dilution. Detection of IMC3 was achieved using rat monoclonal anti-IMC3 antibody (kindly supplied by Dr. Marc-Jan Gubbels, Boston College) at 1:2,000 dilution overnight at 4°C, followed by goat anti-rat Alexa Fluor 594 antibody (Thermo Fisher) at 1:4,000 dilution. 4',6-diamidino-2-phenylindole (DAPI, Vector Labs) was applied for 5 min as a co-stain to visualize nuclei.

IFAs of bradyzoite cultures: Rat monoclonal anti-HA primary antibody (Roche # 11867423001) was applied at 1:1,000 dilution for 1 hour at room temperature, followed by goat anti-rat AlexaFluor 594 secondary antibody (Thermo Fisher #11007) at 1:1,000 dilution. For the visualization of bradyzoite cyst walls, rhodamine- or FITC-conjugated *Dolichos biflorus* lectin (Vector Laboratories # RL-1032 or # FL-1031) was applied at 1:1,000 dilution for 30 minutes at room temperature. In IFAs co-stained for IMC3 or SAG1, rabbit polyclonal anti-HA primary antibody (Invitrogen #715500) was applied at 1:2,000 dilution, followed by goat anti-rabbit Alexa Fluor 568 secondary antibody (Thermo Fisher # A-11011) at 1:4,000 dilution. Detection of IMC3 was achieved using rat monoclonal anti-IMC3 antibody (kindly supplied by Dr. Marc-Jan Gubbels, Boston College) at 1:2,000 dilution overnight at 4°C, followed by goat anti-rat Alexa Fluor 647 antibody (Thermo Fisher # A-21247) at 1:4000 dilution. Detection of SAG1 was achieved using mouse monoclonal anti-SAG1 antibody

(Abcam # ab156836) followed by goat anti-mouse AlexaFluor 568 secondary antibody (Thermo Fisher # A-11004).

IV. Gene expression analysis

A. Purification of total RNA

At least 500 ng of total RNA was used to synthesize target sequences for microarray hybridization. Tachyzoite total RNA was purified from intracellular PruQ or $\Delta ap2IX-4$ parasites maintained at pH 7.0 (32-36 hours post-infection) or PruQ, $\Delta ap2IX-4$ or $\Delta ap2IX-4::AP2IX-4^{HA}$ parasites maintained at pH 8.2 (48 hours) using the RNeasy Mini kit (Qiagen) according to manufacturer's instructions. Tachyzoite cultures were harvested by first scraping the monolayer and syringe-passing the culture through a 27-gauge needle. Host debris was filtered out by passing the syringe-lysed culture through a filter membrane with 3 micron pores. Alkaline-induced cultures were harvested by first scraping the monolayer and syringe-passing the culture through a 27-gauge needle, and host debris was separated by filtering the culture twice through a filter with 5 micron pores. The purified parasites were then centrifuged at 4°C 1,500xg for fifteen minutes. The sample was then washed three times total with PBS, with centrifugation at 10,000 rpm at 4°C for 5 minutes between each wash. After the final wash and centrifugation, the supernatant was removed and the pellet was immediately used for total RNA extraction.

The RNeasy Mini kit (Qiagen, # 74104) was used to extract total RNA per manufacturer's instructions. A Nanodrop was used to quantify the total RNA. To check the quality of the total RNA and amount of contaminating host material, an aliquot of the sample was run on a 0.8% agarose gel. The Nanodrop 260/280 reading was used to assess organic contaminants, and a final analysis of quality was performed by the Agilent 2100 Bioanalyzer instrument.

B. ToxoGeneChip description

The availability of a sequenced, annotated genome from the *T. gondii* strain ME49 along with the identification of single nucleotide polymorphisms (SNPs) from genome mapping and expression sequence tag (EST) projects made it possible to populate the *T. gondii* GeneChip with probe sets for a variety of applications. The design of the *T. gondii* GeneChip considers practical applications such as global parasite transcriptome comparisons, gene discovery, comparisons of single nucleotide polymorphisms between strains, and pilot projects such as chromatin immunoprecipitation and antisense expression (168). Each gene is represented by at least eleven 3' biased perfect-match (PM) probes, which are 25-mer oligonucleotides spotted using photolithography. Of the ~8,000 annotated ME49 genes, 3' biased PM probes were designed for 7,793 (168). Annotated genes include nuclear genes which comprise the largest portion of the array (39%) and apicoplast and mitochondrial genes (168). Other probe sets include those ESTs without predicted gene models and *T. gondii* markers for highly polymorphic genes such as SAG1/2/3/4, SRS1/2/9/ ROP1/16, AMA1,

MIC2, GRA3/6/7 and BSR4 (168). The GeneChip also includes probesets for human and mouse genes, notably immune response cytokines and receptors (168).

C. Target sequence synthesis, hybridization, and statistical analysis

A total of 500 ng RNA was used in the Affymetrix One-Cycle kit (ThermoFisherSci, # A10752030) to produce cRNA. The fragmented cRNA was hybridized to the ToxoGeneChip using standard hybridization protocols. Two hybridizations were done for each sample. Hybridization data was processed with the Robust Multi-array Average (RMA) approach which subtracted background, normalized the intensity signals between gene chips, log₂-transformed the probe level intensities and summarized the intensity values within each probe set using per chip and per gene median polishing. The processed probe values were then analyzed using the GeneSpring 7.2 (version 12.6.1) software package (Agilent Technologies, Santa Clara CA). Fold changes that were significant ($p < 0.05$) between probe sets were determined using a moderated t-test followed by Benjamini-Hochberg multiple-testing correction. Transcriptome data from previous publications was used to denote whether genes in our datasets were associated with expression in the bradyzoite stage (103,159).

V. Modeling of parasite infection in mice

A. Acquisition, housing and general care of mice

Four week old female Balb/c mice were purchased from Harlan. After arrival, mice were grouped four per cage, with as close to the same total weight per cage as possible, and allowed at least one week to adjust to their environment. Mice were fed dry chow pellets which they were able to access through a wire overlay. Water was provided through a self-use spigot.

B. Preparation of parasites for injection of mice

In the infection modeling studies presented in this thesis, each group of eight mice was injected with either PruQ, $\Delta ap2IX-4$, or $\Delta ap2IX-4::AP2IX-4^{HA}$ parasites, with each cage receiving either 10^7 , 10^6 or 10^5 parasites. Parasite dosages were prepared through serial dilutions. On the day of injections, intracellular tachyzoites were harvested by scraping the infected HFF monolayer, passing the culture through 25g syringe needle, and filtering out HFF debris using a sterile 3 micron filter. Purified parasites were quantified and inspected for degree of HFF contamination using a hemocytometer. To prepare serial dilutions, the quantity of parasites ten-fold the highest inoculum dosage was aliquoted, centrifuged at 1500g for 10 minutes at room temperature, and resuspended in 1xPBS. This “parasite stock” was used for ten-fold serial dilutions in 1xPBS to a final volume of 100 uL. To assess parasite viability across parasite strains, plaque assays were performed by inoculating each sample onto confluent HFF

monolayers in a 12-well plate with 500, 1000, 2000, and 5000 parasites. These plaque assay plates were left undisturbed in a 37°C incubator with 5% CO₂ for six days. Plaque numbers for each strain were quantified to ensure approximate viability percentage.

C. Injection and monitoring of mice

Mice were weighed before injection to obtain the weight at day 0 of the experiment. Mice were injected intraperitoneally with 28-gauge needles and monitored for weight, scruffiness of appearance and survival. For the acute infection study, mortality was recorded daily for up to 14 days and significant differences in mice survival were calculated using the log-rank test. For the chronic infection study, survivors of the acute infection study were sacrificed at day 35 using CO₂ asphyxiation followed by cervical dislocation. To confirm infection, cardiac bleeds were performed on the mice immediately following euthanasia. Cardiac bleeds were deposited into Eppendorf tubes and kept on ice. The brains of the dead mice were then extracted and homogenized in 1.3 mL PBS, by first grinding with a mortar and pestle followed by pipetting repeatedly into finer particulates. Brains were deposited into Eppendorf tubes and kept on ice.

D. Preparation of IFA samples for *in vivo* cyst burden quantification

To prepare immunofluorescence assay samples from brain homogenates, 250 uL of brain homogenate was obtained from the 1.3 mL preparation and spun

down at 3000xg for 5 minutes. All subsequent steps, from fixation to final wash, were performed by resuspending the pellet with the indicated reagent and time, with centrifugation at 3000xg for 5 minutes at room temperature and removal of the supernatant between each step. The pellet was fixed under the sterile fume hood for 20 minutes with 150 uL 3% methanol-free formaldehyde (prepared from 16% stock, Electron Microscopy Sciences # 50980487) and quenched with 150uL of 0.1 M glycine in 1xPBS for 5 minutes. Blocking was performed with 3% BSA in PBS in 0.2% Triton X-100 for one hour at room temperature.

To stain the cyst walls of any bradyzoites, rhodamine-conjugated *Dolichos biflorus* lectin (source) was applied at 1:250 for one hour at room temperature or overnight at 4°C. The sample was washed three times with PBS. After the final wash, 5 uL of the pellet was deposited onto a glass microscope slide and covered with a circular coverslip. Three samples of 5uL each were prepared per mouse brain homogenate. The slides were allowed to dry overnight on the benchtop before the coverslips were sealed on the rims with nail polish.

E. Quantification of mouse brain cysts

For each mouse brain, all three IFA samples were scored for the number of cysts using the Nikon Eclipse 80i 37 fluorescent microscope. Structures within the brain homogenates that were lectin-positive and spherical or ovoid with distinct smooth outer “lectin rims” were counted as cysts. Total cyst burden approximates per brain were calculated from individual slide counts as previously described in (169).

VI. Yeast two-hybrid library construction

A. General schematic

The yeast two-hybrid (Y2H) assay is an approach that identifies interaction between two proteins. It utilizes the reconstitution of a yeast transcription factor upon interaction of two proteins – the “bait” and the “prey.” The bait protein is fused to the DNA-binding domain of the yeast transcription factor, and the prey is fused to the activation domain. Interaction of bait and prey reconstitutes the transcription factor, allowing recruitment of transcriptional machinery for the expression of a reporter gene that allows growth of yeast colonies on selective media. The Y2H system described in this thesis employs activation of yeast transcription factor LexA following interaction of LexA DNA-binding domain and Gal4 activation domain (**Figure 6**). The reporter gene is *His3* (imidazoleglycerol-phosphate dehydratase), which allows yeast growth on histidine-lacking medium (170).

Full-length AP2IX-4 protein was prepared as bait by fusing AP2IX-4 to the LexA DNA-binding domain. The prey library was developed from cDNA that was generated from RH total RNA (see **Section B** below). Synthesis of cDNA was accomplished using random primers (Petra Tafelmeyer of Hybrigenics, personal communication, March 8, 2017). Adapters were then appended to the cDNA, and adapter-ligated cDNA fragments were inserted at the *Sfi*I restriction site downstream of the Gal4 activation domain in the pP6 library vector. The average sizes of the inserts were 1,500 nucleotides (Petra Tafelmeyer of Hybrigenics,

personal communication, March 8, 2017). Tests for bait auto-activation and toxicity, construction of the prey library via fusion of prey cDNAs to the Gal4 activation domain, and screening was performed by Hybrigenics Services (<https://www.hybrigenics-services.com>).

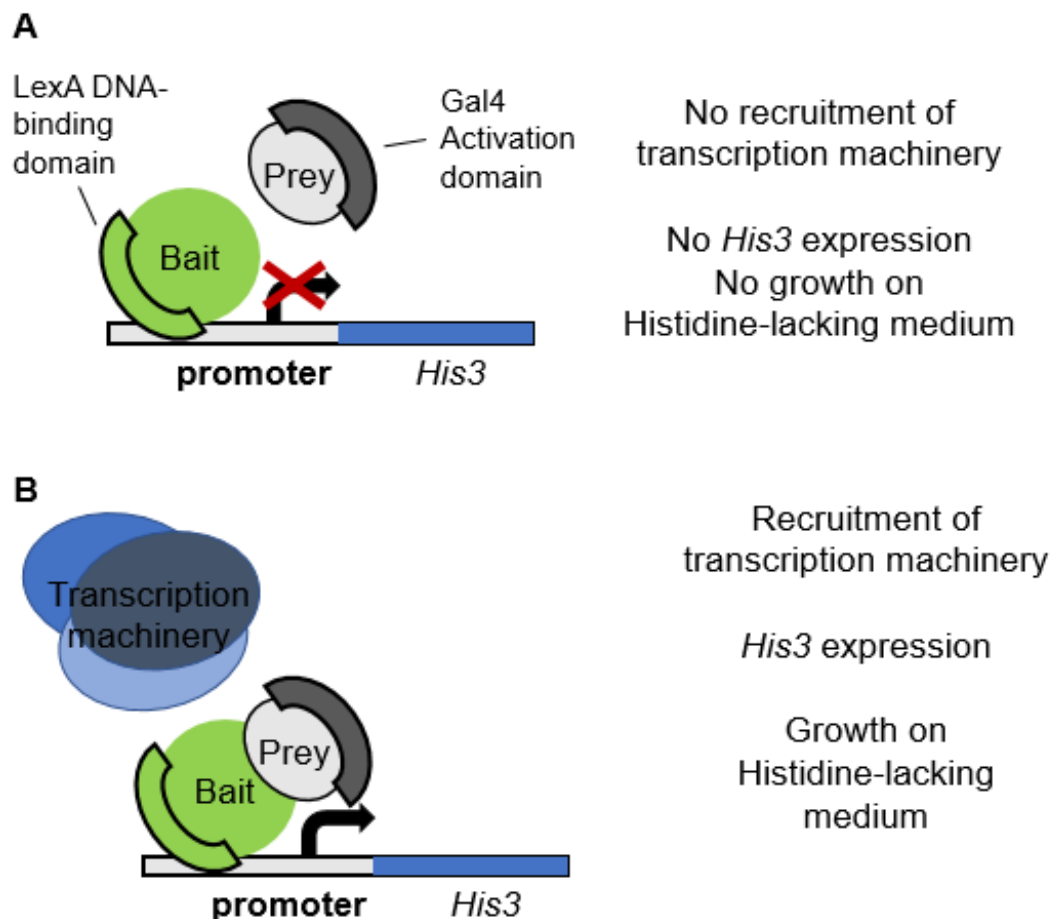


Figure 6. Schematic of yeast two-hybrid concept. Top panel (A). In the absence of a bait-prey interaction, the Gal4 activation domain remains separate from the LexA DNA-binding domain and no recruitment of transcription machinery occurs. **Bottom panel (B).** Reconstitution of the transcription factor by bait-prey interaction results in recruitment of transcription machinery allowing *His3* expression.

To test for auto-activation, yeast cells transformed with bait plasmid were spread on plates lacking tryptophan (to select for the bait plasmid) and lacking histidine. The plates also contained 3-aminotriazol (3-AT) at a concentration of 5 mM. 3-AT is a competitive inhibitor of the product of *His3* gene, a protein called imidazole glycerol phosphate dehydratase which allows yeast growth on histidine-deficient plates (171). To overcome 3-AT inhibition and to grow on the selective medium, yeast cells must express sufficient levels of *His3* (171). In turn, the expression levels of *His3* depend on the strength of the interaction between bait and prey, with stronger interactions allowing for increased promoter activation resulting in increased *His3* (171). Thus, higher levels of 3-AT reduce auto-activation while lower levels promote identification of low-affinity interactions (171). Yeast cells transformed with the AP2IX-4 bait plasmid did not grow on plates with 5 mM 3-AT, suggesting that auto-activation was insignificant at this concentration of 3-AT.

Next, an optimal concentration of 3-AT for the screen was determined; lower concentrations of 3-AT are more amenable to yeast growth and potential false-positives, while higher concentrations are limiting to yeast growth and may potentially mask bait and prey interactions. Yeast containing bait plasmid and yeast containing prey plasmid were mated, and the mating reactions were spread on plates lacking three amino acids ("DO-3 medium" for Drop Out with 3 Amino Acids): tryptophan (to select for bait plasmid), leucine (to select for prey plasmid), and histidine (to select for interaction). The plates contained either 0.5 mM, 1 mM, 2 mM, 5 mM or no 3-AT. In this AP2IX-4 3-AT optimization test, 27 clones

grew on the plates lacking 3AT, while only 4 clones grew on plates with 0.5 mM. Thus, 0.5 mM 3-AT was selected as the optimal 3-AT concentration.

Bait toxicity was tested by plating one set of mating reactions on full medium, containing all amino acids, and another set on medium with all amino acids except tryptophan (to select for the bait plasmid). If the bait is not toxic, approximately the same number of colonies should grow on both plates. If the bait is toxic, fewer colonies will grow on the tryptophan-lacking plate. The AP2IX-4 bait did not exhibit toxicity. This was consistent with the high number of colonies tested in the full-screen, which was more than 50 million (Petra Tafelmeyer of Hybrigenics, personal communication, February 10, 2017).

A total of 54 million colonies in the AP2IX-4 yeast two-hybrid screen were tested, representing 5-fold coverage of the library, and a total of 343 clones grew successfully on DO-3 medium and were sequenced (Valerie Hindie of Hybrigenics, personal communication, October 13, 2016). Out of these 343, there were a total of 58 independent hits, and these were ranked by the “predicted biological scores (PBS).” The PBS score considers the frequency of interactions observed with each prey fragment, the distribution of reading frames and stop codons in the prey sequence, and any interactions confirmed by other screens (172). Numerically, it ranges from 0 to 1, and is an indication of the probability of a non-specific interaction. The range of PBS scores is separated by letters indicating each score range: $A < 1e-10 < B < 1e-5 < C < 1e-2.5 < D < 1$ (172). PBS D hits represent those whose interaction was detected by one prey fragment, suggesting either a true interaction from a protein expressed from a

low-expression mRNA in the prey library or a false-positive interaction (172). PBS E and F categories were added by Hybrigenics (173); PBS E hits represent those containing protein domains that have been mapped to with numerous interactions with proteins in a human protein database, while PBS F hits represent artifacts of the Y2H assay, such as proteins that bound to LexA, Gal4, or DNA sequences upstream of the reporter gene (173).

B. Preparation of total RNA

1 mg of total RNA for the generation of prey cDNA in the Y2H screen was prepared from wild-type RH. RH parasites were seeded onto confluent HFF monolayers in T150cm² flasks and grown to the intracellular, 48 parasite-per-vacuole stage. Parasites were harvested by scraping the infected HFF monolayer and passing the culture through a 25-gauge syringe needle. HFF debris was separated from the parasites by passing the syringe-lysed mixture through a 3-micron pore filter. Parasites were pelleted by centrifugation at 3000xg, 4°C for 10 minutes. Total RNA isolation was performed using TRIzol Reagent (Thermo Fisher #15596026) according to manufacturer's protocol (https://tools.thermofisher.com/content/sfs/manuals/trizol_reagent.pdf). DNase treatment was performed using the DNA-free kit (Thermo Fisher #AM1906) per manufacturer's protocol (https://tools.thermofisher.com/content/sfs/manuals/cms_055739.pdf).

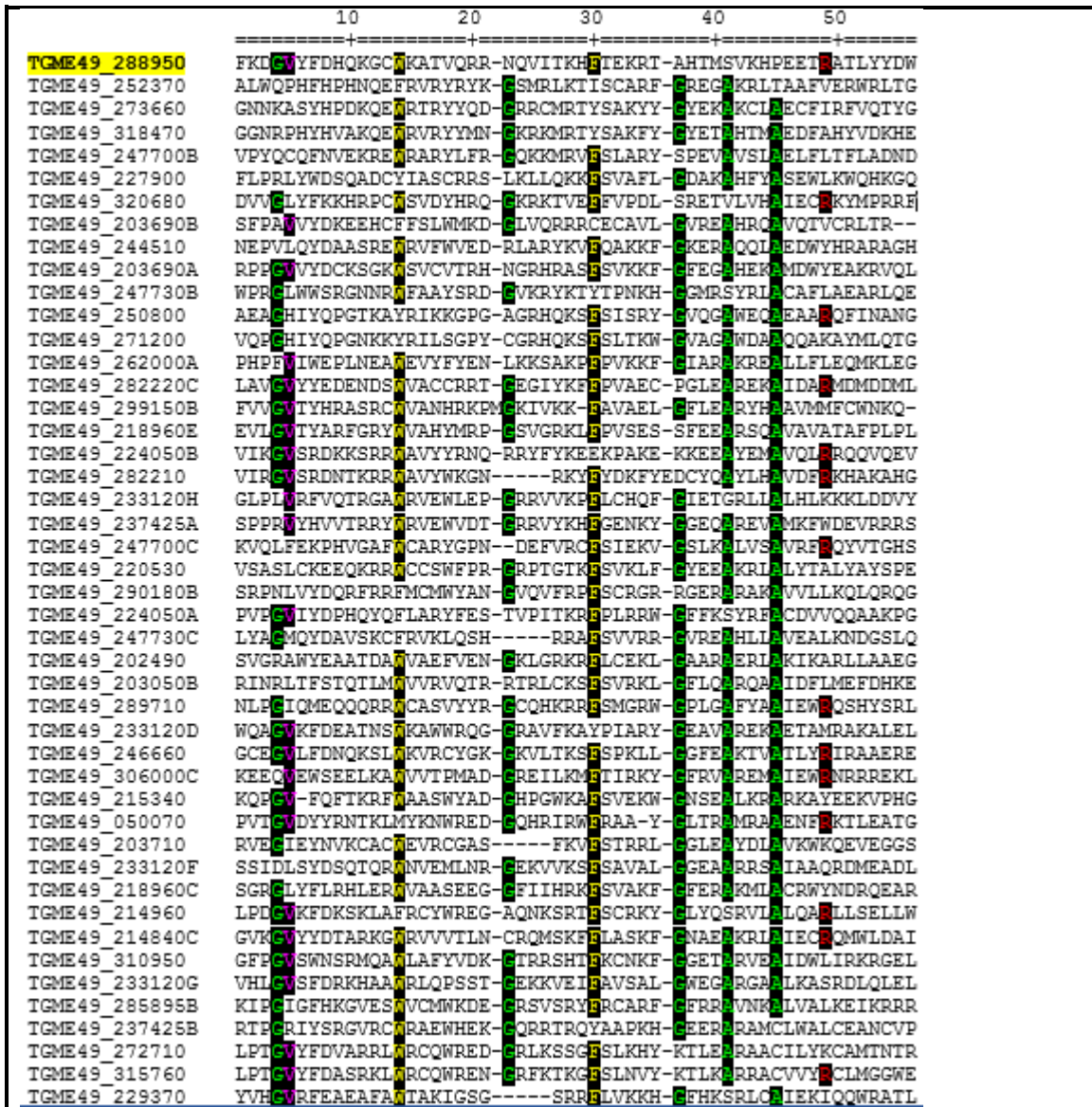
CHAPTER 3: RESULTS

A previous study employed microarray analysis to measure the transcript expression of *T. gondii* genes during 12-hour time courses in the tachyzoite stage (109). Data from this study revealed that AP2IX-4 (TGME49_288950) exhibits cell cycle regulation, with transcript abundance peaking at the boundary between the S and M phase. AP2IX-4 is predicted to be a 2,856 bp intron-less gene located on chromosome IX (Toxodb.org). The protein mass of AP2IX-4 is predicted to be 104 kDa, and the protein sequence is composed of 951 amino acids that harbor a single predicted AP2 domain. No other protein domains were detected with SMART or Interpro algorithms, and there is no evidence for post-translational modifications on AP2IX-4.

I. Alignment and phylogenetic analysis of the predicted AP2 DNA-binding domain of AP2IX-4

We performed phylogenetic analyses of the AP2IX-4 protein sequence in collaboration with Dr. Chunlin Yang (Gustavo Arrizabalaga Lab, IUSM). BLAST searches performed on a 60-amino acid globular region C-terminal to the AT-hook DNA-binding motif in *Plasmodium* revealed that this globular region was conserved in other Apicomplexa as well (139). Secondary structure prediction performed on this globular region found that it includes a core of three consecutive β strands followed by an α helix, consistent with the secondary structure of AP2 DNA-binding domains found in plants (139). 68 AP2 domain-containing proteins are predicted in the *T. gondii* genome, with some proteins

containing multiple AP2 domains. To explore the relationships between the 103 total AP2 domains across *T. gondii* AP2 proteins, the amino acid sequences for the predicted AP2 domains were aligned using Gblock program, which aligns multiple sequences by conserved features that are organized into “blocks” (http://molevol.cmima.csic.es/castresana/Gblocks_server.html; 174). The results of the alignment are shown in **Figure 7**.



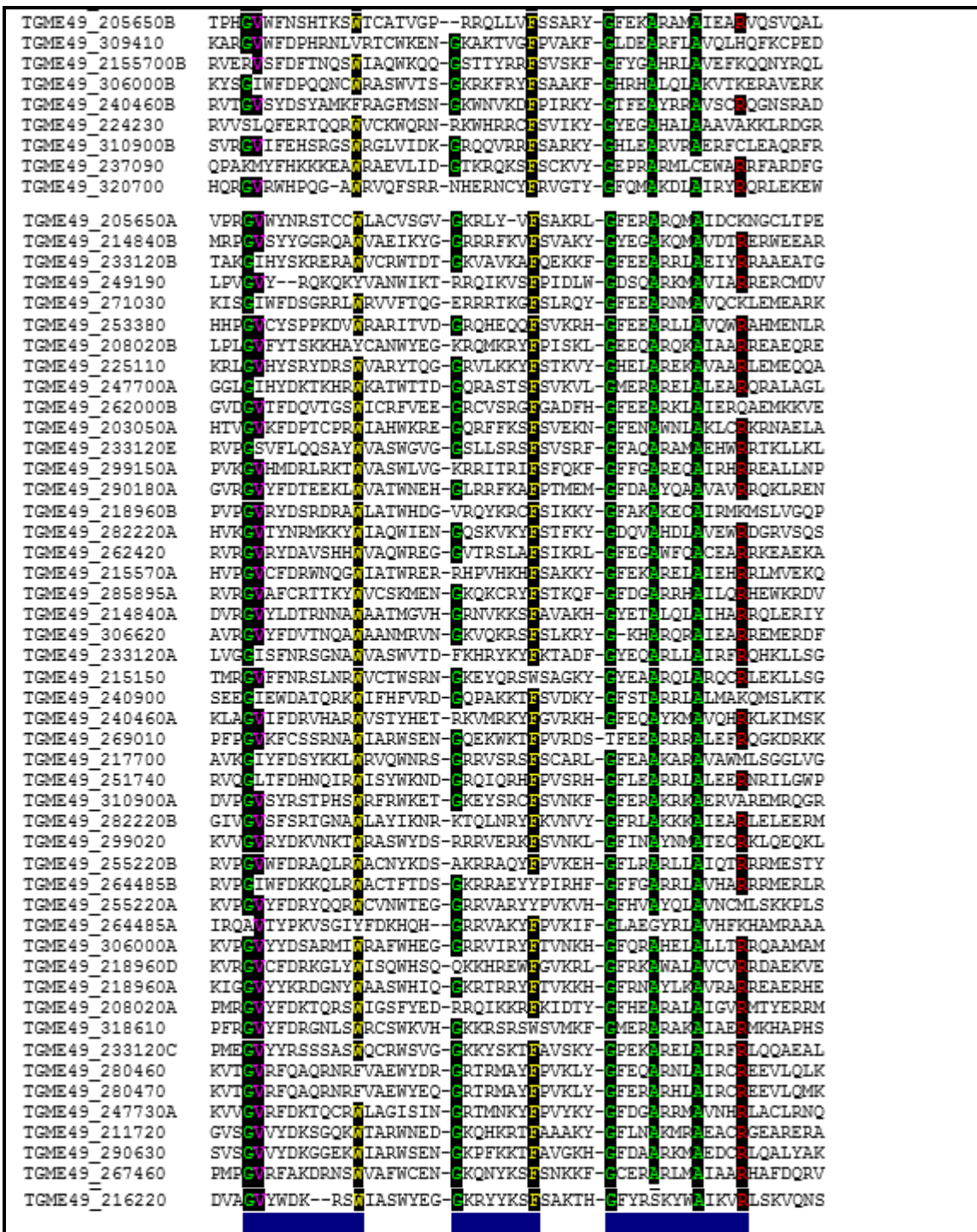


Figure 7. Amino acid sequence alignment of AP2 domain of AP2IX-4. The predicted AP2 domain of AP2IX-4 was aligned with the other 102 AP2 domains across the *T. gondii* genome. Conserved residues are highlighted in black. Blue bars at the bottom of the alignment indicate the three alignment blocks. AP2IX-4 (TGME49_288950) is highlighted at the top of the list.

Compared to the 102 total AP2 domains across the other *T. gondii* AP2 proteins, the predicted AP2 domain of AP2IX-4 was revealed to contain conserved glycine, valine and tryptophan residues in the first alignment block and a conserved phenylalanine residue in the second block. The third alignment block is missing all conserved residues except for an arginine residue. JPRED 4 algorithms (<http://www.compbio.dundee.ac.uk/jpred4/index.html>; 175) were used to identify any secondary structures in the amino acid sequence of the AP2 domain of AP2IX-4. AP2IX-4 was determined to include three β strands followed by a C-terminal α helix, congruent with the secondary structures of the AP2 domains found in *Plasmodium* (139, **Figure 8**).

```

FKDGVYFDHQKGCWKATVQRRNQVITKHFTEKRTAHTMSVKHPEETRA
      TLYYDW
-----EEE-----EEEEHH---HEEEEEEE-----HHHHHHHHHHHHHHHE---

```

Figure 8. Predicted secondary structures in the AP2IX-4 AP2 domain.

JPRED algorithms were used to predict the secondary structures in the amino acid sequence of AP2IX-4 following multiple alignment of the amino sequences of the 103 AP2 domains predicted across the 68 AP2 proteins in the *T. gondii* genome. The program assigns each amino acid as belonging to a β sheet (“E”), an α helix (“H”) or neither β sheet or α helix (“-”).

The GBlock alignment of the 103 *T. gondii* AP2 domains was inputted into the PhyML 3.0 program (<http://www.atgc-montpellier.fr/phyml/>; 176) to construct a phylogenetic tree using the likelihood-based statistical method (**Figure 9**). The AP2 domain of AP2IX-4 (TGME49_288950) clustered with the AP2 domain of AP2X-10 (TGME49_215340), the most C-terminal AP2 domain (483 aa-538 aa) of AP2IX-8 (TGME49_306000), and the AP2 domain of AP2IV-2 (TGME49_320680). AP2X-10 (TGME49_215340) transcripts are upregulated

during *in vitro* and *in vivo* bradyzoite induction (103, 159), and AP2IV-2 (TGME49_320680) expression is elevated during chronic infection in mice (159). Thus, the amino acid alignment and phylogeny tree revealed conserved features and secondary structures of the AP2 domain of AP2IX-4.

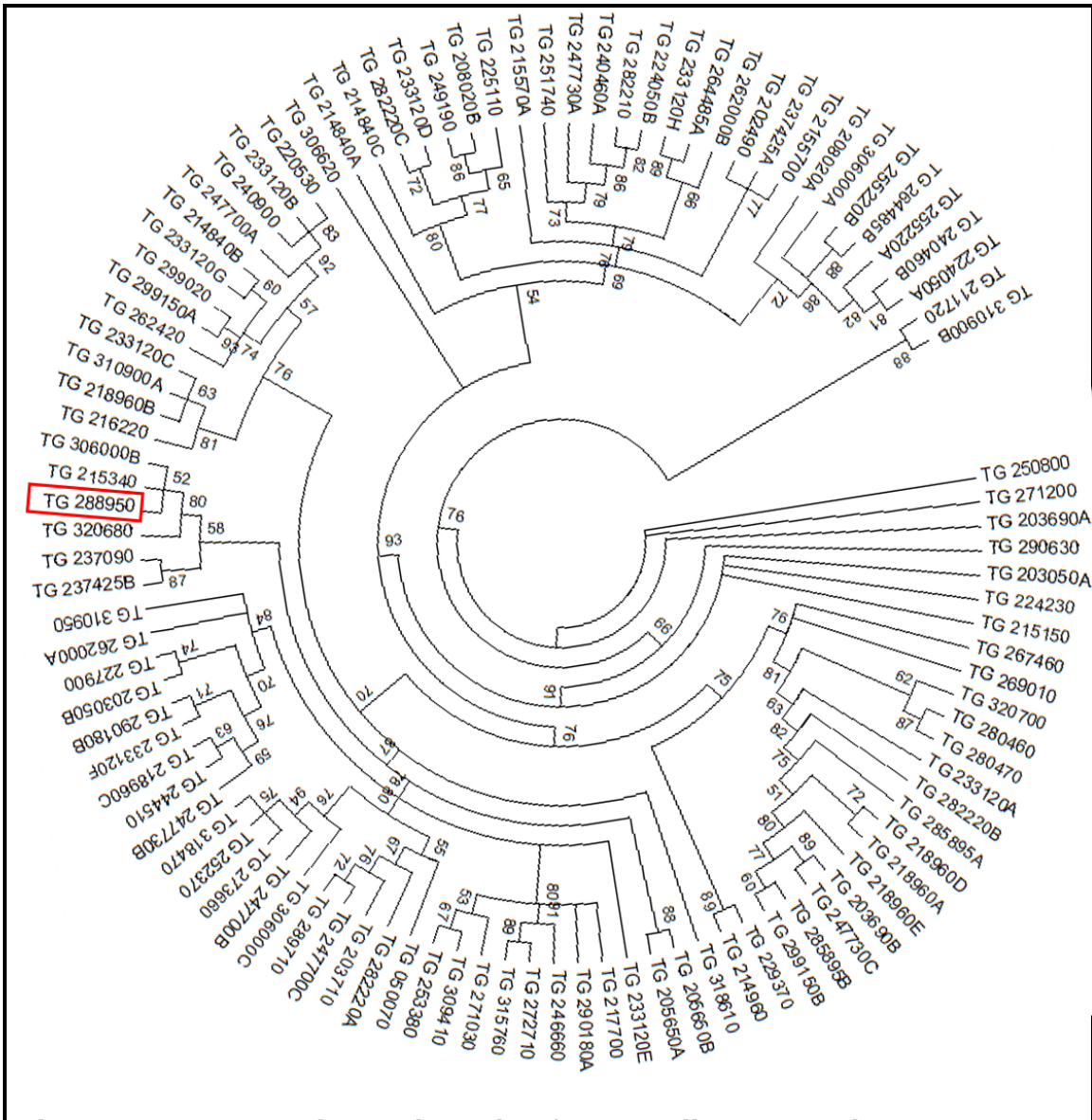
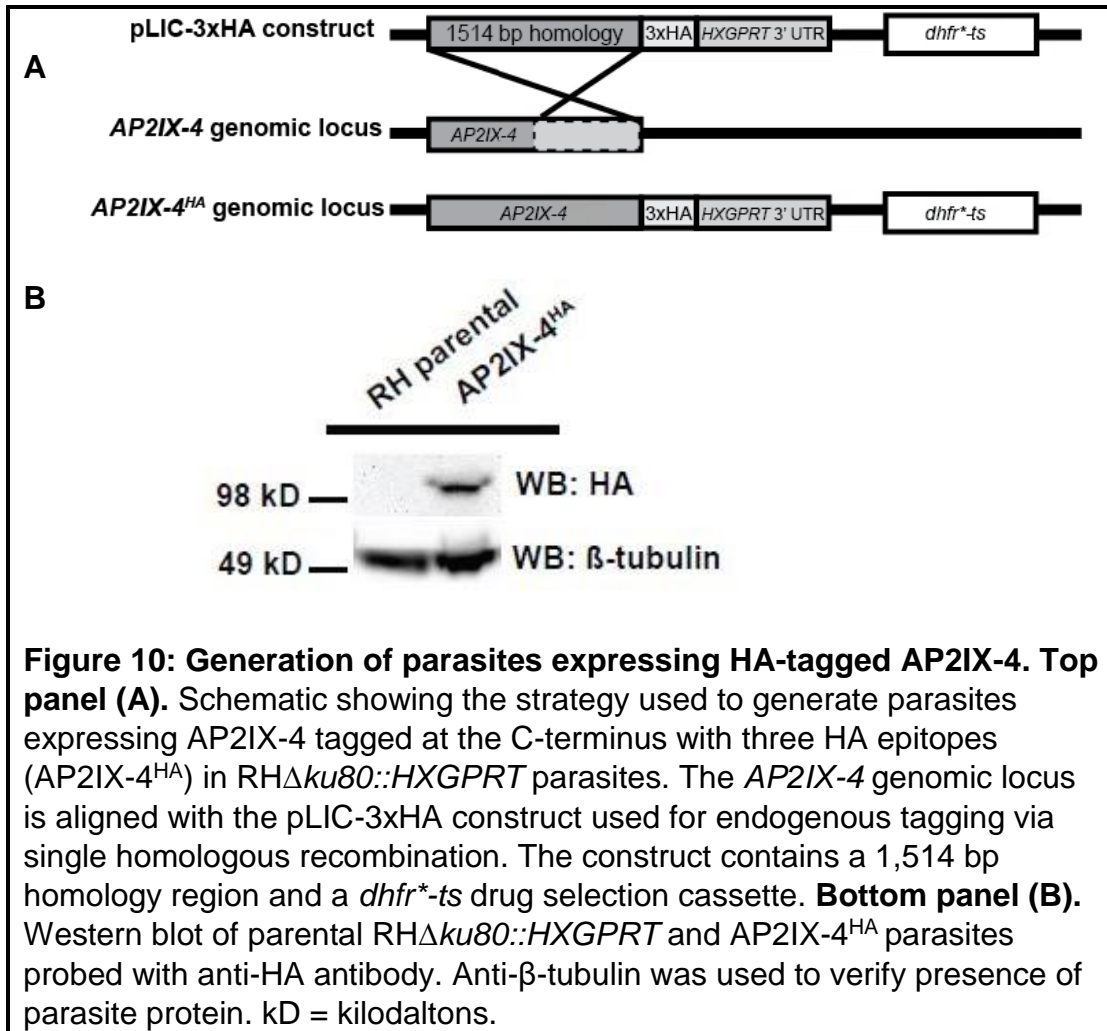


Figure 9. Phylogenetic relationship of *T. gondii* AP2 domains. A phylogeny tree was constructed with PhyML 3.0 using the likelihood-based method and visualized using the MEGA 7.0.20 software. Branch numbers represent the percentage the branch point occurred out of all assembled trees. The accession numbers for the *T. gondii* reference strain ME49 are given. AP2IX-4 (TGME49_288950) is boxed in red.

II. The predicted and confirmed protein size of AP2IX-4

Our first aim was to validate the predicted protein size and examine the protein expression pattern of AP2IX-4. Towards this goal, a previous postdoctoral fellow in the Sullivan Lab, Dr. Ting-Kai Liu, tagged endogenous AP2IX-4 with three tandem HA epitopes on its C-terminus in *RH Δ ku80::HXGPRT* parasites. The loss of the non-homologous end-joining repair enzyme KU80 in these parasites facilitates homologous recombination, allowing more efficient allelic replacement of the endogenous *ap2IX-4* locus (161). Construct pLIC-AP2IX-4-3HA-DHFRTS was engineered to contain the last 1,514 bp of the *AP2IX-4* genomic sequence followed by the three HA tags, allowing integration of the epitope sequences at the *AP2IX-4* genomic region (**Figure 10A**). The construct contained a DHFR*-TS drug selection cassette which confers resistance to pyrimethamine and was transfected into *RH Δ ku80::HXGPRT* parasites, and transgenic clones were selected for with pyrimethamine and isolated through limiting dilution cloning. IFA was used to screen for parasites containing nuclear HA signal. One parasite clone that demonstrated nuclear HA signal was named AP2IX-4^{HA} and subjected to further analysis by Western blot. Probing with anti-HA antibody in the Western blot analysis revealed a single band at 112 kDa, which matched the predicted 3xHA-tagged protein size (**Figure 10B**). Anti- β -tubulin antibody was used as a gel loading control. The generation of the AP2IX-4^{HA} parasite line confirmed the Toxodb.org prediction for the protein size of AP2IX-4 and allowed further examination of protein expression pattern through the tachyzoite cell cycle by IFA.



III. AP2IX-4 is expressed in the parasite nucleus during the S-M phase of the tachyzoite cell cycle

AP2IX-4^{HA} parasites were employed to study the protein expression of AP2IX-4 through the parasite cell cycle. IFAs were performed to detect subcellular localization throughout the tachyzoite cell cycle, using co-staining with Inner Membrane Complex-3 (IMC3) antibody to help delineate cell cycle stages. IMC3 is part of a group of structural, filament proteins called alveolins which are located in the subpellicular network underneath the parasite plasma membrane

(177). The IMC proteins lend the parasite structural stability. IMC3 is enriched in budding daughter cells during late S phase through cytokinesis, so it is a useful marker for tracing parasites undergoing daughter cell formation (178).

In our IFA results, AP2IX-4^{HA} protein localized to the parasite nuclei (**Figure 11, merged** panels). Co-staining with IMC3 identified parasites in various cell cycle phases in a population: G1 or S phase parasites exhibited fainter IMC3 enrichment at the parasite membrane and absence of budding daughter cells, while late S/M parasites exhibited the beginning of daughter cell formation, and parasites undergoing mitosis or cytokinesis exhibited more complete daughter cell formation (**Figure 11, IMC3** panel). Using IMC3 co-staining, we found that AP2IX-4^{HA} was undetectable in the G1 phase, appeared during the S-M stages, then decreased in expression during cytokinesis (**Figure 11**). Therefore, the protein expression of this factor is consistent with its reported mRNA profile. In addition, we noted that in parasite vacuoles positive for the factor, expression was homogenous amongst all tachyzoites within the vacuole.

IV. AP2IX-4 is dispensable for *in vitro* tachyzoite replication

Dr. Ting-Kai Liu generated a gene knockout of *AP2IX-4* in the Prugniaud (Pru) parasite background by replacing the endogenous *AP2IX-4* gene coding region using double homologous recombination with the DHFR*-TS selectable marker. The allelic replacement vector shown in **Figure 12A** was transfected into the Pru parasite strain lacking KU80 (henceforth abbreviated PruQ).

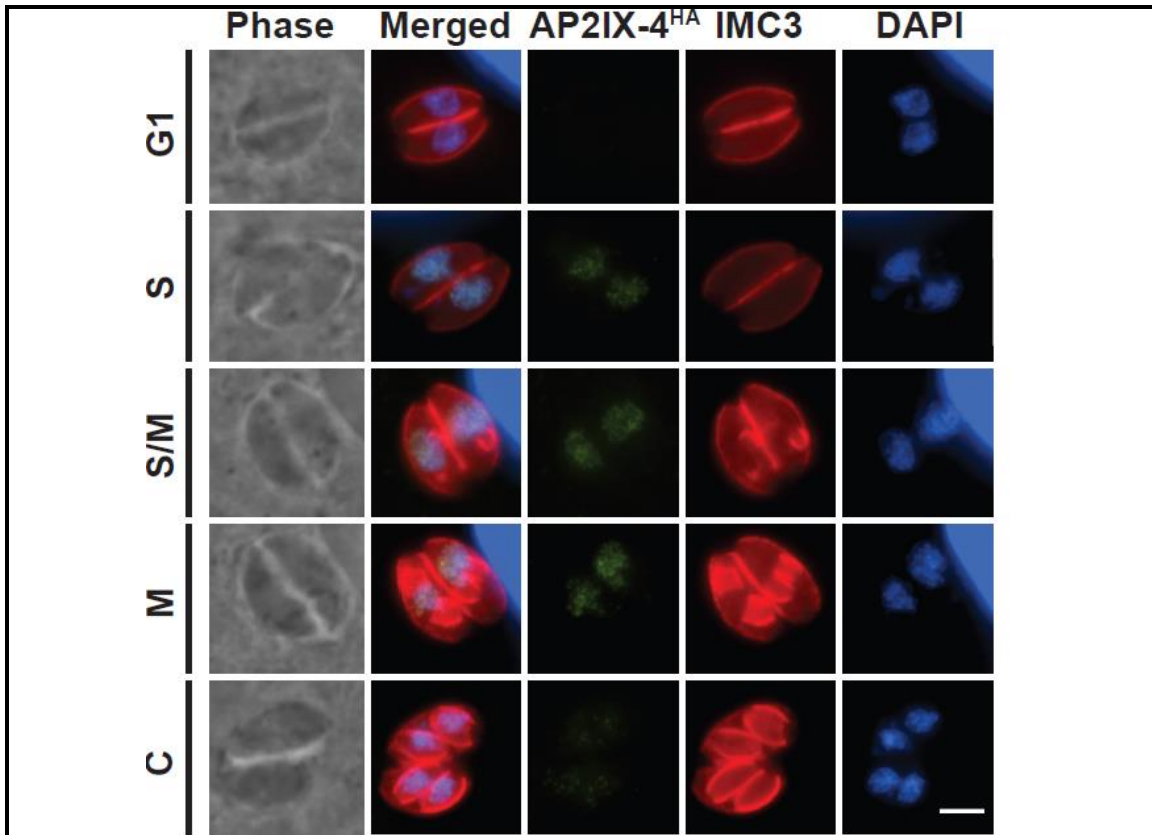
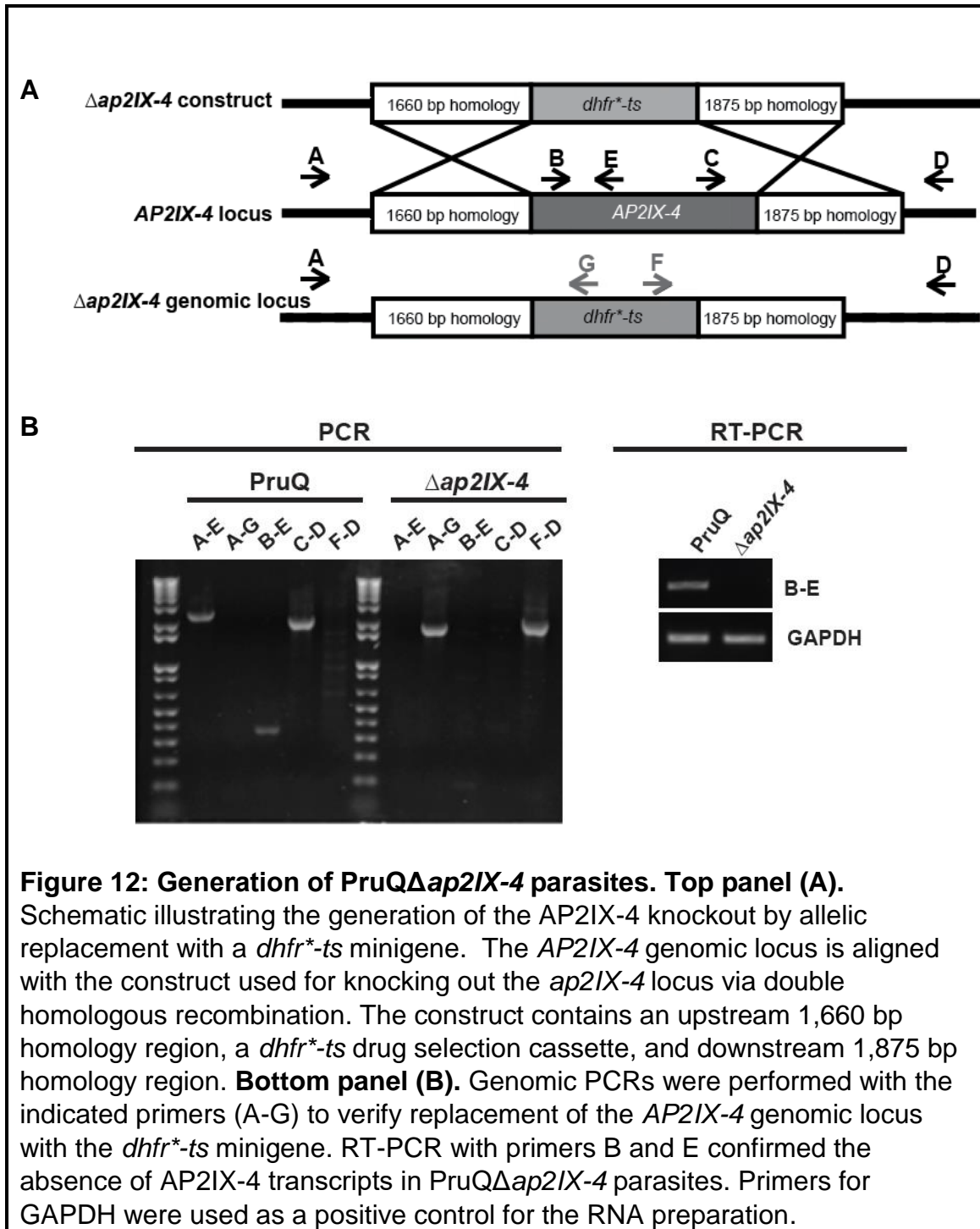
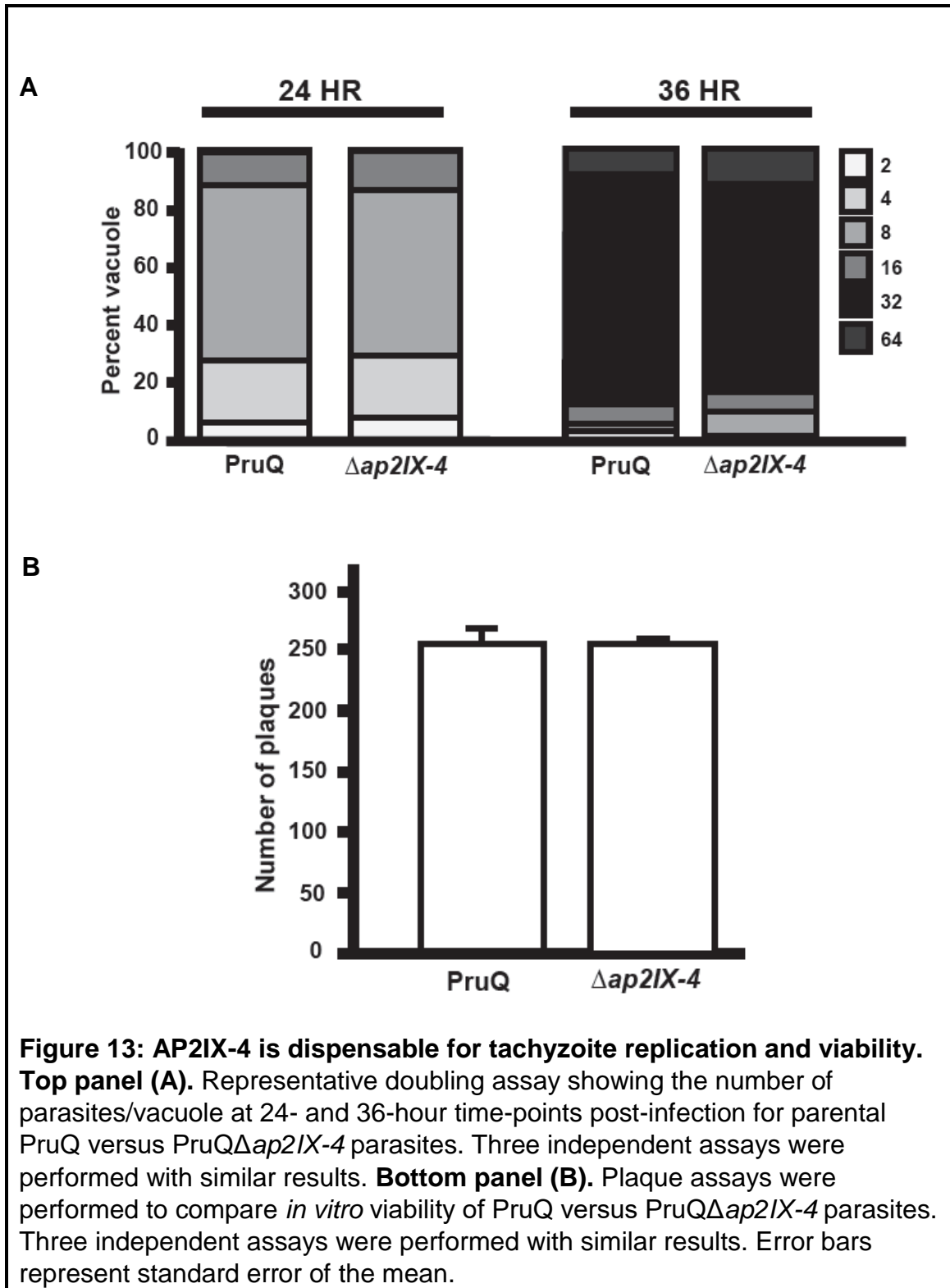


Figure 11: AP2IX-4 is localized to the parasite nucleus and expressed predominantly in the S and M phases. IFAs were performed on AP2IX-4^{HA} tachyzoites using anti-HA (green). To monitor cell cycle phases, parasites were co-stained with anti-IMC3 (red) and DAPI (blue). G1, gap phase; S, synthesis phase; M, mitotic phase; C, cytokinesis. Scale bar = 3 microns.





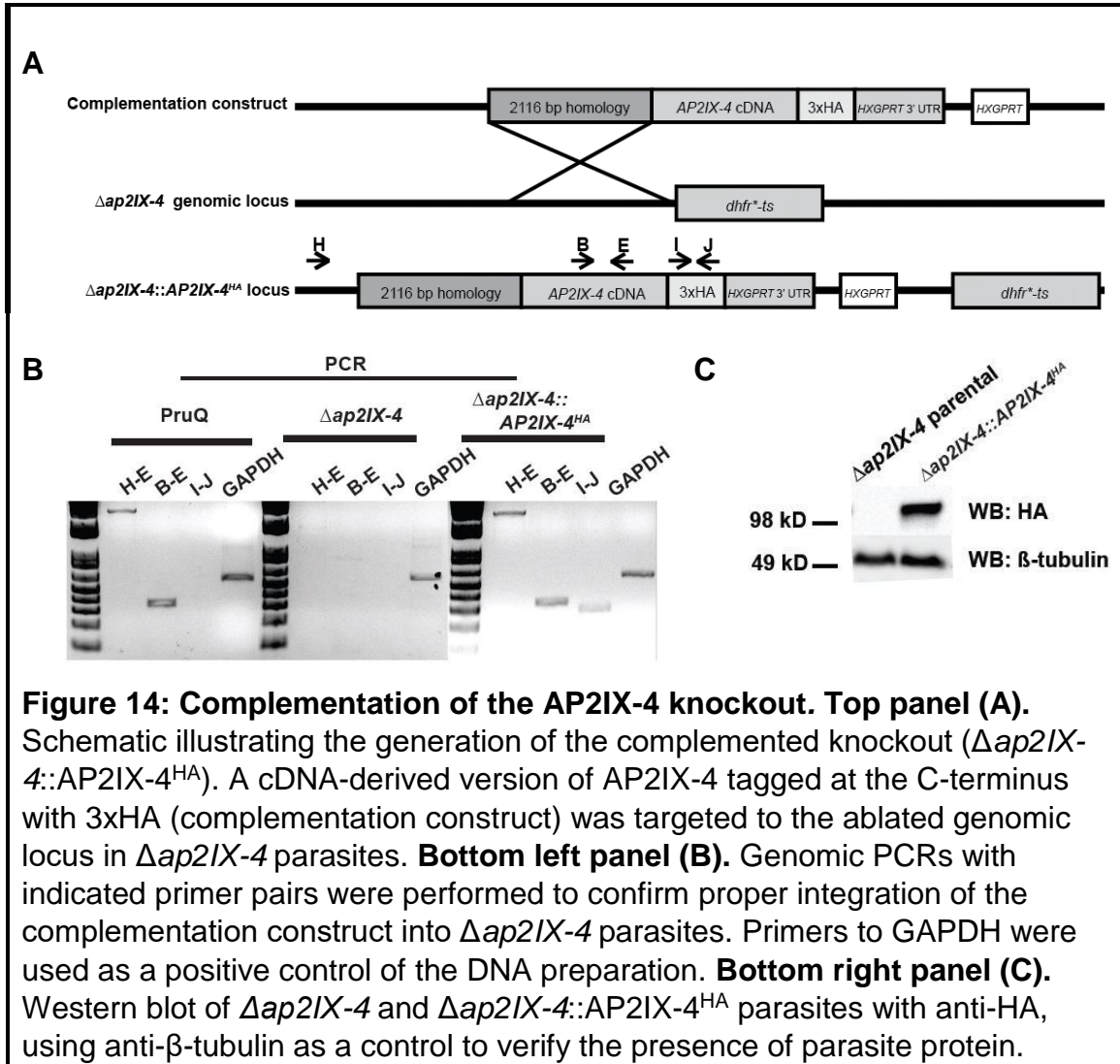
The generation of the parasite lines containing a deletion of AP2IX-4 allowed us to investigate the role of AP2IX-4 in *T. gondii*. Following the isolation of transgenic parasite clones via limiting dilution, genomic PCRs were performed to screen for *ap2IX-4* knockout parasites (**Figure 12B**, primer set **B-E**). Primer sets were also designed to confirm integration of the DHFR*-TS selection cassette at the *AP2IX-4* genomic locus (**Figure 12B**, primer sets **A-G** and **F-D**). Figure 12B shows the results confirming successful allelic replacement of the *AP2IX-4* gene in the PruQ background (named $\Delta ap2IX-4$). RT-PCR was performed on mRNA harvested from $\Delta ap2IX-4$ parasites to verify loss of transcript (**Figure 12B**).

Parasite replication rates were determined using a doubling assay (**Figure 13A**) and viability was examined using a plaque assay (**Figure 13B**). Neither assay revealed a significant difference in the *in vitro* growth between parental and $\Delta ap2IX-4$ parasites in the PruQ strain (**Figures 13A-B**). These results suggest that, despite its appearance during the S-M stages of the cell cycle, AP2IX-4 is not required for tachyzoite replication.

V. AP2IX-4 is expressed throughout bradyzoite development

Previous evaluation of the transcript expression of cell cycle-regulated AP2 proteins during *in vitro* bradyzoite induction conditions revealed a near three-fold elevation of AP2IX-4 transcripts in the type II strain ME49 (142). AP2IX-4 transcript was elevated as well during chronic infection of mice (146). To examine the function of AP2IX-4 in bradyzoites, we complemented the

PruQ Δ *ap2IX-4* parasites with a cDNA-derived version of AP2IX-4 tagged with HA at its C-terminus to be expressed under the native *AP2IX-4* promoter (**Figure 14A**). Genomic PCRs using primer sets spanning *AP2IX-4* and its flanking genomic loci confirmed integration of the complementation construct at the disrupted *AP2IX-4* locus (**Figure 14B**).



To validate the predicted size of AP2IX-4, Western blot analysis was performed on this transgenic line. As shown in **Figure 14C**, Western blot analysis confirmed the expected size of the AP2IX-4^{HA} protein to be 112 kDa taking into

account the three tandem HA epitopes. In addition, IFA analysis of the complemented knockout line demonstrates that AP2IX-4^{HA} in tachyzoites is properly localized to the nucleus and matches the cell cycle-regulated pattern we observed in the type I parasites containing endogenously tagged AP2IX-4, whereby peak expression occurs during the S-M phase of the cell cycle (**Figures 11 and 15**). Together, these data confirm the fidelity of the complemented knockout and uncover no differences in localization or cell cycle regulation of AP2IX-4 between type I and type II strains.

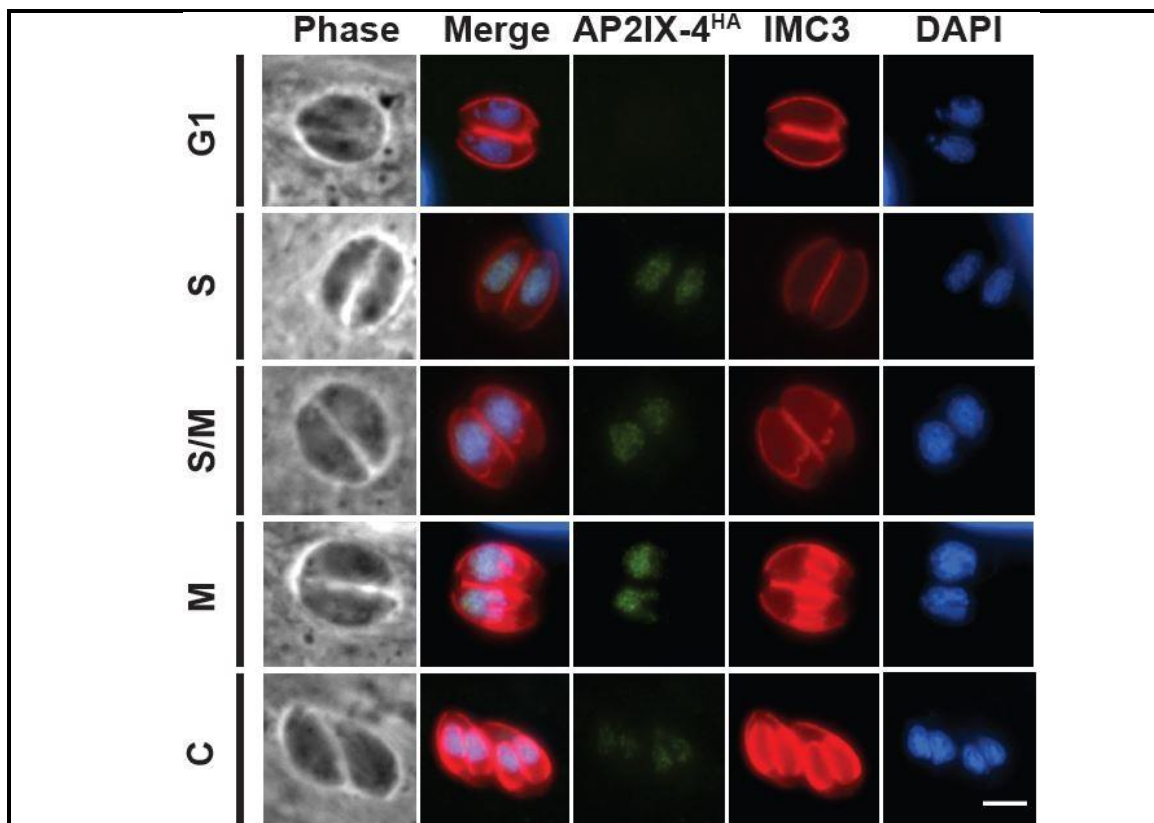
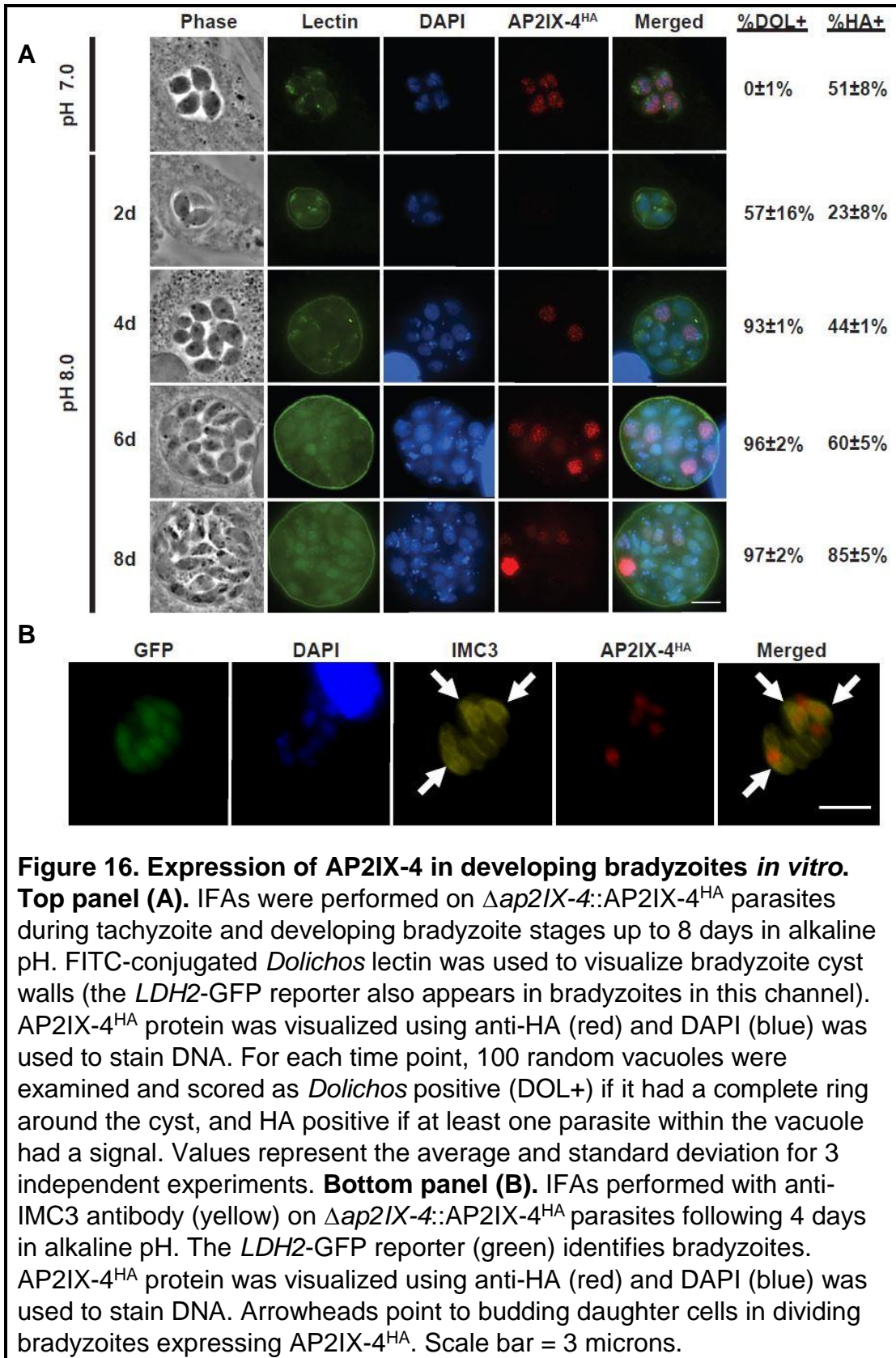


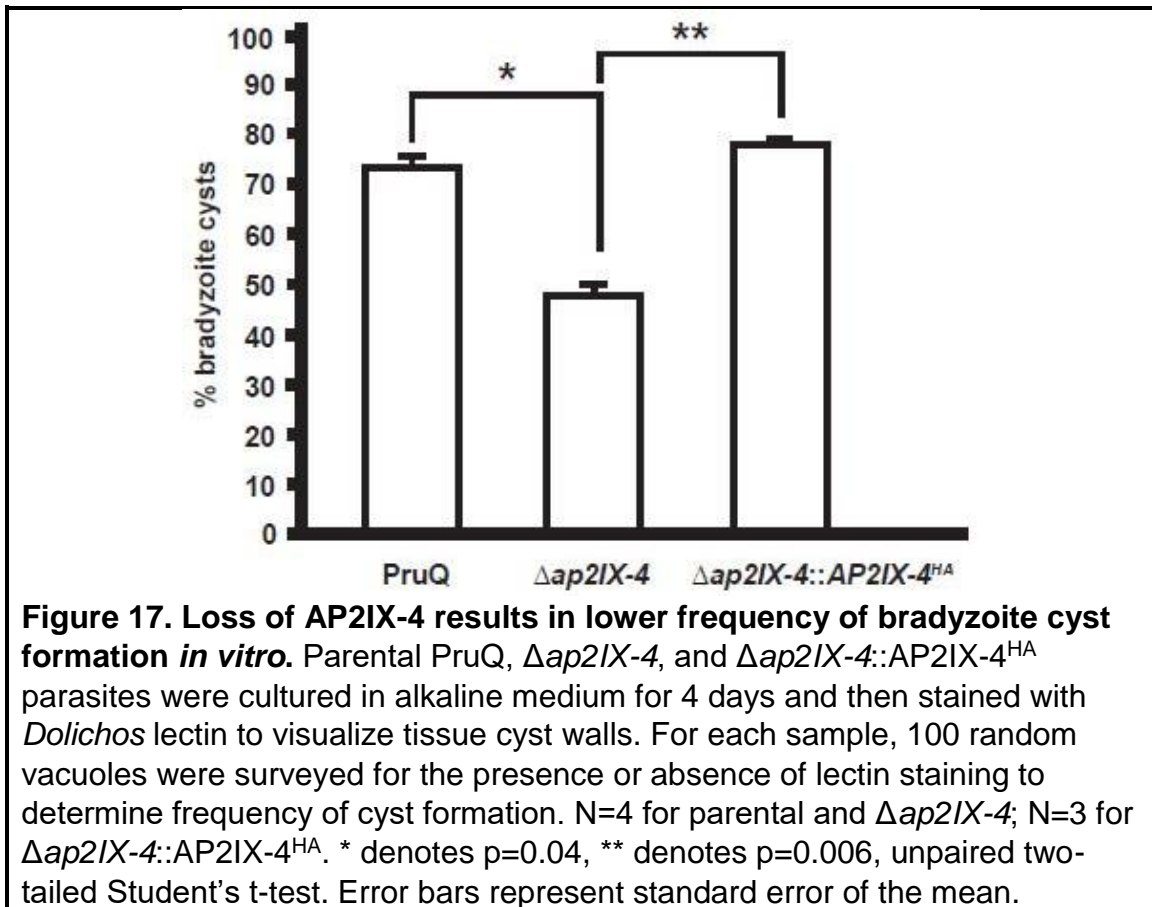
Figure 15: Expression of AP2IX-4 in $\Delta ap2IX-4::AP2IX-4^{HA}$ tachyzoites. IFAs were performed on $\Delta ap2IX-4::AP2IX-4^{HA}$ tachyzoites as described in **Figure 11**. AP2IX-4^{HA} was detected using anti-HA (green). To monitor cell cycle phases, parasites were co-stained with anti-IMC3 (red) and DAPI (blue). G1, gap phase; S, synthesis phase; M, mitotic phase; C, cytokinesis. Scale bar = 3 microns.

To study the expression of AP2IX-4^{HA} in bradyzoites, $\Delta ap2IX-4::AP2IX-4^{HA}$ parasites were examined at two-day intervals during bradyzoite-induction (**Figure 16A**, performed by postdoctoral fellow Michael Holmes). Parasites were subjected to alkaline stress for two, four, six and eight days. For comparison, an IFA was also performed on the transgenic line under tachyzoite conditions. *Dolichos* lectin staining was performed to identify the cysts encasing the bradyzoites. AP2IX-4^{HA} expression was detected in a subset of the cysts in the culture and localized to the bradyzoite nucleus. In addition, AP2IX-4^{HA} expression was heterogeneous and confined to a subset of the bradyzoites within each cyst. Although the proportion of cysts containing at least one parasite expressing AP2IX-4^{HA} increased from day two through day eight of bradyzoite differentiation, only 16% of the total number of bradyzoites within each cyst expressed AP2IX-4^{HA}. This suggested the possibility that the factor may be expressed in the subset of parasites that are dividing within the cyst. To test this idea, we co-stained anti-HA with IMC3 (**Figure 16B**). The IMC3 co-stain revealed that parasites expressing AP2IX-4^{HA} are in the process of forming budding daughter cells. In addition, the presence of AP2IX-4^{HA} was accompanied by GFP expression that was driven ectopically under the bradyzoite-specific LDH2 promoter in these parasites. Together, these observations suggest that AP2IX-4^{HA} expression continues to be cell cycle-regulated during encystation and that its expression is present within dividing parasites that express the GFP bradyzoite marker.



VI. Deletion of AP2IX-4 reduces *in vitro* bradyzoite cyst efficiency

We next compared the frequency of bradyzoite cyst development in PruQ and $\Delta ap2IX-4$ parasites grown in alkaline induction conditions for four days. We employed staining with *Dolichos biflorus* lectin to identify bradyzoite cyst walls, recording the number of positive-staining cysts in 100 vacuoles sampled randomly. After four days in alkaline pH, 73% of parental PruQ parasites converted into bradyzoites, but this was reduced to 46% in parasites lacking AP2IX-4 (Figure 17). Complementation of the AP2IX-4 knockout parasites restored the rate of bradyzoite cyst formation to levels matching the parental PruQ strain. These data show that ablation of AP2IX-4 impairs the frequency at which cysts form *in vitro*.



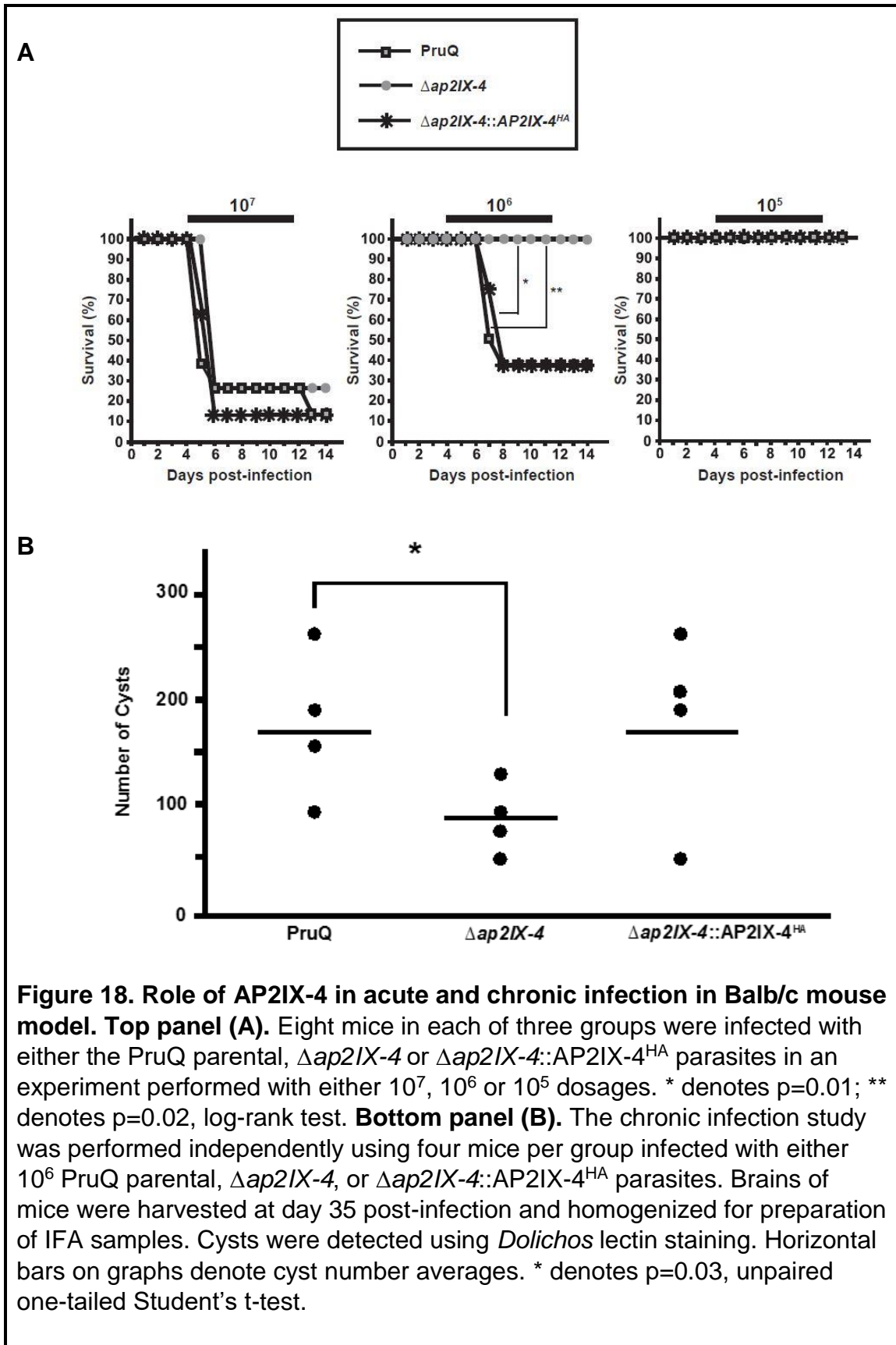
VII. Analysis of $\Delta ap2IX-4$ in mouse models of acute and chronic toxoplasmosis

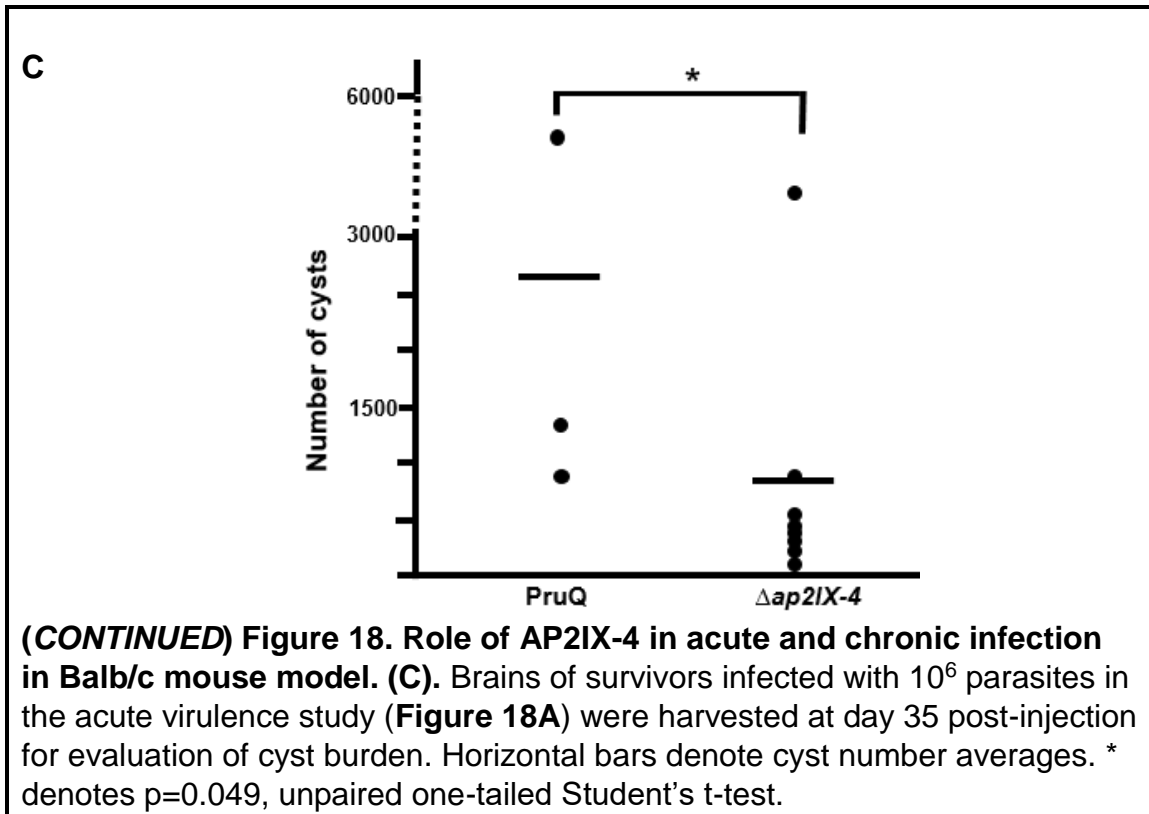
To determine the role of AP2IX-4 in *in vivo* pathogenesis, female Balb/c mice were infected with either PruQ, $\Delta ap2IX-4$ or $\Delta ap2IX-4:AP2IX-4^{HA}$ parasites and monitored daily for survival for up to two weeks. In this acute virulence study, inocula of 10^7 , 10^6 , and 10^5 parasites were employed to encompass the highly lethal (10^7), intermediate (10^6) and sub-lethal (10^5) dosages. By day six post-injection, at least 75% of mice infected with 10^7 parasites for all strains had perished (**Figure 18A**). At the end of the study, there was no significant difference in survival between mice infected 10^7 PruQ, $\Delta ap2IX-4$ or $\Delta ap2IX-4:AP2IX-4^{HA}$ parasites. All mice infected with each of the three strains at a dosage of 10^5 parasites survived the course of acute infection. However, while five mice died in both groups of mice infected with 10^6 PruQ or 10^6 $\Delta ap2IX-4:AP2IX-4^{HA}$ parasites, all mice infected with 10^6 $\Delta ap2IX-4$ parasites survived (**Figure 18A**). This suggests that the loss of *ap2IX-4* confers a modest virulence defect in $\Delta ap2IX-4$ parasites.

To determine the role of AP2IX-4 in cyst development *in vivo*, a chronic infection study was performed independently using four mice per group infected with either 10^6 PruQ parental, $\Delta ap2IX-4$, or $\Delta ap2IX-4::AP2IX-4^{HA}$ tachyzoites. Mice infected with parental parasites contained an average of 169 brain cysts while those infected with $\Delta ap2IX-4$ yielded a significantly reduced average of 91 brain cysts. Complementation of $\Delta ap2IX-4$ reversed the phenotype, producing an average of 176 brain cysts (**Figure 18B**). Consistent with the reduced frequency

of bradyzoite development noted *in vitro*, these data suggest that loss of AP2IX-4 also results in decreased bradyzoite frequency *in vivo*.

A virulence defect in the $\Delta ap2IX-4$ parasites as observed in the acute virulence study (**Figure 18A**) may impact cyst frequency *in vivo*. For example, the decreased virulence in $\Delta ap2IX-4$ parasites may reduce the number of parasites successfully initiating bradyzoite development in the brains of the mice. Therefore, survivors of the acute infection phase of the experiment were sacrificed at day 35 and their brains harvested. The three surviving mice in the PruQ-infected group demonstrated an average cyst burden of 2,652 cysts, while the eight mice surviving in the $\Delta ap2IX-4$ group demonstrated significantly reduced average cyst burden of 711 (**Figure 18C**). Thus, the reduction in cyst burden in the brains of $\Delta ap2IX-4$ -infected acute virulence survivors is consistent with the reduction observed in the independent chronic infection study.





VIII. Loss of AP2IX-4 results in enhanced bradyzoite gene expression

To study how AP2IX-4 impacts the parasite transcriptome in response to alkaline stress, we collaborated with Drs. Joshua Radke and Dong-Pyo Hong (Michael White Lab, University of South Florida) to perform a microarray analysis on PruQ, $\Delta ap2IX-4$ and $\Delta ap2IX-4::AP2IX-4^{HA}$ parasites cultured in either tachyzoite (pH 7.6) conditions or 48 hours in bradyzoite (pH 8.2) conditions. Total RNA of cultured parasites was prepared in our laboratory, and generation of hybridization probes for the ToxoGeneChip and statistical analyses were performed by the White Lab.

Only 24 genes were differentially expressed two-fold or more between PruQ and $\Delta ap2IX-4$ parasites under tachyzoite conditions (**Table 4**). Three genes

(TGME49_239580, TGME49_312905, and TGME49_312905) encoding genes of hypothetical function, were upregulated in the $\Delta ap2IX-4$ compared to parental parasites. The rest of the genes were downregulated. These included bradyzoite surface antigens or cyst wall proteins such as MCP4, SRS35A/SAG4.2, and SRS13. The presence of bradyzoite proteins in tachyzoites may help “poise” the parasites for efficient differentiation; decreased expression of these proteins in the AP2IX-4 knockout tachyzoites could partly explain the diminished numbers of cysts in response to alkaline stress.

In contrast, under bradyzoite conditions, a total of 119 genes were differentially expressed two-fold or more between PruQ and $\Delta ap2IX-4$ parasites. 64 were downregulated in the $\Delta ap2IX-4$ compared to the parental while 55 were upregulated. Approximately 89% of these genes were complemented in knockout parasites in which AP2IX-4 expression had been restored. Further discussion is limited to genes that exhibited ≥ 1.5 -fold restoration of gene expression in complemented parasites relative to the knockout (**Table 5**). By this stringent criteria, 20 of the downregulated genes (including AP2IX-4) and 34 of the upregulated genes were complemented.

Four bradyzoite-associated genes were downregulated in the knockout following alkaline stress. These included enoyl coA hydratase/isomerase, and hypothetical proteins TGME49_205680, TGME49_287040, and TGME49_306270 (**Table 5**). Enoyl coA hydratase/isomerase, along with a MoeA domain-containing protein (involved in biosynthesis of molybdopterin), were downregulated in the AP2IX-4 knockout in both tachyzoite and bradyzoite-

inducing conditions. The majority of genes showing upregulated expression in the AP2IX-4 knockout upon stress were those encoding well-established bradyzoite-associated proteins such as ENO1, BAG1, PMA1, B-NTPase, LDH2, DnaK-TPR, SAG2C, and MCP4 (**Table 5**). A previously uncharacterized bradyzoite-specific CMGC kinase MAPK family (TGME49_221550) was also upregulated in the AP2IX-4 knockout.

Table 4. Differentially expressed genes (FC≥2) under tachyzoite conditions in PruQΔap2IX-4 compared to parental PruQ parasites.

Probe Set ID	Gene	Annotation	PruQΔap2IX-4 vs. PruQ Parental (FC)
80.m02181_at	TGME49_288950	AP2IX-4	-32.9
611.m00052_at	TGME49_317705	enoyl-CoA hydratase/isomerase family protein	-5.7
55.m00162_at	TGME49_261650	hypothetical protein	-4.7
83.m01216_at	TGME49_293480	MoeA N-terminal region (domain I and II) domain-containing protein	-4.3
25.m01822_at	TGME49_208730	microneme protein, putative; MCP4	-3.9
551.m00220_at	TGME49_307760	tubulin-tyrosine ligase family protein	-3.3
31.m00936_at	TGME49_212940	hypothetical protein	-3.2
20.m00337_at	TGME49_203720	vitamin K epoxide reductase complex subunit 1	-3.2
37.m00739_at	TGME49_217400	hypothetical protein	-3.2
641.m00181_at	TGME49_320740	hypothetical protein	-3.0
23.m00155_at	TGME49_207210	hypothetical protein	-3.0
72.m00004_at	TGME49_280570	SAG-related sequence SRS35A (SRS35A) aka bradyzoite surface antigen (SAG4.2, p18)	-2.8
541.m02517_at	TGME49_304930	hypothetical protein	-2.7
25.m00212_at	TGME49_208740	microneme protein, putative	-2.5
50.m03090_at	TGME49_245770	hypothetical protein	-2.5
80.m02369_s_at	TGME49_292375	KRUF family protein	-2.4
94.m00031_s_at	TGME49_296340	hypothetical protein	-2.2
76.m01568_s_at	TGME49_284420	hypothetical protein	-2.2
41.m01360_at	TGME49_222370	SAG-related sequence SRS13 (SRS13)	-2.2
55.m04865_at	TGME49_260190	microneme protein MIC13 (MIC13)	-2.2
49.m03275_at	TGME49_242110	Rhoptry kinase family protein ROP38	-2.2
55.m00276_at	TGME49_255210	ATPase, AAA family protein	-2.1
52.m00020_at	TGME49_253710	hypothetical protein	-2.1
49.m03157_at	TGME49_239580	hypothetical protein	4.6
583.m00678_at	TGME49_312905	hypothetical protein	3.8
583.m00665_at	TGME49_312905	hypothetical protein	2.3

Table 5. Differentially expressed genes (FC>2) in $\Delta ap2IX-4$ and $\Delta ap2IX-4::AP2IX-4^{HA}$ during bradyzoite induction conditions.

Highlighted in gray are genes previously found to be expressed during the bradyzoite stage (See **Chapter 2 Section IV.C**).

Accession no.	Annotation	PruQ $\Delta ap2IX-4$ vs. PruQ parental (FC)	$\Delta ap2IX-4::AP2IX-4^{HA}$ vs PruQ $\Delta ap2IX-4$ (FC)
DOWNREGULATED GENES			
TGME49_288950	AP2IX-4	-38.1	22.00
TGME49_319890	hypothetical protein	-7.6	1.8
TGME49_293480	MoeA N-terminal region (domain I and II) domain-containing protein	-7.4	3.4
TGME49_243940	hypothetical protein	-7.0	1.8
TGME49_204050	subtilisin SUB1 (SUB1)	-4.9	1.7
TGME49_317705	enoyl coA hydratase/isomerase	-3.8	2.2
TGME49_297910	hypothetical protein	-3.7	2.1
TGME49_256792	hypothetical protein	-3.6	2.1
TGME49_217400	hypothetical protein	-3.5	3.2
TGME49_205680	hypothetical protein	-3.2	1.7
TGME49_287040	hypothetical protein	-3.1	1.8
TGME49_306270	hypothetical protein	-3.0	1.7
TGME49_280500	inorganic anion transporter, sulfate permease (SulP) family protein	-2.6	2.2
TGME49_261250	histone H2A1	-2.6	1.7
TGME49_240090	roptry kinase family protein ROP34, putative	-2.5	1.6
TGME49_214190	SRS46	-2.3	1.6
TGME49_239260	histone H4	-2.2	1.7
TGME49_261240	histone H3	-2.1	2.4
TGME49_305160	histone H2Ba	-2.0	2.9
TGME49_255060	cytochrome b(N-terminal)/b6/petB subfamily protein	-2.0	3.9

Note: Table 5 (upregulated genes) continued on next page

(CONTINUED) Table 5

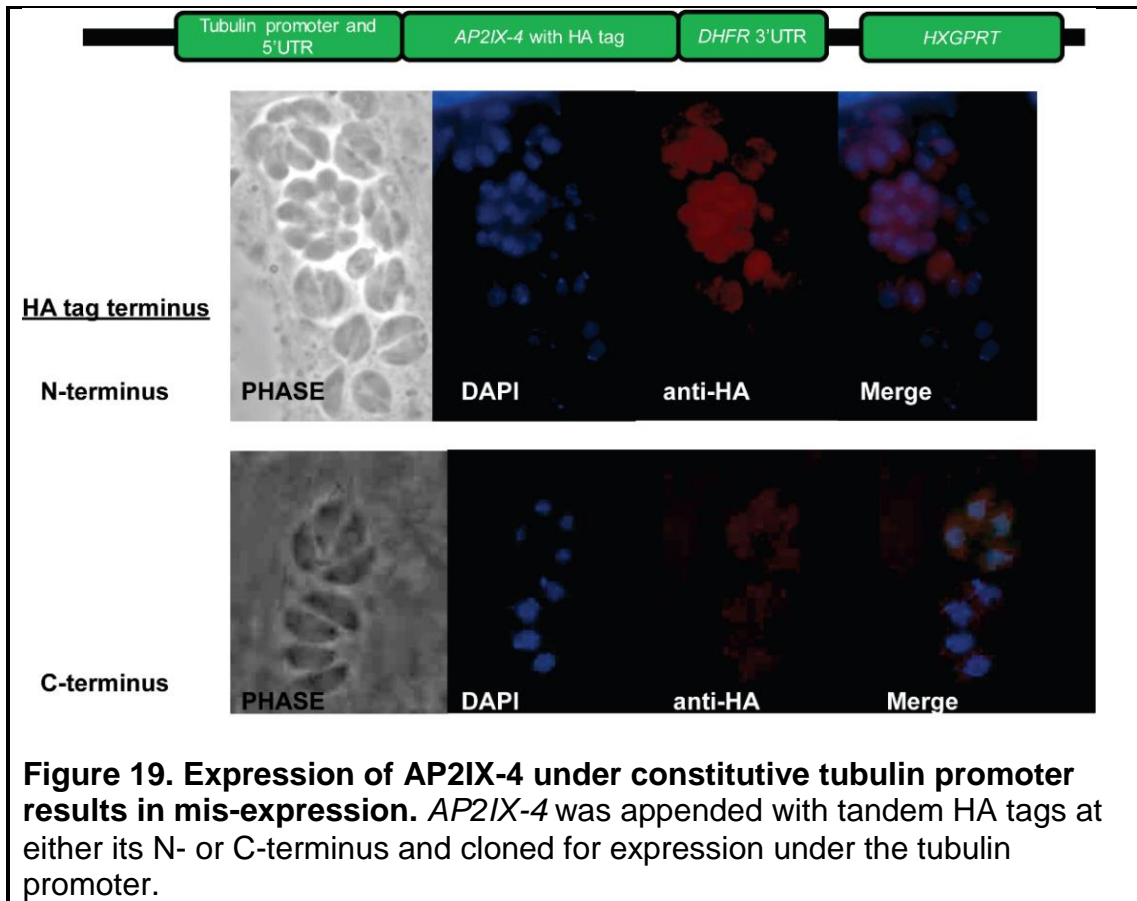
Accession no.	Annotation	PruQΔap2IX-4 vs. PruQ parental (FC)	Δap2IX-4::AP2IX-4^{HA} vs PruQΔap2IX-4 (FC)
UPREGULATED GENES			
TGME49_268860	ENO1	10.2	-2.3
TGME49_312905	hypothetical protein	9.7	-7.3
TGME49_209755	hypothetical protein	7.0	-2.5
TGME49_259020	BAG1	5.7	-1.6
TGME49_293790	hypothetical protein	4.9	-2.1
TGME49_278080	Toxoplasma gondii family A protein	4.9	-1.7
TGME49_216140	tetratricopeptide repeat-containing protein	4.4	-1.8
TGME49_252640	P-type ATPase PMA1	4.4	-1.7
TGME49_225290	GDA1/CD39 (nucleoside phosphatase) (B-NTPase)	4.1	-2.1
TGME49_315560	ATP-binding cassette G family transporter ABCG77	4.0	-1.5
TGME49_291040	lactate dehydrogenase LDH2 (LDH2)	4.0	-1.6
TGME49_202020	DnaK-TPR	3.9	-1.8
TGME49_221550	CMGC kinase, MAPK family, MEK kinase-related	3.7	1.9
TGME49_292260	SAG-related sequence SRS36B (SAG5D)	3.6	-1.9
TGME49_266700	hypothetical protein	3.5	-1.9
TGME49_240470	hypothetical protein	3.2	-1.7
TGME49_207160	SAG-related sequence SRS49D (SAG2C)	3.1	-2.2
TGME49_267470	cold-shock DNA-binding domain- containing protein	3.1	-1.7
TGME49_253680	hypothetical protein	3.0	1.5
TGME49_208730	microneme protein, putative (MCP4)	3.0	-1.6
TGME49_207150	SAG-related sequence SRS49C (SAG2D)	2.9	-1.9
TGME49_287960	hypothetical protein	2.7	-1.6
TGME49_218470	protein disulfide-isomerase	2.6	1.9
TGME49_253710	hypothetical protein	2.6	-1.7
TGME49_306338	dynein gamma chain, flagellar outer arm, putative	2.5	-1.9
TGME49_243720	peroxisomal biogenesis factor PEX11 (PEX11)	2.5	-1.9
TGME49_259960	nucleoside-diphosphatase	2.4	-1.5
TGME49_312905	hypothetical protein	2.4	-2.0
TGME49_314250	bradyzoite rhoptry protein BRP1 (BRP1)	2.4	-1.8
TGME49_253330	rhoptry kinase family protein (BPK1)	2.3	-1.5
TGME49_224830	hypothetical protein	2.2	1.5
TGME49_221840	hypothetical protein	2.2	-1.5
TGME49_311370	methylmalonate-semialdehyde dehydrogenase	2.1	-2.0
TGME49_213460	hypothetical protein	2.0	-1.7
TGME49_266900	Cyclin, N-terminal domain-containing protein	2.0	-1.6

IX. Strategies to generate overexpression of AP2IX-4

Attempts were made to generate parasites that express AP2IX-4 ectopically under the constitutively active tubulin promoter. Two separate plasmid constructs were designed, one with AP2IX-4 tagged at its C-terminus with three tandem HA tags and another with AP2IX-4 tagged at its N-terminus (**Figure 19**). Both constructs were sequenced and shown to be in-frame with the HA tags. Both the C- and N-terminus HA-tagged lines demonstrated similar phenotypes of slow growth, with the slowest growers taking more than two weeks to fully lyse a monolayer. The morphology of the parasites within their vacuoles was abnormal for both parasite lines, appearing round instead of banana-shaped, with abnormal numbers of parasites within the vacuoles (**Figure 19**). IFA with anti-HA showed the recombinant AP2IX-4 to be diffuse throughout the parasite. No further phenotypic experiments were pursued with these lines since the ectopic AP2IX-4 was mis-expressed in the parasite cytosol.

X. Yeast two-hybrid screen uncovers AP2IX-4 protein interactors

We performed a yeast two-hybrid screen using the entire AP2IX-4 coding sequence as bait to identify interacting proteins. The prey library was constructed from RH strain total RNA generated in our laboratory, and library construction and screening were performed by Hybrigenics Services (<https://www.hybrigenics-services.com/>; see **Chapter 2 Section VI**).



The list of all *T. gondii* AP2IX-4 interactors identified through the yeast two-hybrid screen is summarized in **Table 6**. Several proteins in the list of potential interactors are most likely false positive interactions based on functional characterizations and localizations of these and similar proteins: myosin light chain MLC1 (TGME49_257680), histidyl-tRNA synthetase (HisRS) (TGME49_280600), rhoptry neck protein RON5 (TGME49_311470), microneme protein MIC15 (TGME49_247195), and ATP-citrate lyase (TGME49_223840) (180-182). In addition, three interactions occurred with proteins from the human proteome, and this is most likely the result of human cDNAs in the prey library representing low levels of contamination with total RNA from the HFFs in which

the parasites were grown (see **Appendix** for complete list of all yeast two-hybrid interactions and corresponding PBS scores).

Among the list of interacting proteins are five AP2 proteins: AP2X-9, (TGME49_215150), AP2XII-1 (TGME49_218960), AP2VIIa-8 (TGME49_282210), AP2X-11 (TGME49_215570) and AP2X-2 (TGME49_225110). The microarray data assessing transcript levels of these AP2s through the tachyzoite cell cycle demonstrates that the transcripts for the first four of these AP2 proteins all exhibit cell cycle regulation with peak expression at the S/M phase (Toxodb.org; 109). The cell cycle transcript data for AP2X-2 is unavailable from Toxodb.org. Therefore, the temporal regulation of the four AP2s whose cell cycle transcript data is available is consistent with the cell cycle regulation of AP2IX-4 and should be confirmed with evaluation of protein expression through the tachyzoite cell cycle. In addition, the interaction of AP2IX-4 with other AP2s is consistent with the passive repressor model by which plant AP2 and other eukaryotic transcriptional repressors operate (see **Discussion**). Reciprocal interactions of these AP2IX-4 should be validated in co-immunoprecipitation. These AP2s are promising candidates for further studies as they provide clues to the mechanism of AP2IX-4 on gene expression and bradyzoite biology. A remaining question is whether AP2IX-4 interacts with these AP2s during the tachyzoite cell cycle, during bradyzoite development, or both stages.

Another AP2IX-4 interactor, TGME49_311400, contains a MAPK-interacting and spindle-stabilizing protein-like (MISS) domain that includes MAPK

phosphorylation sites. In mouse oocytes, the MISS protein is a MAPK substrate that maintains spindle integrity during meiosis. The protein also contains a WD40 domain; in higher eukaryotes WD40 repeat proteins are involved in diverse cellular processes, including nucleosome and chromatin organization and transcriptional regulation (179).

AP2IX-4 also interacted with an ImpB/MucB/SamB family protein (TGME49_ TGME49_308880) that belongs to the DNA polymerase type- γ family involved in response to DNA lesions. Among other interesting candidates from the yeast two-hybrid results is TGME49_320300, a SWI2/SNF2 Brahma-like putative that may represent a putative chromatin remodeling protein important for AP2IX-4 transcriptional function. TGME49_294610 is predicted to encode a SET-domain containing lysine methyltransferase whose interaction with AP2IX-4 should also be validated and examined, as this class of proteins may either activate or repress gene expression depending on which lysine residue they modify.

Table 6. Protein interactors of AP2IX-4 from yeast two-hybrid screen

Gene	Annotation
TGME49_246340	DnaJ domain-containing protein
TGME49_215150	AP2X-9
TGME49_257680	myosin light chain MLC1
TGME49_280600	histidyl-tRNA synthetase (HisRS)
TGME49_218960	AP2XII-1
TGME49_282210	AP2VIIa-8
TGME49_311400	WD domain, G-beta repeat-containing protein
TGME49_213067	hypothetical protein
TGME49_311470	rhopty neck protein RON5
TGME49_247195	microneme protein MIC15
TGME49_239910	cyclin-dependent kinase
TGME49_263060	Proteasome/cyclosome repeat-containing protein
TGME49_223840	ATP-citrate lyase
TGME49_308880	ImpB/MucB/SamB family protein
TGME49_288240	hypothetical protein
TGME49_224970	nucleolar protein
TGME49_215570	AP2X-11
TGME49_234990	hypothetical protein
TGME49_239885	hypothetical protein
TGME49_293320	hypothetical protein
TGME49_212190	RNA recognition motif-containing protein
TGME49_320300	SWI2/SNF2 Brahma-like putative
TGME49_270595	UBA/TS-N domain-containing protein
TGME49_288700	RecF/RecN/SMC N terminal domain-containing protein
TGME49_304990	guanylate-binding protein
TGME49_280600	histidyl-tRNA synthetase (HisRS)
TGME49_314410	aquarius
TGME49_225110	AP2X-2
TGME49_212300	hypothetical protein
TGME49_294610	histone lysine methyltransferase, SET
TGME49_287480	hypothetical protein
TGME49_304630	ATG C terminal domain-containing protein
TGME49_213020	hypothetical protein
TGME49_306320	Myb family DNA-binding domain-containing protein
TGME49_261660	hypothetical protein
TGME49_270930	hypothetical protein
TGME49_222350	hypothetical protein
TGME49_230000	hypothetical protein
TGME49_250700	hypothetical protein
TGME49_275430	hypothetical protein
TGME49_272155	hypothetical protein
TGME49_245990	hypothetical protein
TGME49_264830	hypothetical protein

TGME49_231200	hypothetical protein
TGME49_286270	hypothetical protein
TGME49_294060	hypothetical protein
TGME49_261960	hypothetical protein
TGME49_290678	hypothetical protein
TGME49_312630	anonymous antigen-1
TGME49_312190	hypothetical protein
TGME49_212880	surface antigen repeat-containing protein
TGME49_254710	serine esterase (DUF676) protein
TGME49_227450	hydrolase, NUDIX family protein
TGME49_221640	hypothetical protein
TGME49_244450	protein phosphatase 2C domain-containing protein
TGME49_264880	NEDD8-activating enzyme E1 catalytic subunit
TGME49_294690	rhomboid protease ROM5

CHAPTER 4: DISCUSSION

This thesis described the characterization of AP2IX-4, a novel member of the AP2 class of DNA-binding proteins in *T. gondii*. AP2IX-4 contains one putative AP2 DNA-binding domain. Microarray data suggested that the transcript expression of this factor peaked at the S/M phase of the tachyzoite cell cycle and is upregulated in response to alkaline stress (103, 156). AP2IX-4 transcript expression is also elevated during chronic infection of mice (159). From these observations, we hypothesized that **AP2IX-4 is a cell cycle-regulated transcription factor that contributes to the biology of bradyzoite cysts.**

To address this hypothesis, we examined AP2IX-4 protein expression during the parasite tachyzoite and bradyzoite stages and generated a knockout of this factor to study its role in tachyzoite replication and bradyzoite development. To assess the effect of AP2IX-4 on gene modulation, we performed microarray analysis to compare gene expression in AP2IX-4 knockout and parental parasites under both tachyzoite and bradyzoite conditions. Finally, we initiated a yeast two-hybrid study to screen for AP2IX-4 interactors. Our results showed that AP2IX-4 is expressed in both dividing tachyzoites and dividing bradyzoites. In response to alkaline stress, $\Delta ap2IX-4$ parasites exhibited reduced frequency of cysts accompanied by enhancement of the expression of bradyzoite-associated genes. *In vivo*, $\Delta ap2IX-4$ parasites demonstrated a modest virulence defect that was accompanied by decreased cyst burden in the brains of Balb/c mice.

I. AP2IX-4 is a nuclear factor expressed in the S/M phase of the tachyzoite cell cycle, but is dispensable for tachyzoite replication.

To compare AP2IX-4 protein expression to transcript data, we generated a parasite line in which AP2IX-4 was tagged at its C-terminus with three tandem HA tags. IFAs employing anti-HA and DAPI revealed the presence of AP2IX-4 in the parasite nucleus, a result consistent with the role of this factor as a putative transcription factor. Co-staining with IMC3 demonstrated that AP2IX-4 is expressed predominantly in the S through M phases of the tachyzoite cell cycle, which is consistent with its transcript data. Therefore, we demonstrated that AP2IX-4 is a cell cycle-regulated nuclear factor.

The “just-in-time” expression of AP2IX-4 in dividing tachyzoites suggests it may be important in tachyzoite replication. Therefore, to examine the role of AP2IX-4 in tachyzoite replication and viability, we generated a knockout of this factor. Parasite replication rates were assessed using a doubling assay, and viability was evaluated using a plaque assay. Neither assay revealed a significant difference in the *in vitro* growth between parental and $\Delta ap2IX-4$ parasites.

In tachyzoites, daughter cell formation begins in the late S phase, and nuclear and organelle partitioning are concurrent and terminate in the generation of daughter parasites in cytokinesis. Yet, the replication and viability data demonstrates that AP2IX-4 is not essential for tachyzoite replication. To date, only one other publication assessed the knockout of a cell cycle-regulated AP2. A knockout of AP2XI-5, whose transcript expression peaks during mitosis and cytokinesis, was generated in both type I and type II strains and neither

demonstrated a growth defect (158). Interestingly, knockout of AP2XI-5 in type II Pru reduced brain cyst burden in mice (158). This suggests that cell cycle-regulated factors in *T. gondii* may not necessarily direct replication in the tachyzoite stage but may play important roles in bradyzoite development.

As mentioned in the introduction, parasites positive for both tachyzoite and bradyzoite markers appear at the junction of the S and mitotic phases of the tachyzoite cell cycle (108). The appearance of these parasites precedes appearances of BAG1-positive and SAG1-negative parasites, suggesting that the S/M phase may be a point of commitment to bradyzoite development. Therefore, peak protein expression of AP2IX-4 may relate to its potential function in bradyzoite biology instead of a dominant role in tachyzoite replication. The negative tachyzoite data on tachyzoite replication and viability combined with the association of the S/M phase in bradyzoite development encouraged us to focus on the role of AP2IX-4 in bradyzoite development.

II. AP2IX-4 is expressed in dividing bradyzoites.

To begin dissecting the role of AP2IX-4 in bradyzoite development, we examined the expression of this factor under bradyzoite induction conditions. IFAs were performed using $\Delta ap2IX-4::AP2IX-4^{HA}$ parasites, a type II Pru line which expressed AP2IX-4 with three tandem HA tags in its C-terminus, under alkaline conditions using DAPI and anti-HA staining. This experiment revealed four key observations. First, AP2IX-4 is expressed in the nuclei of bradyzoites, consistent with a putative role as a transcription factor. Second, unlike its

expression in all parasites within a subset of tachyzoite vacuoles, AP2IX-4 is expressed in only 16% of parasites contained in a subset of cysts. Third, IMC3 co-staining with HA demonstrated that AP2IX-4 is expressed in dividing bradyzoites. This is a novel finding as AP2IX-4 is the first AP2 to be found expressed in both dividing tachyzoites and bradyzoites.

Lastly, the presence of budding daughter cells in parasites expressing HA-tagged AP2IX-4 was found alongside expression of GFP, which in these parasites was expressed under the bradyzoite-specific LDH2 promoter. Together, these observations indicate heterogeneity of AP2IX-4 expression within the cyst and that it is expressed in parasites that are dividing yet express a bradyzoite marker.

The heterogeneity of AP2IX-4 expression is consistent with emerging data showing that bradyzoites within a cyst are dynamic, dividing entities. Varying stages of daughter cell assembly has been observed among bradyzoites in a cyst (180, 181). *In vivo*, dividing and non-dividing parasites can be observed within a cyst, with dividing parasites exhibiting two patterns of IMC3 staining derived from asynchronous division of parasites within a cyst (181). Populations of parasites within a cyst can exhibit “cluster” replication, in which groups of parasites in close vicinity appear to exhibit budding daughter cell formation at the same time (181). This is in comparison to “sporadic” replication, in which isolated parasites scattered throughout the cyst exhibit division (181). Synchronized replication, in which all parasites within the cyst exhibit robust IMC3 staining, has also been observed. Furthermore, the number of cysts

containing asynchronously dividing parasites increases in the time course of bradyzoite development (180). Our observation that AP2IX-4 is expressed in asynchronously dividing bradyzoites and that the number of vacuoles positive for AP2IX-4 increases through bradyzoite development further supports the heterogeneous nature of dividing bradyzoites within tissue cysts.

The expression of AP2IX-4 in dividing and GFP-positive bradyzoites is consistent with emerging data that illustrate bradyzoite development as occurring through multiple transitions. Preceding the progression to the mature bradyzoite are events linking the tachyzoite cell cycle with commitment to differentiation, whereby the tachyzoite cell cycle lengthens and growth rate decreases accompanied by the enrichment of a population of parasites with DNA content of 1.8-2N (38, 107, 108). These G2/S phase parasites are both SAG1 and BAG1-positive (108). A developing bradyzoite cyst may contain parasites exhibiting bradyzoite-specific, tachyzoite-specific or bradyzoite and tachyzoite-specific markers (106, 182). Gene expression data also support the view of the cyst as developing in a temporal cascade of bradyzoite expression (103, 117, 118).

While the expression of AP2IX-4 in bradyzoites is consistent with existing literature demonstrating transitioning and dividing bradyzoites within a cyst, further questions remain due to missing links in bradyzoite biology knowledge. Of note, while existing literature suggests that bradyzoite development occurs in a step-wise, multi-transition manner, the role of bradyzoite division in this process is unclear. AP2IX-4 may be a useful candidate for uncovering more of bradyzoite biology by dissecting the purpose of bradyzoite division in this multi-step process.

Therefore it serves as a useful marker of transitioning bradyzoites, and the role of AP2IX-4 in bradyzoite transition and division remains to be elucidated in future studies.

III. Ablation of AP2IX-4 decreased cyst frequency in alkaline induction and in brains of chronically infected mice.

The presence of AP2IX-4 in bradyzoites suggest it plays a role in bradyzoite development. We therefore subjected PruQ and $\Delta ap2IX-4$ parasites to differentiation assays, in which parasite cultures were grown in alkaline conditions for four days before they were stained with *Dolichos biflorus* lectin to mark bradyzoite cyst walls. These differentiation assays revealed that 73% of PruQ vacuoles exhibited lectin staining compared to 46% in $\Delta ap2IX-4$ parasite cultures. Consistent with the reduction in cyst frequency observed *in vitro* in $\Delta ap2IX-4$ parasite cultures, we observed a reduction in cyst burden in the brains of mice infected with $\Delta ap2IX-4$ parasites. This suggests that AP2IX-4 contributes to the frequency of lectin-positive cysts. However, the exact role AP2IX-4 exerts in bradyzoite biology remains to be dissected, and future *in vitro* studies should be undertaken to address the following questions:

- What is the role of AP2IX-4 in dividing parasites within the alkaline-induced cyst?
- How does the dysregulation of gene expression in $\Delta ap2IX-4$ parasites result in decreased cyst frequency *in vitro* and *in vivo*?

- Where in the genome (such as gene-specific *cis*-regulatory sequences, intergenic regions, and introns) does AP2IX-4 localize and enrich? What are AP2IX-4 interactors and do these interactors impact bradyzoite biology?

IV. AP2IX-4 as a transcriptional repressor of a subset of bradyzoite-associated genes.

Following the initial commitment to bradyzoite differentiation at the S/M phase of the tachyzoite cell cycle, the gradual maturation of the cyst is based upon a temporal cascade of gene expression, whereby bradyzoite-specific genes are turned on step-wise in the development time course (103, 117, 118). BAG1 mRNA expression has been consistently demonstrated to be induced around day three of differentiation, later than the induction of other bradyzoite markers such as ENO1 and LDH2 (117, 118). Although the molecular mechanisms underlying progression from the early to late bradyzoite remain to be fully elucidated, Radke et al. proposed a model employing data on AP2IX-9, whose expression in alkaline conditions is persistent only in early stage bradyzoites (156). This model suggests that AP2IX-9 inhibits progression of the premature bradyzoite, a repression that might serve useful in conditions where further development is not necessary or favored (156).

Moreover, the identification of a bradyzoite development activator, AP2XI-4, suggests that bradyzoite progression may in part occur mechanistically through competition between molecular activators and repressors (156, 157,

183). This competition mechanism is well-conserved in higher eukaryotes, in which the cellular decision to differentiate occurs in the G1 phase of the cell cycle and is mediated by the interaction between E2F transcription factors and activating or repressing complexes (184, 185). AP2XI-4 was demonstrated to activate the expression of bradyzoite genes in addition to BAG1, while AP2IX-9 represses the expression of BAG1 (156, 157). Together, the AP2XI-4 and AP2IX-9 data support a model by which transcriptional activator and repressor complexes may compete for binding on stage-specific promoters. Future studies should consider our yeast two-hybrid results to elucidate AP2IX-4's mechanism as a potential transcriptional repressor.

V. Conclusions and future studies

In reviewing our hypothesis, we first demonstrated that AP2IX-4 is a cell cycle-regulated nuclear factor. Second, the enhancement of bradyzoite-associated gene expression in response to alkaline stress, combined with reduced cyst frequency of $\Delta ap2IX-4$ parasites in the brains of chronically infected mice indicate a role for AP2IX-4 in bradyzoite biology. However, two key questions remain which will be evaluated in this section:

- i. What is the role of AP2IX-4 in dividing bradyzoites?
- ii. How does AP2IX-4 operate as a transcription factor, especially with regards to its potential repressor role?

i. Role of AP2IX-4 in dividing bradyzoites.

Its expression in dividing bradyzoites in the tissue cyst suggests that AP2IX-4 may repress bradyzoite progression in these intermediate entities. One possibility, therefore, is that AP2IX-4 represses bradyzoite development in favor of continued parasite replication. Continued parasite replication would confer an advantage to the parasite by expanding parasite burden for eventual dissemination in the host, while maintained latency would ensure the host survival until the parasite is ready to disseminate.

Another possibility is that AP2IX-4 represses both bradyzoite development *and* replication, that is, towards the goal of maintaining latency. The expression of this factor in the subset of bradyzoites that exhibit IMC3-positive daughter cell formation is appropriate, as it is possible that these dividing parasites are simply those in the decision process of whether to continue dividing, progress further in the bradyzoite progression or to pursue neither route. This model thereby introduces another intermediate in the bradyzoite development timeline in which a non-developing, latent parasite exists.

Future Studies. Further experiments should dissect out these models:

- (1) IMC3 staining should be examined in $\Delta ap2IX-4$ parasites cultured in alkaline stress. If more parasites exhibit IMC3 staining following loss of AP2IX-4, this supports the model in which AP2IX-4 suppresses bradyzoite replication, resulting in increased daughter cell formation in the knockout parasites.

(2) Increased replication of parasites lacking AP2IX-4 will also favor the model in which this factor is a suppressor of replication. An increased replication phenotype may be accompanied by increased glycolytic flux or oxidative phosphorylation, such as that measured by the SeaHorse XF Analyzer. Other phenotypes of increased parasite replication include acidification of alkaline medium in which the parasites are cultured.

ii. AP2IX-4 as a transcriptional repressor.

In our microarray performed under alkaline conditions, 22 out of 35 or 63% of the genes whose transcripts were upregulated in the $\Delta ap2IX-4$ parasites are bradyzoite-associated, including *BAG1*. This suggests that AP2IX-4 may be a transcriptional repressor of these bradyzoite-associated genes. Since it was not known whether AP2IX-4 localizes to the loci of genes dysregulated in the microarray, we attempted ChIP-qPCR to examine whether HA-tagged AP2IX-4 would localize to promoter regions of *BAG1*. The HA-tagged version of TgGCN5B ($GCN5B^{HA}$), expressed under the tubulin promoter, was used as positive control (186). Two T-150cm² flasks, each containing intracellular AP2IX-4^{HA} or $GCN5B^{HA}$ parasites, were fixed in 16% paraformaldehyde and pellets were subjected to sonication on ice at 30% output and six times 30s on/off. When sonicated genomic material from the lysates were resolved on agarose gel, the $GCN5B^{HA}$ sample revealed a DNA smear representing sonicated chromatin at desired sizes of 500-1000 bp. However, in all trials in the same conditions, sonicated genomic material from AP2IX-4^{HA} parasites resolved as a single band of about 400bp. AP2IX-4 may be involved in chromatin compaction, and the HA

epitopes may interfere with this function. One way to test this is through a DNase I hypersensitivity assay as described in (187). This assay works under the premise that less compacted, exposed chromatin is more sensitive to DNase I access. Exposed chromatin can be found in transcriptionally active areas. If AP2IX-4 function targets it differentially to structurally compact or open chromatin, and epitope tagging can interfere with this function, then the DNase I assay may reveal differences in digested chromatin pattern in wild-type versus tagged parasite lines. For example, less compact chromatin may be more amenable to shearing by sonication such that the same sonication conditions which yield a smear for GCN5^{HA} may yield the single band composed of uniformly shorter (~400 bp) fragments for AP2IX-4^{HA}.

Given that AP2 proteins contain plant-like homology, it is important to note that at least two models of repression by transcriptional protein complexes exist for plant AP2s (188). Transcriptional repressors may inhibit gene expression as either active or passive repressors. The mechanism of passive repressors can be mediated through either direct DNA binding or DNA binding-independent, protein-protein steric interference (189, 190). For example, passive repressors may interfere with transcriptional activation complexes such as by binding directly to DNA, thereby competing for the same DNA binding sites. They may also directly bind to transcriptional activators, precluding the ability of these activators to bind DNA and activate gene expression. Active repressors, on the other hand, are able to intrinsically repress gene expression such as through recruitment of chromatin modifying complexes.

Previous attempts to identify a DNA-binding motif for the AP2 domain of AP2IX-4 using protein binding microarrays (PBMs) did not reveal a potential DNA-binding motif. While there are limitations to this artificial approach and the ability of AP2IX-4 to bind to DNA cannot be completely ruled out, the data supports a model by which AP2IX-4 represses gene expression independent of DNA binding. Analysis of AP2IX-4 interactors can provide important clues on the mechanism of AP2IX-4 repression.

Protein-protein interactions can be screened using various approaches, including co-immunoprecipitation followed by mass spectrometry or a yeast two-hybrid assay. In the co-immunoprecipitation approach, an antibody is used to target and “pull-down” a protein-of-interest, whose interacting proteins are then resolved on a gel for subsequent identification via mass spectrometry. The major technical challenge with this approach is due to the limiting levels of AP2IX-4, which is cell cycle-regulated. Attempts to pull down sufficient amounts of AP2IX-4 and its associating partners could be tried after synchronizing tachyzoite populations, in order to maximize the number in S/M where the protein expression peaks. We employed a yeast two-hybrid approach to overcome these limitations of protein concentration. With Hybrigenics Services, we performed a yeast two-hybrid screen to identify bait (AP2IX-4) interactions with prey generated from a *T. gondii* cDNA library. However, this is an artificial system and may identify false protein interactions; candidate interacting proteins will have to be verified through independent methods.

Our yeast two-hybrid results revealed interactions with five other potential transcriptional modulators of the AP2 class. Interestingly, the cell cycle regulation transcript data for four of these five revealed peak expression during the S/M phase. The interaction of AP2IX-4 with these AP2's should be validated with reciprocal co-immunoprecipitation using lysates from tachyzoites and from bradyzoites to examine stage-specificity of interactions. Finally, the function of these AP2s should be further studied using genetic deletion and transcriptomic analysis.

If AP2IX-4 is a transcriptional repressor of these genes, it can also operate by recruiting repressor complexes. Our yeast two-hybrid results identified a SWI2/SNF2 Brahma-like putative (TGME49_320300) and SET domain-containing histone lysine methyltransferase (TGME49_294610), whose reciprocal interactions with AP2IX-4 should be validated with co-immunoprecipitation. The SWI2/SNF2 Brahma-like protein merits further analysis as it may serve as a potential chromatin remodeler. SET domain-containing histone lysine methyltransferases may activate or repress gene expression depending on the particular lysine residue modified. Toxodb.org reveals that this protein is downregulated during *in vitro* bradyzoite conditions; in addition, its cell cycle transcript profile demonstrates peak expression in the S/M phase (Toxodb.org, 109). The function of this SET domain containing lysine methyltransferase is unknown and should be examined to assess its role in possible gene expression repression.

To date, no FDA-approved drugs which eradicate *T. gondii* tissues cysts exist. Effective targeting of the chronic of *T. gondii* infection requires knowledge about the molecular processes underlying differentiation and reactivation. Emerging literature reveals that differentiation is a complex, multi-step process. Understanding the function and mechanism of AP2IX-4, a nuclear, cell-cycle regulated factor, will inform how differentiation is coordinated with parasite division. Moreover, the dysregulation in bradyzoite gene expression observed in $\Delta ap2IX-4$ parasites suggest a balancing act of gene expression must be maintained for efficient cyst formation.

APPENDIX

Yeast two-hybrid hits with global predicted biological score (PBS)

Note: The PBS score calculation and relevance is explained in **Chapter 2, Section V.I.** "N/A" denotes PBS scores which could not be calculated due to missing sequences or sequences that are out-of-frame, within 5' or 3' UTR regions, or antisense compared to their reference CDS.

Gene	Annotation	PBS
TGME49_246340	DnaJ domain-containing protein	A
TGME49_215150	AP2X-9	A
TGME49_257680	myosin light chain MLC1	A
TGME49_280600	histidyl-tRNA synthetase	B
TGME49_218960	AP2XII-1	B
TGME49_282210	AP2VIIa-8	B
TGME49_311400	WD domain, G-beta repeat-containing protein	C
TGME49_213067	hypothetical protein	C
TGME49_311470	rhopty neck protein RON5	C
TGME49_247195	microneme protein MIC15	C
TGME49_239910	cyclin-dependent kinase	C
TGME49_263060	Proteasome/cyclosome repeat-containing protein	D
TGME49_223840	ATP-citrate lyase	D
TGME49_308880	ImpB/MucB/SamB family protein	D
TGME49_288240	hypothetical protein	D
TGME49_224970	nucleolar protein	D
TGME49_215570	AP2X-11	D
TGME49_234990	hypothetical protein	D
TGME49_212190	RNA recognition motif-containing protein	D
TGME49_320300	SWI2/SNF2 Brahma-like putative	D
TGME49_270595	UBA/TS-N domain-containing protein	D
TGME49_288700	RecF/RecN/SMC N terminal domain-containing protein	D
TGME49_304990	guanylate-binding protein	D
TGME49_280600	histidyl-tRNA synthetase	D
TGME49_314410	aquarius	D
TGME49_225110	AP2X-2	D
TGME49_212300	hypothetical protein	D
TGME49_294610	histone lysine methyltransferase, SET	D
TGME49_287480	hypothetical protein	D
TGME49_215570	AP2X-11	D
TGME49_304630	ATG C terminal domain-containing protein	D
TGME49_213020	hypothetical protein	D
TGME49_306320	Myb family DNA-binding domain-containing protein	D

TGME49_261660	hypothetical protein	D
TGME49_270930	hypothetical protein	D
TGME49_222350	hypothetical protein	D
TGME49_230000	hypothetical protein	D
TGME49_250700	hypothetical protein	D
TGME49_275430	hypothetical protein	D
TGME49_272155	hypothetical protein	D
TGME49_245990	hypothetical protein	D
TGME49_264830	hypothetical protein	D
TGME49_231200	hypothetical protein	D
TGME49_286270	hypothetical protein	D
TGME49_224870	hypothetical protein	D
TGME49_294060	hypothetical protein	D
TGME49_261960	hypothetical protein	D
TGME49_290678	hypothetical protein	D
TGME49_312630	anonymous antigen-1	D
TGME49_312190	hypothetical protein	D
TGME49_212880	surface antigen repeat-containing protein	D
TGME49_254710	serine esterase (DUF676) protein	D
TGME49_227450	hydrolase, NUDIX family protein	D
TGME49_221640	hypothetical protein	D
TGME49_244450	protein phosphatase 2C domain-containing protein	D
TGME49_264880	NEDD8-activating enzyme E1 catalytic subunit	D
TGME49_257680	myosin light chain MLC1?	D
TGME49_294690	rhomboid protease ROM5?	D
TGME49_249180	DHFR	N/A
TGME49_211650	hypothetical protein	N/A
TGME49_312300	Sec7 domain-containing protein	N/A
TGME49_286420	elongation factor 1-alpha	N/A
TGME49_210800	activator of hsp90 ATPase	N/A
TGME49_243460	hypothetical protein	N/A
TGME49_232350	lactate dehydrogenase LDH1	N/A
TGME49_257680	myosin light chain MLC1	N/A
TGME49_318230	phosphoglycerate kinase PGKI	N/A
TGME49_228170	inner membrane complex protein IMC2A	N/A
TGME49_285240	3-oxo-5-alpha-steroid 4-dehydrogenase	N/A
TGME49_205650	AP2VIIa-3	N/A
None	Homolog of SPRED1 (Homo sapiens)	D
None	Homolog of p87/89 (Homo sapiens)	D
None	Homolog of prosaposin (Homo sapiens)	D
None	Homolog of COL1A1 (Homo sapiens)	N/A

REFERENCES

1. Pappas, G., Roussos, N. and Falagas, M.E., 2009. Toxoplasmosis snapshots: global status of *Toxoplasma gondii* seroprevalence and implications for pregnancy and congenital toxoplasmosis. *International journal for parasitology*, 39(12), pp.1385-1394.
2. FIN, A.M., Heckerroth, A.R. and Weiss, L.M., 2000. *Toxoplasma gondii*: from animals to humans. *International journal for parasitology*, 30(12), pp.1217-1258.
3. Dubey, J.P., Miller, N.L. and Frenkel, J.K., 1970. The *Toxoplasma gondii* oocyst from cat feces. *The Journal of experimental medicine*, 132(4), pp.636-662.
4. Dubey, J.P. and Frenkel, J.K., 1972. Cyst-induced toxoplasmosis in cats. *Journal of Eukaryotic Microbiology*, 19(1), pp.155-177.
5. Dubey, J.P., Lindsay, D.S. and Speer, C.A., 1998. Structures of *Toxoplasma gondii* tachyzoites, bradyzoites, and sporozoites and biology and development of tissue cysts. *Clinical microbiology reviews*, 11(2), pp.267-299.
6. Dubey, J.P., 1995. Duration of immunity to shedding of *Toxoplasma gondii* oocysts by cats. *The Journal of parasitology*, pp.410-415.
7. Dubey, J.P., Speer, C.A., Shen, S.K., Kwok, O.C. and Blixt, J.A., 1997. Oocyst-induced murine toxoplasmosis: life cycle, pathogenicity, and stage conversion in mice fed *Toxoplasma gondii* oocysts. *The Journal of parasitology*, 83(5), pp.870-882
8. Remington JS, McLeod R, Thuilliez P, et al. Toxoplasmosis. In: Remington JS, Klein JO, Wilson CB, et al, eds. *Infectious Diseases of the Fetus and Newborn Infant*. 7th ed. Philadelphia, PA: Elsevier Saunders; 2011.
9. Remington, JS.; Desmonts, G. Toxoplasmosis. In: Remington, JS.; Klein, JO., editors. *Infectious diseases of the fetus and newborn infant*. 3. Philadelphia: WB Saunders; 1990. p. 89-195.
10. Velimirovic, B., 1984. Toxoplasmosis in immunosuppression and AIDS. *Infection*, 12(5), pp.315-317.
11. Derouin, F. and Pelloux, H., 2008. Prevention of toxoplasmosis in transplant patients. *Clinical Microbiology and Infection*, 14(12), pp.1089-1101.
12. Sacks, J.J., Roberto, R.R. and Brooks, N.F., 1982. Toxoplasmosis infection associated with raw goat's milk. *Jama*, 248(14), pp.1728-1732.
13. Jacobs, L., Remington, J.S. and Melton, M.L., 1960. A survey of meat samples from swine, cattle, and sheep for the presence of encysted *Toxoplasma*. *The Journal of parasitology*, 46(1), pp.23-28.
14. Jacobs, L. and Moyle, G.G., 1963. The prevalence of toxoplasmosis in New Zealand sheep and cattle. *American Journal of Veterinary Research*, 24, pp.673-675.
15. Deckert-Schlüter, M., Rang, A., Weiner, D., Huang, S., Wiestler, O.D., Hof, H. and Schlüter, D., 1996. Interferon-gamma receptor-deficiency renders mice highly susceptible to toxoplasmosis by decreased macrophage

- activation. *Laboratory investigation; a journal of technical methods and pathology*, 75(6), pp.827-841.
16. Suzuki, Y., Orellana, M.A., Schreiber, R.D. and Remington, J.S., 1988. Interferon-gamma: the major mediator of resistance against *Toxoplasma gondii*. *Science*, 240(4851), p.516.
 17. Suzuki, Y. and Remington, J.S., 1990. The effect of anti-IFN-gamma antibody on the protective effect of Lyt-2+ immune T cells against toxoplasmosis in mice. *The Journal of Immunology*, 144(5), pp.1954-1956.
 18. Nathan, C.F., Murray, H.W., Wiebe, M.E. and Rubin, B.Y., 1983. Identification of interferon- γ as the lymphokine that activates human macrophage oxidative metabolism and antimicrobial activity. *J. exp. Med*, 158(670), p.1983.
 19. Murray, H.W., Gellene, R.A., Libby, D.M., Rothermel, C.D. and Rubin, B.Y., 1985. Activation of tissue macrophages from AIDS patients: in vitro response of AIDS alveolar macrophages to lymphokines and interferon-gamma. *The Journal of Immunology*, 135(4), pp.2374-2377.
 20. Scharon-Kersten, T.M., Wynn, T.A., Denkers, E.Y., Bala, S., Grunvald, E., Hieny, S., Gazzinelli, R.T. and Sher, A., 1996. In the absence of endogenous IFN-gamma, mice develop unimpaired IL-12 responses to *Toxoplasma gondii* while failing to control acute infection. *The Journal of Immunology*, 157(9), pp.4045-4054.
 21. Gazzinelli, R.T., Hieny, S., Wynn, T.A., Wolf, S. and Sher, A., 1993. Interleukin 12 is required for the T-lymphocyte-independent induction of interferon gamma by an intracellular parasite and induces resistance in T-cell-deficient hosts. *Proceedings of the National Academy of Sciences*, 90(13), pp.6115-6119.
 22. Khan, I.A., Matsuura, T. and Kasper, L.H., 1994. Interleukin-12 enhances murine survival against acute toxoplasmosis. *Infection and immunity*, 62(5), pp.1639-1642.
 23. Bliss, S.K., Marshall, A.J., Zhang, Y. and Denkers, E.Y., 1999. Human polymorphonuclear leukocytes produce IL-12, TNF- α , and the chemokines macrophage-inflammatory protein-1 α and-1 β in response to *Toxoplasma gondii* antigens. *The Journal of Immunology*, 162(12), pp.7369-7375.
 24. Plattner, F., Yarovinsky, F., Romero, S., Didry, D., Carlier, M.F., Sher, A. and Soldati-Favre, D., 2008. *Toxoplasma* profilin is essential for host cell invasion and TLR11-dependent induction of an interleukin-12 response. *Cell host & microbe*, 3(2), pp.77-87.
 25. Yarovinsky, F., Zhang, D., Andersen, J.F., Bannenberg, G.L., Serhan, C.N., Hayden, M.S., Hieny, S., Sutterwala, F.S., Flavell, R.A., Ghosh, S. and Sher, A., 2005. TLR11 activation of dendritic cells by a protozoan profilin-like protein. *Science*, 308(5728), pp.1626-1629.
 26. Koblansky, A.A., Jankovic, D., Oh, H., Hieny, S., Sungnak, W., Mathur, R., Hayden, M.S., Akira, S., Sher, A. and Ghosh, S., 2013. Recognition of profilin by Toll-like receptor 12 is critical for host resistance to *Toxoplasma gondii*. *Immunity*, 38(1), pp.119-130.

27. Andrade, W.A., do Carmo Souza, M., Ramos-Martinez, E., Nagpal, K., Dutra, M.S., Melo, M.B., Bartholomeu, D.C., Ghosh, S., Golenbock, D.T. and Gazzinelli, R.T., 2013. Combined action of nucleic acid-sensing Toll-like receptors and TLR11/TLR12 heterodimers imparts resistance to *Toxoplasma gondii* in mice. *Cell host & microbe*, 13(1), pp.42-53.
28. Roach, J.C., Glusman, G., Rowen, L., Kaur, A., Purcell, M.K., Smith, K.D., Hood, L.E. and Aderem, A., 2005. The evolution of vertebrate Toll-like receptors. *Proceedings of the National Academy of Sciences of the United States of America*, 102(27), pp.9577-9582.
29. Subauste, C.S. and Wessendarp, M., 2000. Human dendritic cells discriminate between viable and killed *Toxoplasma gondii* tachyzoites: dendritic cell activation after infection with viable parasites results in CD28 and CD40 ligand signaling that controls IL-12-dependent and-independent T cell production of IFN- γ . *The Journal of Immunology*, 165(3), pp.1498-1505.
30. Sher, A., Tosh, K. and Jankovic, D., 2016. Innate recognition of *Toxoplasma gondii* in humans involves a mechanism distinct from that utilized by rodents. *Cellular & molecular immunology*.
31. Johnson, L.L. and Sayles, P.C., 2002. Deficient humoral responses underlie susceptibility to *Toxoplasma gondii* in CD4-deficient mice. *Infection and immunity*, 70(1), pp.185-191.
32. Shirahata, T., Yamashita, T., Ohta, C., Goto, H. and Nakane, A., 1994. CD8+ T lymphocytes are the major cell population involved in the early gamma interferon response and resistance to acute primary *Toxoplasma gondii* infection in mice. *Microbiology and immunology*, 38(10), pp.789-796.
33. Montoya, J.G., Lowe, K.E., Clayberger, C., Moody, D., Do, D., Remington, J.S., Talib, S. and Subauste, C.S., 1996. Human CD4+ and CD8+ T lymphocytes are both cytotoxic to *Toxoplasma gondii*-infected cells. *Infection and immunity*, 64(1), pp.176-181.
34. Purner, M.B., Berens, R.L., Nash, P.B., van Linden, A.N.N.A.M.I.E., Ross, E., Kruse, C., Krug, E.C. and Curiel, T.J., 1996. CD4-mediated and CD8-mediated cytotoxic and proliferative immune responses to *Toxoplasma gondii* in seropositive humans. *Infection and immunity*, 64(10), pp.4330-4338.
35. Gazzinelli, R.I.C.A.R.D.O., Xu, Y., Hieny, S.A.R.A., Cheever, A.L.L.E.N. and Sher, A.L.A.N., 1992. Simultaneous depletion of CD4+ and CD8+ T lymphocytes is required to reactivate chronic infection with *Toxoplasma gondii*. *The Journal of Immunology*, 149(1), pp.175-180.
36. Lütjen, S., Soltek, S., Virna, S., Deckert, M. and Schlüter, D., 2006. Organ- and disease-stage-specific regulation of *Toxoplasma gondii*-specific CD8-T-cell responses by CD4 T cells. *Infection and immunity*, 74(10), pp.5790-5801.
37. Gazzinelli, R.T., Hakim, F.T., Hieny, S., Shearer, G.M. and Sher, A., 1991. Synergistic role of CD4+ and CD8+ T lymphocytes in IFN-gamma production and protective immunity induced by an attenuated *Toxoplasma gondii* vaccine. *The Journal of Immunology*, 146(1), pp.286-292.

38. Bohne, W., Heesemann, J. and Gross, U., 1994. Reduced replication of *Toxoplasma gondii* is necessary for induction of bradyzoite-specific antigens: a possible role for nitric oxide in triggering stage conversion. *Infection and immunity*, 62(5), pp.1761-1767.
39. Lüder, C.G., Algner, M., Lang, C., Bleicher, N. and Groß, U., 2003. Reduced expression of the inducible nitric oxide synthase after infection with *Toxoplasma gondii* facilitates parasite replication in activated murine macrophages. *International journal for parasitology*, 33(8), pp.833-844.
40. Hayashi, S., Chan, C.C., Gazzinelli, R. and Roberge, F.G., 1996. Contribution of nitric oxide to the host parasite equilibrium in toxoplasmosis. *The Journal of Immunology*, 156(4), pp.1476-1481.
41. Lüder, C.G., Giraldo-Velásquez, M., Sendtner, M. and Gross, U., 1999. *Toxoplasma gondii* in primary rat CNS cells: differential contribution of neurons, astrocytes, and microglial cells for the intracerebral development and stage differentiation. *Experimental parasitology*, 93(1), pp.23-32.
42. Suzuki, Y., Conley, F.K. and Remington, J.S., 1989. Importance of endogenous IFN-gamma for prevention of toxoplasmic encephalitis in mice. *The Journal of Immunology*, 143(6), pp.2045-2050.
43. Remington, J.S., Jacobs, L. and Kaufman, H.E., 1960. Toxoplasmosis in the adult. *New England Journal of Medicine*, 262(5), pp.237-241.
44. Taila, A.K., Hingwe, A.S. and Johnson, L.E., 2011. Toxoplasmosis in a patient who was immunocompetent: a case report. *Journal of medical case reports*, 5(1), p.1.
45. Stevens, Christine and Linda Miller. *Clinical Serology And Immunology*, 4E. Philadelphia: F.A. Davis, 2016. Print.
46. Park, Y.H. and Nam, H.W., 2013. Clinical features and treatment of ocular toxoplasmosis. *The Korean journal of parasitology*, 51(4), pp.393-399.
47. Bodaghi, B., Touitou, V., Fardeau, C., Paris, L. and LeHoang, P., 2012. Toxoplasmosis: new challenges for an old disease. *Eye*, 26(2), pp.241-244.
48. "Preventing Congenital Toxoplasmosis". Cdc.gov. N.p., 2017. Web. 10 Feb. 2017.
49. Boyer, K.M., Holfels, E., Roizen, N., Swisher, C., Mack, D., Remington, J., Withers, S., Meier, P., McLeod, R. and Toxoplasmosis Study Group, 2005. Risk factors for *Toxoplasma gondii* infection in mothers of infants with congenital toxoplasmosis: implications for prenatal management and screening. *American journal of obstetrics and gynecology*, 192(2), pp.564-571.
50. Weiss, L.M. and Dubey, J.P., 2009. Toxoplasmosis: A history of clinical observations. *International journal for parasitology*, 39(8), pp.895-901.
51. Deka, Deepika. *Congenital Intrauterine Infections*. 1st ed. New Dwlhi: Jaypee Brothers Medical Publishers, 2009. Print.
52. Dunn, D., Wallon, M., Peyron, F., Petersen, E., Peckham, C. and Gilbert, R., 1999. Mother-to-child transmission of toxoplasmosis: risk estimates for clinical counselling. *The Lancet*, 353(9167), pp.1829-1833.

53. Olariu, T.R., Remington, J.S., McLeod, R., Alam, A. and Montoya, J.G., 2011. Severe congenital toxoplasmosis in the United States: clinical and serologic findings in untreated infants. *The Pediatric infectious disease journal*, 30(12), pp.1056-1061.
54. Goldstein, E.J., Montoya, J.G. and Remington, J.S., 2008. Management of *Toxoplasma gondii* infection during pregnancy. *Clinical Infectious Diseases*, 47(4), pp.554-566.
55. Tekkesin, N., 2012. Diagnosis of toxoplasmosis in pregnancy: a review. *HOAJ Biology*, 1(1), p.9.
56. McAuley JM, Jones JL, Singh AM. *Toxoplasma*. In: Jorgensen JH, Pfaller MA, Carroll KC, Funke G, Landry ML, Richter SS, Warnock DW, editors. *Manual of Clinical Microbiology*. 11th ed. Washington, D.C.: American Society for Microbiology; 2015. p. 2373--2386.
57. Robert-Gangneux, F. and Dardé, M.L., 2012. Epidemiology of and diagnostic strategies for toxoplasmosis. *Clinical microbiology reviews*, 25(2), pp.264-296.
58. Liesenfeld, O., Montoya, J.G., Kinney, S., Press, C. and Remington, J.S., 2001. Effect of testing for IgG avidity in the diagnosis of *Toxoplasma gondii* infection in pregnant women: experience in a US reference laboratory. *Journal of Infectious Diseases*, 183(8), pp.1248-1253.
59. Wallon, M., Franck, J., Thulliez, P., Huissoud, C., Peyron, F., Garcia-Meric, P. and Kieffer, F., 2010. Accuracy of real-time polymerase chain reaction for *Toxoplasma gondii* in amniotic fluid. *Obstetrics & Gynecology*, 115(4), pp.727-733.
60. Toxoplasmosis In HIV-Infected Patients". Uptodate.com. N.p., 2017. Web. 12 Feb. 2017.
61. Weiss, L.M. and Dubey, J.P., 2009. Toxoplasmosis: A history of clinical observations. *International journal for parasitology*, 39(8), pp.895-901.
62. Kaplan, J.E., Benson, C., Holmes, K.K., Brooks, J.T., Pau, A., Masur, H., Centers for Disease Control and Prevention (CDC), National Institutes of Health and HIV Medicine Association of the Infectious Diseases Society of America, 2009. Guidelines for prevention and treatment of opportunistic infections in HIV-infected adults and adolescents. *MMWR Recomm Rep*, 58(RR-4), pp.1-207.
63. Dannemann, B., McCutchan, J.A., Israelski, D., Antoniskis, D., Leport, C., Luft, B., Nussbaum, J., Clumeck, N., Morlat, P., Chiu, J. and Vilde, J.L., 1992. Treatment of toxoplasmic encephalitis in patients with AIDS: a randomized trial comparing pyrimethamine plus clindamycin to pyrimethamine plus sulfadiazine. *Annals of Internal Medicine*, 116(1), pp.33-43.
64. Khurana, S. and Batra, N., 2016. Toxoplasmosis in organ transplant recipients: Evaluation, implication, and prevention. *Tropical Parasitology*, 6(2), p.123.
65. CDC - Toxoplasmosis - Resources For Health Professionals". Cdc.gov. N.p., 2017. Web. 10 Feb. 2017.

66. Dannemann, B., McCutchan, J.A., Israelski, D., Antoniskis, D., Leport, C., Luft, B., Nussbaum, J., Clumeck, N., Morlat, P., Chiu, J. and Vilde, J.L., 1992. Treatment of toxoplasmic encephalitis in patients with AIDS: a randomized trial comparing pyrimethamine plus clindamycin to pyrimethamine plus sulfadiazine. *Annals of Internal Medicine*, 116(1), pp.33-43.
67. Yan, J., Huang, B., Liu, G., Wu, B., Huang, S., Zheng, H., Shen, J., Lun, Z.R., Wang, Y. and Lu, F., 2013. Meta-analysis of prevention and treatment of toxoplasmic encephalitis in HIV-infected patients. *Acta tropica*, 127(3), pp.236-244.
68. van der Ven, A.J., Schoondermark-van de Ven, E.M., Camps, W., Melchers, W.J., Koopmans, P.P., van der Meer, J.W. and Galama, J.M., 1996. Anti-toxoplasma effect of pyrimethamine, trimethoprim and sulphonamides alone and in combination: implications for therapy. *Journal of antimicrobial chemotherapy*, 38(1), pp.75-80.
69. Allegra, C.J., Kovacs, J.A., Drake, J.C., Swan, J.C., Chabner, B.A. and Masur, H., 1987. Potent in vitro and in vivo antitoxoplasma activity of the lipid-soluble antifolate trimetrexate. *Journal of Clinical Investigation*, 79(2), p.478.
70. Allegra, C.J., Boarman, D., Kovacs, J.A., Morrison, P., Beaver, J., Chabner, B.A. and Masur, H., 1990. Interaction of sulfonamide and sulfone compounds with *Toxoplasma gondii* dihydropteroate synthase. *Journal of Clinical Investigation*, 85(2), p.371.
71. Blais, J., Tardif, C. and Chamberland, S., 1993. Effect of clindamycin on intracellular replication, protein synthesis, and infectivity of *Toxoplasma gondii*. *Antimicrobial agents and chemotherapy*, 37(12), pp.2571-2577.
72. Sibley, L.D., Khan, A., Ajioka, J.W. and Rosenthal, B.M., 2009. Genetic diversity of *Toxoplasma gondii* in animals and humans. *Philosophical Transactions of the Royal Society B: Biological Sciences*, 364(1530), pp.2749-2761.
73. Ajzenberg, D., Yera, H., Marty, P., Paris, L., Dalle, F., Menotti, J., Aubert, D., Franck, J., Bessières, M.H., Quinio, D. and Pelloux, H., 2009. Genotype of 88 *Toxoplasma gondii* isolates associated with toxoplasmosis in immunocompromised patients and correlation with clinical findings. *Journal of Infectious Diseases*, 199(8), pp.1155-1167.
74. Lehmann, T., Graham, D.H., Dahl, E.R., Bahia-Oliveira, L.M., Gennari, S.M. and Dubey, J.P., 2004. Variation in the structure of *Toxoplasma gondii* and the roles of selfing, drift, and epistatic selection in maintaining linkage disequilibria. *Infection, Genetics and Evolution*, 4(2), pp.107-114.
75. Howe, D.K. and Sibley, L.D., 1995. *Toxoplasma gondii* comprises three clonal lineages: correlation of parasite genotype with human disease. *Journal of infectious diseases*, 172(6), pp.1561-1566.
76. Isoenzymic characterization of seven strains of *Toxoplasma gondii* by isoelectrofocusing in polyacrylamide gels.

77. Howe, D.K., Honoré, S., Derouin, F. and Sibley, L.D., 1997. Determination of genotypes of *Toxoplasma gondii* strains isolated from patients with toxoplasmosis. *Journal of clinical microbiology*, 35(6), pp.1411-1414.
78. Sibley, L.D. and Boothroyd, J.C., 1992. Virulent strains of *Toxoplasma gondii* comprise a single clonal lineage. *Nature*, 359(6390), p.82.
79. Robert-Gangneux, F. and Dardé, M.L., 2012. Epidemiology of and diagnostic strategies for toxoplasmosis. *Clinical microbiology reviews*, 25(2), pp.264-296.
80. Weilhammer, D.R. and Rasley, A., 2011. Genetic approaches for understanding virulence in *Toxoplasma gondii*. *Briefings in functional genomics*, 10(6), pp.365-373.
81. Behnke, M.S., Khan, A., Wootton, J.C., Dubey, J.P., Tang, K. and Sibley, L.D., 2011. Virulence differences in *Toxoplasma* mediated by amplification of a family of polymorphic pseudokinases. *Proceedings of the National Academy of Sciences*, 108(23), pp.9631-9636.
82. Windeck, T. and Gross, U., 1996. *Toxoplasma gondii* strain-specific transcript levels of SAG1 and their association with virulence. *Parasitology research*, 82(8), pp.715-719.
83. Matsubayashi, H. and Akao, S., 1963. Morphological studies on the development of the *Toxoplasma* cyst. *American Journal of Tropical Medicine and Hygiene*, 12(3), pp.321-33.
84. Gross U, Bohne W. *Toxoplasma gondii*: strain- and host cell-dependent induction of stage differentiation. *J Eukaryot Microbiol*. 1994;41:10S–11S.
85. Jerome, M.E., Radke, J.R., Bohne, W., Roos, D.S. and White, M.W., 1998. *Toxoplasma gondii* bradyzoites form spontaneously during sporozoite-initiated development. *Infection and immunity*, 66(10), pp.4838-4844.
86. Horwitz, M.A., 1983. Formation of a novel phagosome by the Legionnaire's disease bacterium (*Legionella pneumophila*) in human monocytes. *Journal of Experimental Medicine*, 158(3), pp.1319-1331.
87. Jones, T.C., Yeh, S. and Hirsch, J.G., 1972. The interaction between *Toxoplasma gondii* and mammalian cells: I. Mechanism of entry and intracellular fate of the parasite. *The Journal of experimental medicine*, 136(5), p.1157.
88. Meylan, E., Curran, J., Hofmann, K., Moradpour, D., Binder, M., Bartenschlager, R. and Tschopp, J., 2005. Cardif is an adaptor protein in the RIG-I antiviral pathway and is targeted by hepatitis C virus. *Nature*, 437(7062), pp.1167-1172.
89. Jain, P., Luo, Z.Q. and Blanke, S.R., 2011. *Helicobacter pylori* vacuolating cytotoxin A (VacA) engages the mitochondrial fission machinery to induce host cell death. *Proceedings of the National Academy of Sciences*, 108(38), pp.16032-16037.
90. Pernas, L., Adomako-Ankomah, Y., Shastri, A.J., Ewald, S.E., Treeck, M., Boyle, J.P. and Boothroyd, J.C., 2014. *Toxoplasma* effector MAF1 mediates recruitment of host mitochondria and impacts the host response. *PLoS Biol*, 12(4), p.e1001845.

91. Rosowski, E.E., Lu, D., Julien, L., Rodda, L., Gaiser, R.A., Jensen, K.D. and Saeij, J.P., 2011. Strain-specific activation of the NF- κ B pathway by GRA15, a novel *Toxoplasma gondii* dense granule protein. *Journal of Experimental Medicine*, 208(1), pp.195-212.
92. Saeij, J.P.J., Collier, S., Boyle, J.P., Jerome, M.E., White, M.W. and Boothroyd, J.C., 2007. *Toxoplasma* co-opts host gene expression by injection of a polymorphic kinase homologue. *Nature*, 445(7125), pp.324-327.
93. Radke, J.R., Behnke, M.S., Mackey, A.J., Radke, J.B., Roos, D.S. and White, M.W., 2005. The transcriptome of *Toxoplasma gondii*. *BMC biology*, 3(1), p.26.
94. Saeij, J.P., Boyle, J.P. and Boothroyd, J.C., 2005. Differences among the three major strains of *Toxoplasma gondii* and their specific interactions with the infected host. *Trends in parasitology*, 21(10), pp.476-481.
95. Sims, T.A., Hay, J. and Talbot, I.C., 1988. Host—parasite relationship in the brains of mice with congenital toxoplasmosis. *The Journal of pathology*, 156(3), pp.255-261.
96. Sethi, K.K., Rahman, A., Pelster, B. and Brandis, H., 1977. Search for the presence of lectin-binding sites on *Toxoplasma gondii*. *The Journal of parasitology*, pp.1076-1080.
97. Boothroyd, J.C., Black, M., Bonnefoy, S., Hehl, A., Knoll, L.J., Manger, I.D., Ortega-Barria, E. and Tomavo, S., 1997. Genetic and biochemical analysis of development in *Toxoplasma gondii*. *Philosophical Transactions of the Royal Society of London B: Biological Sciences*, 352(1359), pp.1347-1354.
98. Zhang, Y.W., Halonen, S.K., Ma, Y.F., Wittner, M. and Weiss, L.M., 2001. Initial Characterization of CST1, a *Toxoplasma gondii* Cyst Wall Glycoprotein. *Infection and immunity*, 69(1), pp.501-507.
99. Tomita, T., Bzik, D.J., Ma, Y.F., Fox, B.A., Markillie, L.M., Taylor, R.C., Kim, K. and Weiss, L.M., 2013. The *Toxoplasma gondii* cyst wall protein CST1 is critical for cyst wall integrity and promotes bradyzoite persistence. *PLoS Pathog*, 9(12), p.e1003823.
100. Ferguson, D.J.P., Cesbron-Delauw, M.F., Dubremetz, J.F., Sibley, L.D., Joiner, K.A. and Wright, S., 1999. The expression and distribution of dense granule proteins in the enteric (Coccidian) forms of *Toxoplasma gondii* in the small intestine of the cat. *Experimental parasitology*, 91(3), pp.203-211.
101. Ferguson, D.J.P., Jacobs, D., Saman, E., Dubremetz, J.F. and Wright, S.E., 1999. In vivo expression and distribution of dense granule protein 7 (GRA7) in the exoenteric (tachyzoite, bradyzoite) and enteric (coccidian) forms of *Toxoplasma gondii*. *Parasitology*, 119(03), pp.259-265.
102. Gross, U., Bormuth, H., Gaissmaier, C., Dittrich, C., Krenn, V., Bohne, W. and Ferguson, D.J., 1995. Monoclonal rat antibodies directed against *Toxoplasma gondii* suitable for studying tachyzoite-bradyzoite interconversion in vivo. *Clinical and Diagnostic Laboratory Immunology*, 2(5), pp.542-548.
103. Buchholz, K.R., Fritz, H.M., Chen, X., Durbin-Johnson, B., Rocke, D.M., Ferguson, D.J., Conrad, P.A. and Boothroyd, J.C., 2011. Identification of

- tissue cyst wall components by transcriptome analysis of in vivo and in vitro *Toxoplasma gondii* bradyzoites. *Eukaryotic cell*, 10(12), pp.1637-1647.
104. Soete, M., Camus, D. and Dubrametz, J.F., 1994. Experimental induction of bradyzoite-specific antigen expression and cyst formation by the RH strain of *Toxoplasma gondii* in vitro. *Experimental parasitology*, 78(4), pp.361-370.
 105. Tomavo, S. and Boothroyd, J.C., 1995. Interconnection between organellar functions, development and drug resistance in the protozoan parasite, *Toxoplasma gondii*. *International journal for parasitology*, 25(11), pp.1293-1299.
 106. Bohne, W.O.L.F.G.A.N.G., Heesemann, J.U.R.G.E.N. and Gross, U., 1993. Induction of bradyzoite-specific *Toxoplasma gondii* antigens in gamma interferon-treated mouse macrophages. *Infection and immunity*, 61(3), pp.1141-1145.
 107. Radke, J.R., Striepen, B., Guerini, M.N., Jerome, M.E., Roos, D.S. and White, M.W., 2001. Defining the cell cycle for the tachyzoite stage of *Toxoplasma gondii*. *Molecular and biochemical parasitology*, 115(2), pp.165-175.
 108. Radke, J.R., Guerini, M.N., Jerome, M. and White, M.W., 2003. A change in the premitotic period of the cell cycle is associated with bradyzoite differentiation in *Toxoplasma gondii*. *Molecular and biochemical parasitology*, 131(2), pp.119-127.
 109. Behnke, M.S., Wootton, J.C., Lehmann, M.M., Radke, J.B., Lucas, O., Nawas, J., Sibley, L.D. and White, M.W., 2010. Coordinated progression through two subtranscriptomes underlies the tachyzoite cycle of *Toxoplasma gondii*. *PLoS one*, 5(8), p.e12354.
 110. Naguleswaran, A., Elias, E.V., McClintick, J., Edenberg, H.J. and Sullivan Jr, W.J., 2010. *Toxoplasma gondii* lysine acetyltransferase GCN5-A functions in the cellular response to alkaline stress and expression of cyst genes. *PLoS Pathog*, 6(12), p.e1001232.
 111. Bohne, W., Gross, U., Ferguson, D.J. and Heesemann, J., 1995. Cloning and characterization of a bradyzoite-specifically expressed gene (*hsp30/bag1*) of *Toxoplasma gondii*, related to genes encoding small heat-shock proteins of plants. *Molecular microbiology*, 16(6), pp.1221-1230.
 112. Ueno, A., Dautu, G., Haga, K., Munyaka, B., Carmen, G., Kobayashi, Y. and Igarashi, M., 2011. *Toxoplasma gondii*: a bradyzoite-specific DnaK-tetratricopeptide repeat (DnaK-TPR) protein interacts with p23 co-chaperone protein. *Experimental parasitology*, 127(4), pp.795-803
 113. Holcik M, Sonenberg N. Translational control in stress and apoptosis. *Nat Rev Mol Cell Biol* 2005; 6: 318–327.
 114. Sullivan, W.J., Narasimhan, J. and Bhatti, M.M., 2004. Parasite-specific eIF2 (eukaryotic initiation factor-2) kinase required for stress-induced translation control. *Biochemical Journal*, 380(2), pp.523-531.
 115. Narasimhan, J., Joyce, B.R., Naguleswaran, A., Smith, A.T., Livingston, M.R., Dixon, S.E., Coppens, I., Wek, R.C. and Sullivan, W.J., 2008.

- Translation regulation by eukaryotic initiation factor-2 kinases in the development of latent cysts in *Toxoplasma gondii*. *Journal of Biological Chemistry*, 283(24), pp.16591-16601.
116. Manger, I.D., Hehl, A., Parmley, S., Sibley, L.D., Marra, M., Hillier, L., Waterston, R. and Boothroyd, J.C., 1998. Expressed sequence tag analysis of the bradyzoite stage of *Toxoplasma gondii*: identification of developmentally regulated genes. *Infection and immunity*, 66(4), pp.1632-1637.
 117. Cleary, M.D., Singh, U., Blader, I.J., Brewer, J.L. and Boothroyd, J.C., 2002. *Toxoplasma gondii* asexual development: identification of developmentally regulated genes and distinct patterns of gene expression. *Eukaryotic Cell*, 1(3), pp.329-340.
 118. Singh, U., Brewer, J.L. and Boothroyd, J.C., 2002. Genetic analysis of tachyzoite to bradyzoite differentiation mutants in *Toxoplasma gondii* reveals a hierarchy of gene induction. *Molecular microbiology*, 44(3), pp.721-733.
 119. Radke, J.R., Behnke, M.S., Mackey, A.J., Radke, J.B., Roos, D.S. and White, M.W., 2005. The transcriptome of *Toxoplasma gondii*. *BMC biology*, 3(1), p.1.
 120. Smith, A.T., Tucker-Samaras, S.D., Fairlamb, A.H. and Sullivan, W.J., 2005. MYST family histone acetyltransferases in the protozoan parasite *Toxoplasma gondii*. *Eukaryotic cell*, 4(12), pp.2057-2065.
 121. Bhatti, M.M., Livingston, M., Mullapudi, N. and Sullivan, W.J., 2006. Pair of unusual GCN5 histone acetyltransferases and ADA2 homologues in the protozoan parasite *Toxoplasma gondii*. *Eukaryotic cell*, 5(1), pp.62-76
 122. Saksouk, N., Bhatti, M.M., Kieffer, S., Smith, A.T., Musset, K., Garin, J., Sullivan, W.J., Cesbron-Delauw, M.F. and Hakimi, M.A., 2005. Histone-modifying complexes regulate gene expression pertinent to the differentiation of the protozoan parasite *Toxoplasma gondii*. *Molecular and cellular biology*, 25(23), pp.10301-10314.
 123. Sullivan Jr, W.J., Monroy, M.A., Bohne, W., Nallani, K.C., Chrivia, J., Yaciuk, P., Smith II, C.K. and Queener, S.F., 2003. Molecular cloning and characterization of an SRCAP chromatin remodeling homologue in *Toxoplasma gondii*. *Parasitology research*, 90(1), pp.1-8.
 124. Soldati, D. and Boothroyd, J.C., 1995. A selector of transcription initiation in the protozoan parasite *Toxoplasma gondii*. *Molecular and cellular biology*, 15(1), pp.87-93.
 125. Nakaar, V., Bermudes, D., Peck, K.R. and Joiner, K.A., 1998. Upstream elements required for expression of nucleoside triphosphate hydrolase genes of *Toxoplasma gondii*. *Molecular and biochemical parasitology*, 92(2), pp.229-239.
 126. Ma, Y.F., Zhang, Y., Kim, K. and Weiss, L.M., 2004. Identification and characterisation of a regulatory region in the *Toxoplasma gondii* hsp70 genomic locus. *International journal for parasitology*, 34(3), pp.333-346.
 127. Matrajt, M., Platt, C.D., Sagar, A.D., Lindsay, A., Moulton, C. and Roos, D.S., 2004. Transcript initiation, polyadenylation, and functional promoter

- mapping for the dihydrofolate reductase-thymidylate synthase gene of *Toxoplasma gondii*. *Molecular and biochemical parasitology*, 137(2), pp.229-238.
128. Bohne, W., Wirsing, A. and Gross, U., 1997. Bradyzoite-specific gene expression in *Toxoplasma gondii* requires minimal genomic elements. *Molecular and biochemical parasitology*, 85(1), pp.89-98.
 129. Behnke, M.S., Radke, J.B., Smith, A.T., Sullivan Jr, W.J. and White, M.W., 2008. The transcription of bradyzoite genes in *Toxoplasma gondii* is controlled by autonomous promoter elements. *Molecular microbiology*, 68(6), pp.1502-1518.
 130. Saeij, J.P., Arrizabalaga, G. and Boothroyd, J.C., 2008. A cluster of four surface antigen genes specifically expressed in bradyzoites, SAG2CDXY, plays an important role in *Toxoplasma gondii* persistence. *Infection and immunity*, 76(6), pp.2402-2410.
 131. Thomas, M.C. and Chiang, C.M., 2006. The general transcription machinery and general cofactors. *Critical reviews in biochemistry and molecular biology*, 41(3), pp.105-178.
 132. Orphanides, G., Lagrange, T. and Reinberg, D., 1996. The general transcription factors of RNA polymerase II. *Genes and development*, 10(21), pp.2657-2683.
 133. Buratowski, S., Hahn, S., Guarente, L. and Sharp, P.A., 1989. Five intermediate complexes in transcription initiation by RNA polymerase II. *Cell*, 56(4), pp.549-561.
 134. Hatzopoulos, A.K., Schlokot, U., and Gruss, P. Enhancers and other cis-acting regulatory sequences. B.D. Hames, D.M. Glover (Eds.) Eucaryotic RNA Synthesis and Processing, Horizons in Molecular Biology Series. IRL Press, Oxford; 1988
 135. Legube, G. and Trouche, D., 2003. Regulating histone acetyltransferases and deacetylases. *EMBO reports*, 4(10), pp.944-947.
 136. Meissner, M. and Soldati, D., 2005. The transcription machinery and the molecular toolbox to control gene expression in *Toxoplasma gondii* and other protozoan parasites. *Microbes and infection*, 7(13), pp.1376-1384.
 137. Riechmann, J.L., Heard, J., Martin, G., Reuber, L., Jiang, C.Z., Keddie, J., Adam, L., Pineda, O., Ratcliffe, O.J., Samaha, R.R. and Creelman, R., 2000. Arabidopsis transcription factors: genome-wide comparative analysis among eukaryotes. *Science*, 290(5499), pp.2105-2110.
 138. Iyer, L.M., Anantharaman, V., Wolf, M.Y. and Aravind, L., 2008. Comparative genomics of transcription factors and chromatin proteins in parasitic protists and other eukaryotes. *International journal for parasitology*, 38(1), pp.1-31.
 139. Balaji, S., Babu, M.M., Iyer, L.M. and Aravind, L., 2005. Discovery of the principal specific transcription factors of Apicomplexa and their implication for the evolution of the AP2-integrase DNA binding domains. *Nucleic acids research*, 33(13), pp.3994-4006.
 140. Okamuro, J.K., Caster, B., Villarroel, R., Van Montagu, M. and Jofuku, K.D., 1997. The AP2 domain of APETALA2 defines a large new family of

- DNA binding proteins in Arabidopsis. *Proceedings of the National Academy of Sciences*, 94(13), pp.7076-7081.
141. Campbell, T.L., De Silva, E.K., Olszewski, K.L., Elemento, O. and Llinás, M., 2010. Identification and genome-wide prediction of DNA binding specificities for the ApiAP2 family of regulators from the malaria parasite. *PLoS Pathog*, 6(10), p.e1001165.
 142. Drews, G.N., Bowman, J.L. and Meyerowitz, E.M., 1991. Negative regulation of the Arabidopsis homeotic gene AGAMOUS by the APETALA2 product. *Cell*, 65(6), pp.991-1002.
 143. Krizek, B., 2009. AINTEGUMENTA and AINTEGUMENTA-LIKE6 act redundantly to regulate Arabidopsis floral growth and patterning. *Plant physiology*, 150(4), pp.1916-1929.
 144. Wilson, K., Long, D., Swinburne, J. and Coupland, G., 1996. A Dissociation insertion causes a semidominant mutation that increases expression of TINY, an Arabidopsis gene related to APETALA2. *The Plant Cell*, 8(4), pp.659-671.
 145. Agarwal, P.K., Agarwal, P., Reddy, M.K. and Sopory, S.K., 2006. Role of DREB transcription factors in abiotic and biotic stress tolerance in plants. *Plant cell reports*, 25(12), pp.1263-1274.
 146. Molecular responses to dehydration and low temperature: differences and cross-talk between two stress signaling pathways. *Current opinion in plant biology*, 3(3), pp.217-223.
 147. Chung, S. and Parish, R.W., 2008. Combinatorial interactions of multiple cis-elements regulating the induction of the Arabidopsis XERO2 dehydrin gene by abscisic acid and cold. *The Plant Journal*, 54(1), pp.15-29.
 148. Sun, S., Yu, J.P., Chen, F., Zhao, T.J., Fang, X.H., Li, Y.Q. and Sui, S.F., 2008. TINY, a dehydration-responsive element (DRE)-binding protein-like transcription factor connecting the DRE-and ethylene-responsive element-mediated signaling pathways in Arabidopsis. *Journal of Biological Chemistry*, 283(10), pp.6261-6271.
 149. Flueck, C., Bartfai, R., Niederwieser, I., Witmer, K., Alako, B.T., Moes, S., Bozdech, Z., Jenoe, P., Stunnenberg, H.G. and Voss, T.S., 2010. A major role for the Plasmodium falciparum ApiAP2 protein PfSIP2 in chromosome end biology. *PLoS Pathog*, 6(2), p.e1000784.
 150. Yuda, M., Iwanaga, S., Shigenobu, S., Mair, G.R., Janse, C.J., Waters, A.P., Kato, T. and Kaneko, I., 2009. Identification of a transcription factor in the mosquito-invasive stage of malaria parasites. *Molecular microbiology*, 71(6), pp.1402-1414.
 151. Yuda, M., Iwanaga, S., Shigenobu, S., Kato, T. and Kaneko, I., 2010. Transcription factor AP2-Sp and its target genes in malarial sporozoites. *Molecular microbiology*, 75(4), pp.854-863.
 152. Iwanaga, S., Kaneko, I., Kato, T. and Yuda, M., 2012. Identification of an AP2-family protein that is critical for malaria liver stage development. *PLoS One*, 7(11), p.e47557.
 153. Sinha, A., Hughes, K.R., Modrzynska, K.K., Otto, T.D., Pfander, C., Dickens, N.J., Religa, A.A., Bushell, E., Graham, A.L., Cameron, R. and

- Kafsack, B.F., 2014. A cascade of DNA binding proteins for sexual commitment and development in Plasmodium. *Nature*, 507(7491), p.253.
154. Kafsack, B.F., Rovira-Graells, N., Clark, T.G., Bancells, C., Crowley, V.M., Campino, S.G., Williams, A.E., Drought, L.G., Kwiatkowski, D.P., Baker, D.A. and Cortés, A., 2014. A transcriptional switch underlies commitment to sexual development in human malaria parasites. *Nature*, 507(7491), p.248.
155. Yuda, M., Iwanaga, S., Kaneko, I. and Kato, T., 2015. Global transcriptional repression: An initial and essential step for Plasmodium sexual development. *Proceedings of the National Academy of Sciences*, 112(41), pp.12824-12829.
156. Radke, J.B., Lucas, O., De Silva, E.K., Ma, Y., Sullivan, W.J., Weiss, L.M., Llinas, M. and White, M.W., 2013. ApiAP2 transcription factor restricts development of the Toxoplasma tissue cyst. *Proceedings of the National Academy of Sciences*, 110(17), pp.6871-6876.
157. Walker, R., Gissot, M., Croken, M.M., Huot, L., Hot, D., Kim, K. and Tomavo, S., 2013. The Toxoplasma nuclear factor TgAP2XI-4 controls bradyzoite gene expression and cyst formation. *Molecular microbiology*, 87(3), pp.641-655.
158. Walker, R., Gissot, M., Huot, L., Alayi, T.D., Hot, D., Marot, G., Schaeffer-Reiss, C., Van Dorsselaer, A., Kim, K. and Tomavo, S., 2013. Toxoplasma transcription factor TgAP2XI-5 regulates the expression of genes involved in parasite virulence and host invasion. *Journal of Biological Chemistry*, 288(43), pp.31127-31138.
159. Pittman, K.J., Aliota, M.T. and Knoll, L.J., 2014. Dual transcriptional profiling of mice and Toxoplasma gondii during acute and chronic infection. *BMC genomics*, 15(1), p.1.
160. Fox, B.A., Falla, A., Rommereim, L.M., Tomita, T., Gigley, J.P., Mercier, C., Cesbron-Delauw, M.F., Weiss, L.M. and Bzik, D.J., 2011. Type II Toxoplasma gondii KU80 knockout strains enable functional analysis of genes required for cyst development and latent infection. *Eukaryotic cell*, 10(9), pp.1193-1206.
161. Fox, B.A., Ristuccia, J.G., Gigley, J.P. and Bzik, D.J., 2009. Efficient gene replacements in Toxoplasma gondii strains deficient for nonhomologous end joining. *Eukaryotic cell*, 8(4), pp.520-529.
162. Potter, H., 1988. Electroporation in biology: methods, applications, and instrumentation. *Analytical biochemistry*, 174(2), pp.361-373.
163. Van den Hoff, M.J., Moorman, A.F. and Lamers, W.H., 1992. Electroporation in 'intracellular' buffer increases cell survival. *Nucleic acids research*, 20(11), p.2902.
164. Soldati, D. and Boothroyd, J.C., 1993. Transient transfection and expression in the obligate intracellular parasite Toxoplasma gondii. *SCIENCE-NEW YORK THEN WASHINGTON-*, 260, pp.349-349.
165. Ullman, B. and Carter, D., 1995. Hypoxanthine-guanine phosphoribosyltransferase as a therapeutic target in protozoal infections. *Infectious agents and disease*, 4(1), pp.29-40.

166. Donald, R.G., Carter, D., Ullman, B. and Roos, D.S., 1996. Insertional tagging, cloning, and expression of the *Toxoplasma gondii* hypoxanthine-xanthine-guanine phosphoribosyltransferase gene Use as a selectable marker for stable transformation. *Journal of Biological Chemistry*, 271(24), pp.14010-14019.
167. Donald, R.G. and Roos, D.S., 1993. Stable molecular transformation of *Toxoplasma gondii*: a selectable dihydrofolate reductase-thymidylate synthase marker based on drug-resistance mutations in malaria. *Proceedings of the National Academy of Sciences*, 90(24), pp.11703-11707.
168. Bahl, A., Davis, P.H., Behnke, M., Dzierszynski, F., Jagalur, M., Chen, F., Shanmugam, D., White, M.W., Kulp, D. and Roos, D.S., 2010. A novel multifunctional oligonucleotide microarray for *Toxoplasma gondii*. *BMC genomics*, 11(1), p.1.
169. Lavine, M.D., Knoll, L.J., Rooney, P.J. and Arrizabalaga, G., 2007. A *Toxoplasma gondii* mutant defective in responding to calcium fluxes shows reduced in vivo pathogenicity. *Molecular and biochemical parasitology*, 155(2), pp.113-122.
170. "Yeast Two-Hybrid (Y2H) Principle". Hybrigenics-services.com. N.p., 2017. Web. 8 Mar. 2017.
171. Brennan, M.B. and Struhl, K., 1980. Mechanisms of increasing expression of a yeast gene in *Escherichia coli*. *Journal of molecular biology*, 136(3), pp.333-338.
172. Formstecher, E., Aresta, S., Collura, V., Hamburger, A., Meil, A., Trehin, A., Reverdy, C., Betin, V., Maire, S., Brun, C. and Jacq, B., 2005. Protein interaction mapping: a *Drosophila* case study. *Genome research*, 15(3), pp.376-384.
173. *How to Read Your Results Documents*. 1st ed. Hybrigenics, 2017. Web. 15 Oct. 2016.
174. Castresana, J., 2000. Selection of conserved blocks from multiple alignments for their use in phylogenetic analysis. *Molecular biology and evolution*, 17(4), pp.540-552.
175. Drozdetskiy, A., Cole, C., Procter, J. and Barton, G.J., 2015. JPred4: a protein secondary structure prediction server. *Nucleic acids research*, p.gkv332.
176. Guindon, S. and Gascuel, O., 2003. A simple, fast, and accurate algorithm to estimate large phylogenies by maximum likelihood. *Systematic biology*, 52(5), pp.696-704.
177. Mann, T. and Beckers, C., 2001. Characterization of the subpellicular network, a filamentous membrane skeletal component in the parasite *Toxoplasma gondii*. *Molecular and biochemical parasitology*, 115(2), pp.257-268.
178. Gubbels, M.J., Wieffer, M. and Striepen, B., 2004. Fluorescent protein tagging in *Toxoplasma gondii*: identification of a novel inner membrane complex component conserved among Apicomplexa. *Molecular and biochemical parasitology*, 137(1), pp.99-110.

179. Suganuma, T., Pattenden, S.G. and Workman, J.L., 2008. Diverse functions of WD40 repeat proteins in histone recognition. *Genes & development*, 22(10), pp.1265-1268.
180. Dzierszynski, F., Nishi, M., Ouko, L. and Roos, D.S., 2004. Dynamics of *Toxoplasma gondii* differentiation. *Eukaryotic cell*, 3(4), pp.992-1003.
181. Watts, E., Zhao, Y., Dhara, A., Eller, B., Patwardhan, A. and Sinai, A.P., 2015. Novel approaches reveal that *Toxoplasma gondii* bradyzoites within tissue cysts are dynamic and replicating entities in vivo. *MBio*, 6(5), pp.e01155-15.
182. Soete, M., Fortier, B., Camus, D. and Dubremetz, J.F., 1993. *Toxoplasma gondii*: kinetics of bradyzoite-tachyzoite interconversion in vitro. *Experimental parasitology*, 76(3), pp.259-264.
183. White, M.W., Radke, J.R. and Radke, J.B., 2014. *Toxoplasma* development—turn the switch on or off?. *Cellular microbiology*, 16(4), pp.466-472.
184. Shirodkar, S., Ewen, M., DeCaprio, J.A., Morgan, J., Livingston, D.M. and Chittenden, T., 1992. The transcription factor E2F interacts with the retinoblastoma product and a p107-cyclin A complex in a cell cycle-regulated manner. *Cell*, 68(1), pp.157-166.
185. DeGregori, J., Kowalik, T. and Nevins, J.R., 1995. Cellular targets for activation by the E2F1 transcription factor include DNA synthesis-and G1/S-regulatory genes. *Molecular and cellular biology*, 15(8), pp.4215-4224.
186. Wang, J., Dixon, S.E., Ting, L.M., Liu, T.K., Jeffers, V., Croken, M.M., Calloway, M., Cannella, D., Hakimi, M.A., Kim, K. and Sullivan Jr, W.J., 2014. Lysine acetyltransferase GCN5b interacts with AP2 factors and is required for *Toxoplasma gondii* proliferation. *PLoS pathogens*, 10(1), p.e1003830.
187. Lu, Q. and Richardson, B., 2004. DNaseI hypersensitivity analysis of chromatin structure. *Epigenetics Protocols*, pp.77-86.
188. Licausi, F., Ohme-Takagi, M. and Perata, P., 2013. APETALA2/Ethylene Responsive Factor (AP2/ERF) transcription factors: mediators of stress responses and developmental programs. *New Phytologist*, 199(3), pp.639-649.
189. Fujimoto, S.Y., Ohta, M., Usui, A., Shinshi, H. and Ohme-Takagi, M., 2000. Arabidopsis ethylene-responsive element binding factors act as transcriptional activators or repressors of GCC box-mediated gene expression. *The Plant Cell*, 12(3), pp.393-404.
190. Thiel, G., Lietz, M. and Hohl, M., 2004. How mammalian transcriptional repressors work. *European Journal of Biochemistry*, 271(14), pp.2855-2862

CURRICULUM VITAE

Sherri Y. Huang

Education

- 2013 – 2017 Doctor of Philosophy in Pharmacology
Indiana University
Indianapolis, IN
- 2011 – Expected 2020 Doctor of Medicine
Medical Scientist Training Program
Indiana University School of Medicine
Indianapolis, IN
- 2006 – 2009 Bachelor of Arts
Washington University in St. Louis
St. Louis, MO

Research Experience

- 2013 – 2017 Graduate research
*Indiana University School of Medicine, Department of
Pharmacology and Toxicology*
Indianapolis, Indiana
Mentor – William J. Sullivan Jr., Ph.D., Associate Professor
Pharmacology & Toxicology, Microbiology & Immunology
- My thesis work focused on the role of a putative transcription factor called AP2IX-4 in *Toxoplasma gondii*, a pathogen that reactivates from a latent cyst form in immune-compromised patients. I used genetic and molecular approaches, gene expression analysis and mouse modeling to determine the function of AP2IX-4 in tissue cyst development.
- 2010 – 2011 Research assistant
University of California, Berkeley
Berkeley, California
Mentor – Rosanna Alegado, Ph.D.
- I generated genetic constructs to investigate the role of bacterial sphingolipids in inducing multicellular choanoflagellate formation.
- 2007 – 2009 Undergraduate research assistant
Washington University in St. Louis
St. Louis, Missouri

I investigated two putative regulators from a genetic screen to identify positive regulators of FtsZ assembly in *Bacillus subtilis*. Using molecular approaches, I discovered that one clone was an antisense inhibitor of the FtsZ negative regulator EzrA, while the other, yusX, was an indirect regulator of FtsZ assembly.

Peer Reviewed Publications

Huang, Sherri, Michael J. Holmes, Joshua B. Radke, Dong-Pyo Hong, Ting-Kai Liu, Michael W. White, and William J. Sullivan. "Toxoplasma gondii AP2IX-4 regulates gene expression during bradyzoite development." *mSphere* 2, no. 2 (2017): e00054-17.

Jeffers, Victoria, Chunlin Yang, **Sherri Huang**, and William J. Sullivan. "Bromodomains in Protozoan Parasites: Evolution, Function, and Opportunities for Drug Development." *Microbiology and Molecular Biology Reviews* 81, no. 1 (2017): e00047-16.

Radke, Joshua B., Danielle Worth, Dong-Pyo Hong, **Sherri Huang**, William J. Sullivan, Emma H. Wilson, and Michael White. "Transcriptional repression by ApiAP2 factors is central to chronic toxoplasmosis." *bioRxiv* (2017): 100628.

Zhang, Rui, **Sherri Huang**, Kay Li, Guang Jun Zhang, Chun-Ju Chang, and Jer-Yen Yang. "Dual degradation signals destruct GLI1: AMPK inhibits GLI1 through β -TrCP-mediated proteasome degradation." *Oncotarget*. **Accepted with minor revisions.**

Huang, Sherri Y., and Jer-Yen Yang. "Targeting the Hedgehog Pathway in Pediatric Medulloblastoma." *Cancers* 7, no. 4 (2015): 2110-2123.

Alegado, Rosanna A., Jonathan D. Grabenstatter, Richard Zuzow, Andrea Morris, **Sherri Y. Huang**, Roger E. Summons, and Nicole King. "Algoriphagus machipongonensis sp. nov., co-isolated with a colonial choanoflagellate." *International journal of systematic and evolutionary microbiology* 63, no. Pt 1 (2013): 163-168.

Poster & Presentation Abstracts

Sullivan Jr, William J.; **Sherri Huang**; Michael Holmes; Joshua Radke; Dong-Pyo Hong; Ting-Kai Liu; Michael White. AP2IX-4 is a cell cycle-regulated nuclear factor involved in latent cyst formation in *Toxoplasma gondii*. 2016 Molecular Parasitology Meeting in Woods Hole, Massachusetts.

Huang, Sherri Y., Ting-Kai Liu, Joshua B. Radke, Michael W. White, and William J. Sullivan Jr. A cell-cycle regulated ApiAP2 factor modulates stress induction of bradyzoite gene expression. 2015 Midwest Neglected Infectious Diseases Meeting, South Bend IN. **Abstract selected for Oral presentation.**

Huang, Sherri Y., Ting-Kai Liu, Joshua B. Radke, Michael W. White, and William J. Sullivan Jr. Novel *Toxoplasma gondii* AP2 factor modulates stress induction of bradyzoite gene expression. 2015 National MD/PhD Student Conference, Keystone CO. **Poster presentation.**

Huang, Sherri Y., Ting-Kai Liu, Joshua B. Radke, Michael W. White, and William J. Sullivan Jr. A cell-cycle regulated ApiAP2 factor modulates stress induction of bradyzoite gene expression. 13th International Congress for Toxoplasmosis and *T. gondii* Biology, Gettysburg PA. **Abstract selected for Oral presentation.**

Radke, Joshua B., **Sherri Huang,** Li-Min Ting, William J Sullivan Jr, Kami Kim, Michael W. White. Transcriptional repressors have a key role in *Toxoplasma* development. 13th International Congress for Toxoplasmosis and *T. gondii* Biology, Gettysburg PA.

Huang, Sherri Y., Ting-Kai Liu, Joshua B. Radke, Michael W. White, and William J. Sullivan Jr. Novel putative transcription factor in *Toxoplasma gondii* modulates gene expression in tissue cyst stage. 2015 Great Lakes Chapter, American Society for Pharmacology and Experiment Therapeutics, Chicago IL. **Poster presentation.**

Huang, Sherri Y., Ting-Kai Liu, Joshua B. Radke, Michael W. White, and William J. Sullivan Jr. A cell-cycle regulated ApiAP2 factor that contributes to bradyzoite development in *Toxoplasma gondii*. 25th Annual Molecular Parasitology Meeting in Woods Hole, Massachusetts. **Poster presentation.**

Honors & Awards

- 2016 Selected to attend the Combining Clinical and Research Careers in Neuroscience Symposium in Washington D.C.
- 2015 Selected to attend the National MD/PhD Conference in Keystone, CO
- 2015 Graduate and Professional Educational Grant
- 2014 Paradise Travel Award
- 2013 Solution Center Venture Fund
- 2012 MSTP Lois Letzter Fellowship
- 2009 Graduated with Arts and Sciences College Honors
- 2008 Howard Hughes Medical Institute Summer Undergraduate Research Fellowship

Teaching & Mentoring Experience

- July 2016 Mentored M.D./Ph.D. student on summer rotation
Indiana University School of Medicine – Indianapolis, IN
- Nov. 2015 Mentored undergraduate student
Indiana University School of Medicine – Indianapolis, IN

Memberships

American Physician Scientists Association